AD-A008 206

COMBAT TRACTION II, PHASE II. VOLUME I, NARRATIVE

S. M. Warren, et al

Boeing Commercial Airplane Company

Prepared for:

Federal Aviation Administration
Aeronautical Systems Division
National Aeronautics and Space Administration

October 1974

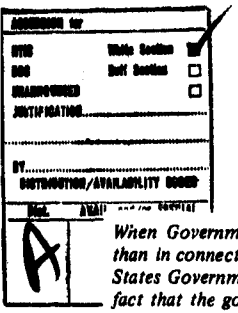

NOTICE

When Government drawings, specifications, or other data are used for any purpose other than in connection with a definitely related Government procurement operation, the United States Government thereby incurs no responsibility nor any obligation whatsoever; and the fact that the government may have formulated, furnished, or in any way supplied the said drawings, specifications, or other data, is not to be regarded by implication or otherwise as in any manner licensing the holder or any other person or corporation, or conveying any rights or permission to manufacture, use, or sell any patented invention that may in any way be related thereto.

This report has been prepared by the Boeing Commercial Aircraft Company, Renton, Washington, under USAF Contract F33657-74-C-0129 for the Deputy for Engineering, Aeronautical Systems Division, Wright-Patterson AFB, Ohio.

This report has been reviewed and cleared for open publication and/or public release by the appropriate Office of Public Information (OI) in accordance with AFR 190-13 and DOD 5230.9. There is no objection to unlimited distribution to the public at large or by the Defense Documentation Center (DDC) to the National Technical Information Service (NTIS).

This report has been reviewed and approved for publication.

William V. Tracy Jr

WILLIAM V. TRACY, JR.
Project Engineer

FOR THE COMMANDER

David B. Tremblay

DAVID B. TREMBLAY
Division Chief
Landing Gear & Mechanical
Equipment Division

Copies of this report should not be returned unless return is required by security considerations, contractual obligations, or notice on a specific document.

AFLC–WPAFB–NOV 74 500

Unclassified

SECURITY CLASSIFICATION OF THIS PAGE (When Data Entered)

REPORT DOCUMENTATION PAGE		READ INSTRUCTIONS BEFORE COMPLETING FORM
1. REPORT NUMBER ASD-TR-74-41 FAA-RD-74-211 Volume I	2. GOVT ACCESSION NO.	3. RECIPIENT'S CATALOG NUMBER AD-A008 206
4. TITLE (and Subtitle) Combat Traction II, Phase II Volume I, Narrative		5. TYPE OF REPORT & PERIOD COVERED Final 6. PERFORMING ORG. REPORT NUMBER
7. AUTHOR(s) S.M. Warren, M.K. Wahi, R.L. Amberg, H.H. Straub, and N.S. Attri		8. CONTRACT OR GRANT NUMBER(s) F33657-74-C-0129
9. PERFORMING ORGANIZATION NAME AND ADDRESS The Boeing Commercial Airplane Company Renton, Washington		10. PROGRAM ELEMENT, PROJECT, TASK AREA & WORK UNIT NUMBERS 021A9363
11. CONTROLLING OFFICE NAME AND ADDRESS Air Force Systems Command Andrews AFB, Maryland		12. REPORT DATE October 1974 13. NUMBER OF PAGES
14. MONITORING AGENCY NAME & ADDRESS(if different from Controlling Office) Deputy for Subsystems Aeronautical Systems Division Wright-Patterson AFB, Ohio		15. SECURITY CLASS. (of this report) Unclassified 15a. DECLASSIFICATION/DOWNGRADING SCHEDULE

16. DISTRIBUTION STATEMENT (of this Report)

Approved for Public Release, Distribution Unlimited

17. DISTRIBUTION STATEMENT (of the abstract entered in Block 20, if different from Report)

18. SUPPLEMENTARY NOTES

19. KEY WORDS (Continue on reverse side if necessary and identify by block number)

Combat Traction
DBV
Mu-Meter
Antiskid
Simulator

20. ABSTRACT (Continue on reverse side if necessary and identify by block number)

A sensitivity analysis of airplane braking distance was conducted on hardware-analog brake control simulator for the Boeing 727-200, 737 Advanced, and 747-200, the Lockheed C-141A, and the McDonnell F-4E aircraft. Parameters affecting braking distance by at least 2% were identified. With the application of dimensional analysis, these parameters were arranged in dimensionless groups, and a braking distance prediction equation was developed for each airplane. A new methodology for predicting airplane braking distance is recommended, based on a dimensional equation, a suitable ground friction prediction system, ar accurate weather data.

DD FORM 1 JAN 73 1473 EDITION OF 1 NOV 65 IS OBSOLETE

SECURITY CLASSIFICATION OF THIS PAGE (When Data Entered)

FOREWORD

This report was prepared by S. M. Warren, M. K. Wahi, R. L. Amberg, H. H. Straub, and N. S. Attri of the Boeing Commercial Airplane Company under combined NASA, USAF, and FAA Contract F33657-74-C-0129. The program was divided into two tasks. Task I involved identifying the factors that significantly influence airplane stopping distance performance. Task II involved the use of Task I results to develop a runway performance prediction system specification and methodology.

This volume describes all essential aspects of the work performed in completing the contract. Volume II describes the hardware and antiskid systems used on the brake control simulator as well as the test conditions and parameters used in developing data required for the dimensional analysis. The work described herein was performed from October 1973 to October 1974.

The authors are indebted to Mr. J. Anselmi and Mr. R. F. Yurzcyk for their contributions to this program. Mr. Anselmi, formerly of the Boeing Commercial Airplane Company and now with General Motors, provided the initial direction in setting up the Boeing analog-hardware brake control simulator. The guidance and technical contribution of Mr. Yurzcyk as a task leader during the initial stages of the contract is appreciated.

The authors are also indebted to Mr. W. V. Tracy, USAF (Program Technical Manager), Mr. W. B. Horne, NASA (Program Monitor), and Mr. H. D'Aulerio, FAA (Program Monitor). Special contributions of Mr. L. Merritt, FAA, Maj. L. Dillon, USAF, and Maj. T. Harty, USAF, are acknowledged.

SUMMARY

This report describes the effort completed to:

- Determine the parameters that most significantly influence airplane stopping distance,
- Formulate a model that could be used to predict airplane braking distance.
- Evaluate the Diagonally Braked Vehicle (DBV) and Mu-Meter with respect to the criteria resulting from the model,
- Recommend the most logical approach to providing this prediction capability for USAF and FAA usage.

During Task I, the Boeing Brake Control Simulator was used to identify the characteristics affecting airplane stopping performance. Five aircraft models (727-200, 737 Advanced, 747-200, C-141A, and F-4E) were the subject of a sensitivity study. Major airplane, landing gear, and brake-wheel-tire parameters were varied systematically from arbitrary baseline conditions. This technique was used to determine the parameters that influence braking distance by at least 2%.

The initial list of parameters was reviewed and reduced by eliminating those involving pilot technique and by grouping interrelated terms. The resultant list is:

- Peak available ground friction (μ)
- Drag device effectiveness (C_L/C_D)
- Brake application speed (v)
- Air density (ρ)
- Engine idle thrust (F_e)

During Task II, a prediction model has been developed that correlates with measured test data to within ±5%. The model consists of a prediction equation expressing the relationships between four dimensionless groups of factors (pi terms) needed to define the braking phenomenon. The equation is of the form:

$$\pi_1 = C_\alpha (\pi_2)^{C_1} (\pi_3)^{C_2} (\pi_4)^{C_3}$$

where $\pi_1 = sg/v^2$, $\pi_2 = \mu$, $\pi_3 = C_L/C_D$, $\pi_4 = \rho v^6/F_e g^2$, and C_α, C_1, C_2, and C_3 are determined from particular aircraft test results.

The DBV and Mu-Meter were evaluated using the developed specification criteria. Both vehicles perform their design functions, but both fail to meet the aircraft criteria developed during this study.

In the recommended approach, the prediction methodology consists of a stopping performance equation; its applicability depends on a meaningful runway-tire friction coefficient and correct weather information.

TABLE OF CONTENTS

TABLE OF CONTENTS (Continued)

TABLE OF CONTENTS (Continued)

TABLE OF CONTENTS (Concluded)

LIST OF ILLUSTRATIONS

LIST OF TABLES

GLOSSARY

air distance summation of approach and flare distances

approach distance distance an aircraft travels from threshold to initiation of flare

baseline airplane aircraft in a three-point taxi attitude (during braking) and of typical landing weight, approach speed, CG location, landing flap setting, and engine thrust

braking distance distance an aircraft travels from brake application to a lower safe-turnoff speed

contamination foreign substance on a runway

flare distance distance an aircraft travels during flare segment

flare load factor normal aircraft acceleration experienced during flare, expressed in g's

glide slope angle in degrees defining aircraft flight path during approach

height above threshold aircraft altitude at start of approach segment

parameter rating index rank-order relationship of parameters

peak available mu computer input defining maximum value of friction available between the tire and ground during test condition

pi term dimensionless term for modeling theory

slip relationship between the braked wheel speed and the synchronous wheel (airplane) speed

stopping distance summation of airplane approach, flare, transition, and braking distances

transition distance distance airplane travels from time of initial main gear touchdown to brake application

LIST OF ABBREAVIATIONS AND SYMBOLS

a	aircraft deceleration
AC	alternating current
C_D	coefficient of drag
CG	center of gravity
C_L	coefficient of lift
DC	direct current
F_e	engine idle thrust
F_{eo}	engine idle thrust at zero velocity
g	acceleration caused by gravity
H	height above threshold
KE	change in idle thrust with velocity
N,n	flare load factor
P_B	brake pressure
PRI	parameter rating index
PSD	power spectral density
s, SB, X_A	braking distance
SA	approach distance
SF	flare distance
ST	transition distance
T_B	brake torque
TA	time to brake application
v, VI	brake application speed
V_w	headwind or tailwind velocity

W	airplane landing weight
γ	glide slope
μ, mu	peak available friction coefficient
η_s	braking distance efficiency
π	pi term
ρ	air density
σ	slip, percentage of slip
ω	wheel velocity

SECTION I

INTRODUCTION

At some time during the approach to an airport, an airplane pilot must decide whether or not he has enough runway length to stop safely. To make this decision, he must consider or anticipate a variety of conditions. Weather, runway conditions, airplane touchdown dynamics, and braking system capability have a major influence on the stopping distance of the aircraft. Thus, the pilot must have information not only on his own aircraft's landing characteristics but also the environment in which he is landing. Because a successful landing is vital to the safety and economy of airplane operation, there has been a continuing effort by the FAA and USAF to provide pilots with information so that he can predict the stopping performance of his aircraft upon landing.

The desire to provide this information requires a thorough understanding of the parameters that determine stopping distance. To determine what technical data is required by the pilot, a joint NASA, FAA, and USAF program was initiated and the Boeing Commercial Airplane Company was awarded USAF Contract F33657-74-C-0129 to identify, evaluate, and rate the parameters affecting airplane stopping performance. The basic approach, shown in Figures 1 and 2, to meeting this objective was to list all parameters which could possibly influence stopping performance. Then, with the aid of a digital computer and an analog-hardware brake control simulation, the parameters were varied about their baseline to determine their actual effect on stopping distance. To draw some general conclusions regarding the significance of individual parameters, five airplanes were studies (727-200, 737 Advanced, 747-200, C-141A, and F-4E). The process of identifying, evaluating, and rating the factors as described above has been termed a sensitivity study.

To produce meaningful results in a sensitivity study, all influencing factors must be considered. Thus, the analysis of stopping performance should include parameters that affect the airplane while it is on the runway and also factors that determine its initial condition at brake application. Thus, runway performance involves the total airplane-runway-weather system from the point at which the airplane crosses the runway threshold to the point where it actually stops. As a result, the stopping distance has been divided into four distinct segments: approach, flare, transition, and braking (Figure 3). The approach and flare segments are air modes that determine the dynamic conditions of the airplane at touchdown. Transition involves the distance the airplane travels as it changes from an air mode to the braking mode. Braking is the distance during which the airplane's forward kinetic energy is dissipated.

Determination of Federal Air Regulations (FAR) field length requires an accounting of each segment. During the air and transition modes, the distance traveled is determined largely by airplane flight characteristics, pilot technique, and the rules governing operation during these segments. The same factors influence the braking distance because they contribute to the airplane dynamics at brake application.

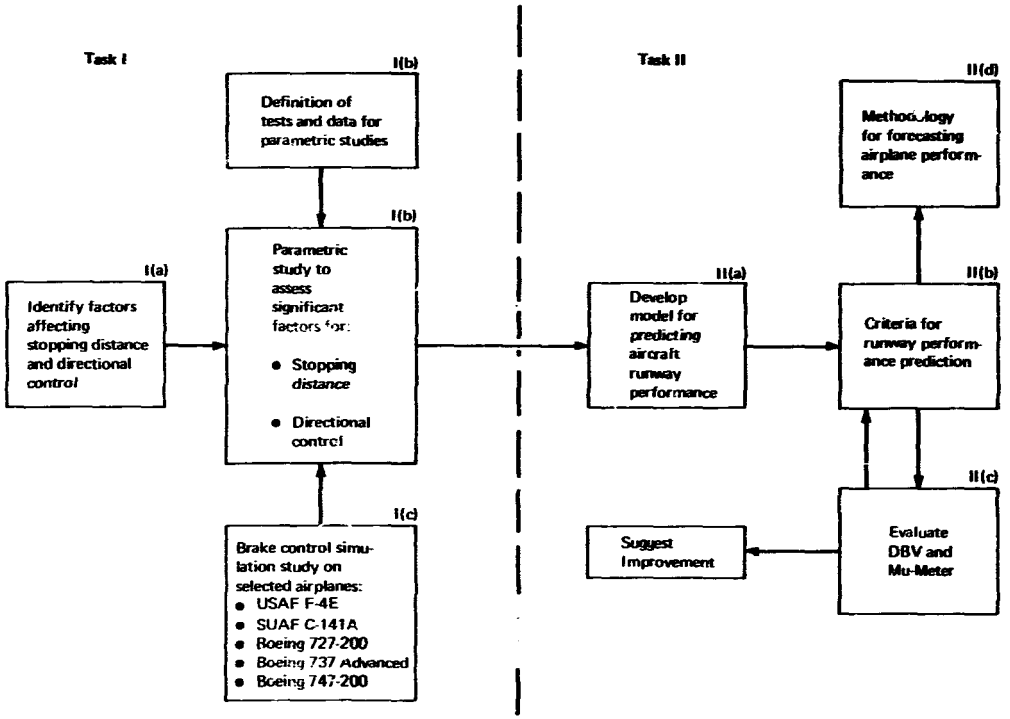

Figure 1.—Basic Program Plan

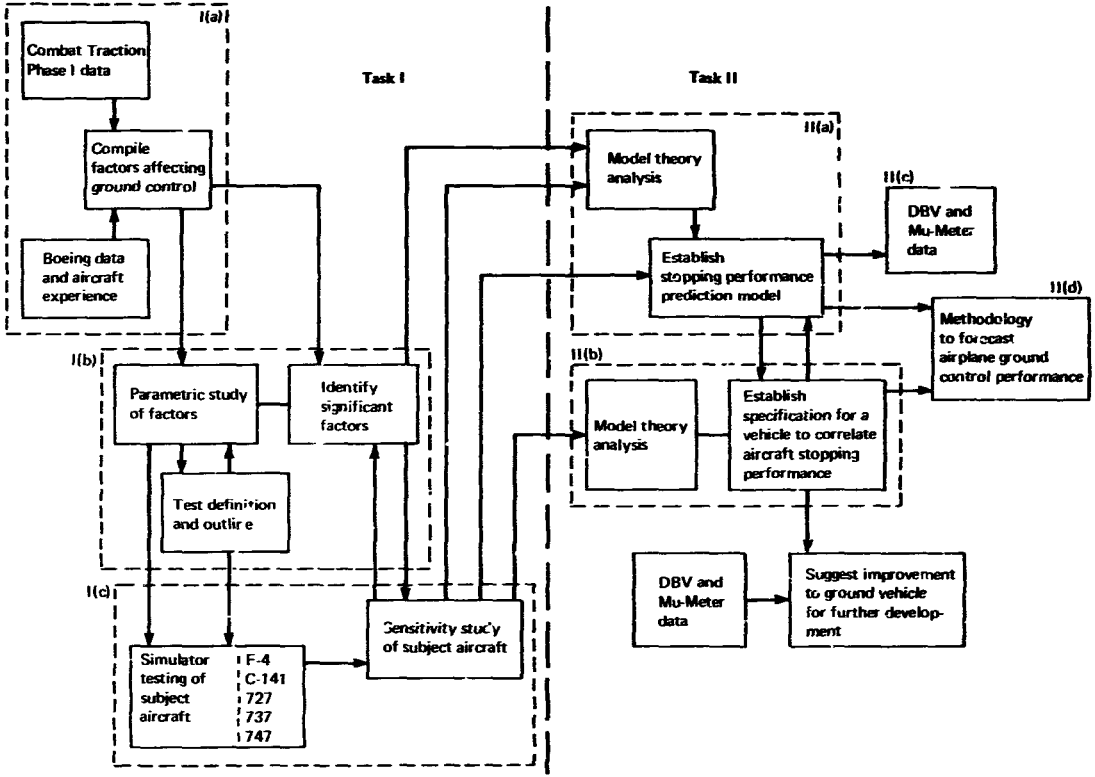

Figure 2.—Basic Program Technical Approach

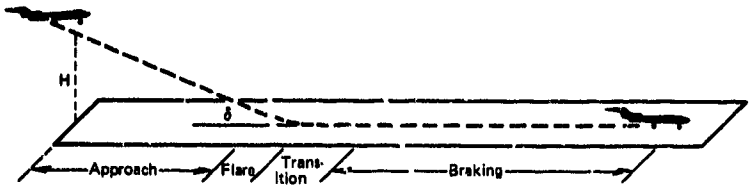

Figure 3.—Landing Segments

Distances from the threshold to touchdown can be readily calculated by considering the individual segments of approach and flare, but a meaningful braking distance can be determined only with an airplane test or a brake control simulation. Because airplane testing is expensive and time-consuming, the simulator is a useful tool, both to evaluate different antiskid systems and to analyze sensitivity where each parameter must be closely controlled. Results of a series of simulator tests can be applied to a dimensional analysis because only one influencing parameter is varied at a time. The goal of the dimensional analysis is the development of a braking distance prediction equation. This equation must include all variables having a significant influence on braking distance during the normal operation of military and commercial aircraft.

Statistical curve fitting techniques can be applied to develop a relationship (or equation) between the dependent and any other independent variable while all other parameters are held constant. This process is repeated for each variable. These component equations can then be combined to form a prediction equation, provided the necessary and sufficient conditions generated during the analysis are met.

The Diagonally Braked Vehicle (DBV) and the Mu-Meter are two ground vehicles in use today to evaluate runway friction conditions. Various methods have been explored and applied in an attempt to correlate the measured ground vehicle data to airplane braking distance. With the use of a dimensional prediction equation, the vehicles can be compared to the dimensional groups. Vehicle usefulness or modification to satisfy the dimensional prediction equation can be assessed.

SECTION II

IDENTIFICATION OF PARAMETERS

Accurate prediction of aircraft stopping distance requires that all significant parameters be taken into account. The many parameters determining aircraft stopping distance have been divided into groups based on the nature of the parameter or the system the parameter affects. The three major groups identified are:

- Airplane flight characteristics
- Runway and environmental system
- Landing gear system

A detailed list of parameters associated with these groups is given in Table 1. The following brief descriptions of the major groups explain the significance of some of the parameters listed in Table 1.

1. AIRPLANE FLIGHT CHARACTERISTICS

The airplane system is the mass being stopped. As such, it provides the inertial, propulsive, and aerodynamic forces that determine the amount of energy to be dissipated by the brakes. The airplane also affects braking in that tire loading is determined from airplane geometry, dynamics, and aerodynamics. The pilot affects stopping by determining the initial conditions of the aircraft.

2. RUNWAY AND ENVIRONMENTAL SYSTEM

The runway and environmental system consists of effects that influence the airplane stopping performance but are external to the aircraft. These include atmospheric conditions, altitude, temperature, runway slope, crown, surface roughness (micro- and macro-texture), material, and contamination.

3. LANDING GEAR SYSTEM

The landing gear system, as it affects stopping, consists of the structure, shock strut, and braking system. The structure transmits the forces developed between the tire and runway to the airplane, while the shock strut is the primary vertical energy absorption system on the airplane. The flexibility and damping characteristics of the structure and the dynamic characteristics of the shock strut have a pronounced effect on stopping system performance. The braking system, consisting of the wheels, brakes, tires, control system, and brake hydraulics, is of primary importance in determining the ground distance. Changes to the braking system will vary the rate and magnitude of kinetic energy transfer

Table 1.—Parameters Influencing Stopping Distance

I. AIRPLANE FLIGHT CHARACTERISTICS

1. Aerodynamics
   a. Brake application speed
   b. Aerodynamic coefficients (lift and drag)
   c. Spoiler deployment rate and effectiveness
   d. Engine idle and spindown thrust

2. Geometry
   a. Center-of-gravity location
   b. Landing gear placement
   c. Airplane weight
   d. Airplane mass moment of inertia
   e. Wing stiffness

3. Operational characteristics
   a. Route structure
   b. Pilot braking technique

II. RUNWAY AND ENVIRONMENTAL SYSTEM

4. Runway
   a. Roughness (micro- and macro-texture)
   b. Contamination
   c. Slope
   d. Crown
   e. Mu

5. Atmospheric
   a. Ambient temperature
   b. Pressure altitude
   c. Wind

III. LANDING GEAR SYSTEM

A. Brake System
   – Brake Actuation System

6. Mechanisms
   a. Pedal crank mechanical advantage
   b. Actuation mechanism mechanical advantage
   c. Mechanism detailed design
   d. Cable length
   e. Cable stiffness
   f. Cable preload

Table 1.–Parameters Influencing Stopping Distance (Continued)

III. LANDING GEAR SYSTEM (Continued)

7. Hydraulics
   a. Hydraulic pump capacity
   b. Pump recovery rate
   c. Accumulator pressure volume characteristics
   d. Fluid bulk modulus
   e. Fluid viscosity
   f. Fluid density
   g. Fluid temperature coefficients
   h. Brake line length
   i. Brake line stiffness
   j. Brake line diameter
   k. Flow restrictions
   l. Hydraulic fuse type
   m. Bleeding characteristics
   n. Return line steady-state back pressure
   o. Return line transient back pressure
   p. Metering valve flow capacity
   q. Metering valve pressure gain

– Antiskid System

8. Wheel speed sensor
   a. Eccentricity
   b. Drive mechanism
   c. Stator mounting
   d. Electrical characteristics
   e. Drive angle
   f. Demodulator characteristics
   g. Sensor type
   h. Sensor detailed design

9. Electronics
   a. System type
   b. Detailed design

10. Servo valve
   a. Valve type
   b. First-stage type
   c. Flow gain
   d. Detailed design
   e. Lapping

– Wheel, Brake, and Tire System

11. Wheel and Brake
   a. Pressure volume characteristics

Table 1.—Parameters Influencing Stopping Distance (Concluded)

III. LANDING GEAR SYSTEM (Continued)

- b. Lining characteristics
- c. Brake detailed design
- d. Heat sink loading
- e. Heat transfer characteristics
- f. Retractor spring pressure
- g. Wear adjusters
- h. Brake mounting system
- i. Wheel design

12. Tire

- a. Footprint area
- b. Inflation pressure
- c. Fore and aft stiffness
- d. Vertical stiffness
- e. Lateral stiffness
- f. Mass
- g. Inertia
- h. Tread pattern
- i. Thermal properties
- j. Rolling resistance
- k. Diameter
- l. Damping characteristics
- m. Wear

B. Shock Strut and Structure

13. Strut

- a. Fore and aft stiffness
- b. Strut mass
- c. Strut effective mass
- d. Fore and aft damping
- e. Vertical stiffness
- f. Metering pin design
- g. Torsional stiffness
- h. Torsional damping
- i. Tolerances
- j. Strut geometry

14. Truck

- a. Mass
- b. Inertia
- c. Truck unbalance

SECTION III

STOPPING DISTANCE DERIVATION

1. AIR AND TRANSITION DISTANCE

Approach, flare, and transition distances are important when considering total stopping distance. The major factors that affect the actual distances involved in these segments are:

- Approach velocity
- Glide slope
- Height above threshold
- Flare load factor
- Time to brake application
- Aircraft deceleration

A digital program was used to analyze the effect of these parameters on stopping distance. Figures 4 through 7 summarize the typical variations in distance that can be expected from a parameter change. The results shown are general and applicable to any aircraft by appropriate variable selection. Figures 4 and 5 point out that glide slope and height above the threshold can cause the approach distance to vary by as much as 250%, while the flare load factor and approach velocity can cause flare distance variations of 300%. The transition distance is primarily a function of approach speed, aircraft deceleration, and time to brake application. Figure 6 indicates that delaying brake application can result in the loss of significant runway length, however reasonable variations in approach speeds do not result in large distance changes. Figure 7 shows that reasonable changes in aircraft deceleration do not cause significant distance variations.

The six factors previously listed are only a partial list of parameters affecting the air and transition distances. Other influencing parameters involve aerodynamic values, the landing gear system, airplane configuration, and environmental factors. These parameters do not, however, cause significant variations in air and transition distances. The significant factors (approach velocity, glide slope, height above the threshold, flare load factor, and time to brake application) are parameters that reflect pilot technique. Because pilot technique is the major factor involved in the determination of air and transition distance, the prediction of total stopping distance is difficult; therefore, the only parametric changes pursued during this program were those involved in the braking portion of the stop. The data scatter resulting from variations in pilot technique can, however, be used to develop advisory information for aircraft operation, which was outside the scope of this program.

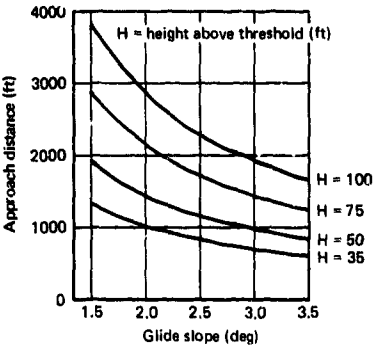

Figure 4.—Approach Distance vs Glide Slope

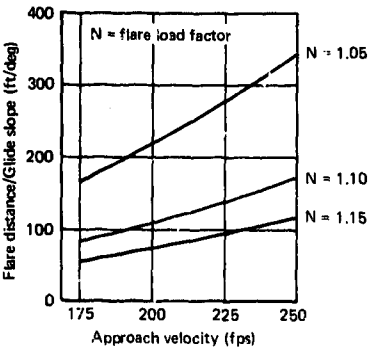

Figure 5.—Flare Distance vs Approach Speed

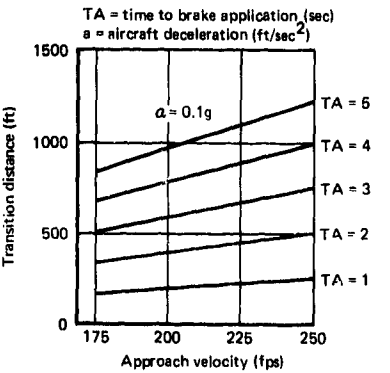

Figure 6.—Transition Distance vs Approach Speed vs Time to Brake Application

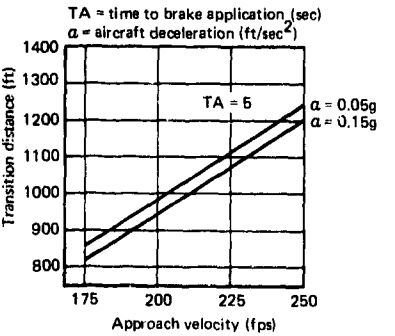

Figure 7.—Transition Distance vs Approach Speed vs Aircraft Deceleration

A summary of the equations used to calculate the approach, flare, and transition distances is given in Appendix A.

2. BRAKING DISTANCE

The brake control simulation (Ref. 1) used to calculate braking distance represents a refinement of an earlier baseline antiskid simulator used at Boeing.

The development of the advanced simulation is the result of many flight test programs Boeing has conducted in recent years. In addition NASA, FAA, and USAF data from recent Boeing 727, F-4, and C-141 aircraft tests was reviewed. Flight test data has been directly compared with simulator and airplane control system tests. The outgrowth of the program has led to many refinements and the development of more sophisticated models. As a result, the simulation more closely represents the airplane and can accurately evaluate the effect of various aircraft, brake, and skid control system parameters on stopping performance and landing gear stability. The payoffs from this undertaking are already incorporated in the 737 Advanced, Advanced 727, and Improved 747F skid control systems.

The simulator is an analog-hardware system consisting of three analog computers simulating the aircraft dynamics and a brake hydraulic system mockup. All actual hydraulic system parts that influence brake system performance are incorporated. In addition, a skid control card or box is used. In this way, the electronic and hydraulic characteristics, which may include nonlinearities, are accurately reproduced.

The computer simulation consists of five interrelated elements: (1) airplane dynamics, (2) strut dynamics, (3) wheel dynamics, (4) brake torque, and (5) ground force. The interrelation of these elements and the hardware portion of the simulation are shown in Figure 8. The basic airplane dynamics include airplane pitching, aerodynamic lift and drag, engine idle thrust, and tire-to-ground forces. Also included are detailed simulations of the landing gear strut and the tire-wheel dynamics. Multiple wheel braking is also provided in the simulation.

Although the actual brake is used to determine the pressure-volume characteristics, the pressure torque relationship is simulated on the computer using the pressure feedback information from the actual brake. The brake simulation also includes steady-state torque gain, retractor spring deadband, torque fade, torque peaking, and frequency response. The analytical models used were derived as a result of many hardware tests conducted at brake vendor facilities and tests conducted at AFFDL Landing Gear Test Facility on two different occasions.

A detailed description of the Boeing Brake Control Simulation is given in Appendix B.

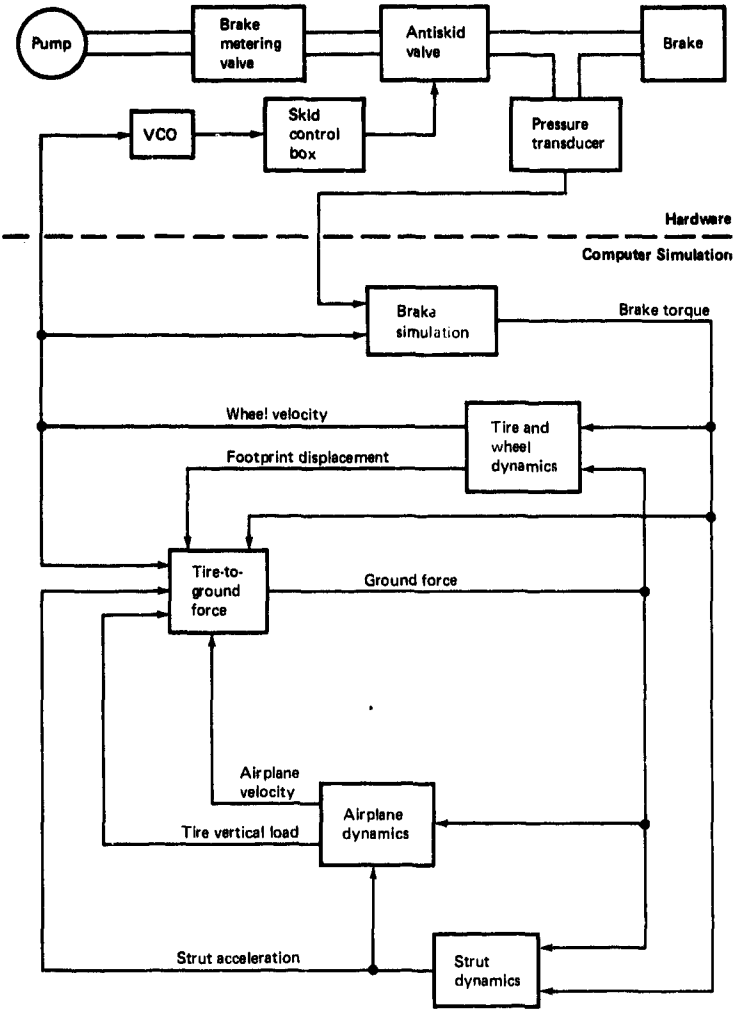

Figure 8.–Simulator Block Diagram

SECTION IV

SENSITIVITY STUDY TEST PROCEDURE

The objective of the sensitivity study was to determine the parameters that influence stopping distance. To properly assess the parameters and draw some general conclusions, five aircraft were studied. The Lockheed-Georgia C-141A, McDonnell-Douglas F-4E, Boeing 747-200, Boeing 737 Advanced, and Boeing 727-200 were chosen, with NASA, FAA, and USAF concurrence.

The data used in the brake control simulator for the Boeing airplanes (727, 737, 747) is well documented within The Boeing Company. It represents a compilation of the currently accepted data used in various Boeing airplane simulators and was checked for accuracy to ensure the reliability of the results obtained from the computer study. Data for the F-4 and the C-141 were obtained from the USAF. This data was reduced to the form required for use in the simulation. Note that this report generally uses a shortened form of the aircraft designations. As used, the short terms are synonymous with the specific model designations.

As a starting point, a baseline airplane was defined for each aircraft. The baseline airplane represents an aircraft in a three-point taxi attitude and of typical (mid-range) landing weight, approach speed, center-of-gravity location, landing flap setting, and engine thrust. The actual parameters required for the airplane simulator are defined in Table 2. Table 3 lists the baseline values used for each airplane.

During the sensitivity study each parameter was changed and the new value of braking distance was evaluated on the simulator. The range over which a parameter was varied reflected values observed in normal service of the airplane. Some of the variables were not independent, and those groups of interrelated parameters were varied appropriately together. An example of this is stall speed and gross weight.

The results of the parametric study are valid for the purpose of this program and contribute a whole new dimension to the state of knowledge for developing more efficient stopping systems and more precise methods of predicting aircraft stopping performance. The parameters are, however, not varied in this manner in real life; therefore, the results should not be misused to judge operational performance of any aircraft studied.

Table 2.–Definition of Simulator Parameters

Parameter	Definition	Unit
	Airplane Parameters	
AW	Effective wing area	ft^2
CD	Drag coefficient	
CDD	Drag coefficient without spoilers	
CL	Lift coefficient	
CLD	Lift coefficient without spoilers	
FEO	Engine idle Thrust at zero velocity	lbf
HB	Height of CG above ground	ft
IYY	Mass moment of inertia, pitch	$ft\text{-}lb\text{-}sec^2$
KE	Change of idle thrust with velocity	lbf-sec/ft
LA	Nose gear to CG distance	ft
LB	Main gear to CG distance	ft
NB	Number of brakes per main strut	
NBA	Number of main gear brakes per airplane	
NBN	Number of nose gear wheels	
NS	Number of main gear struts per airplane	
RHO	Air density	$lbf\text{-}sec^2/ft^4$
VI	Initial airplane velocity	ft/sec
VSTOP	Final airplane velocity	ft/sec
WA	Weight of airplane	lbf
	Brake Parameters	
KP	Torque peaking gain	
MB	Mass of brake heat sink	lbm
OMGP	Wheel velocity at start of torque peaking	rad/sec
PC	Retractor spring pressure	psi
TBG	Torque gain	ft-lbf/psi
THBB	Temperature at initiation of fade	^oF
WN	Natural frequency of torque response	Hz
ZETA	Damping ratio of torque response	
	Tire Parameters	
D	Tire diameter	in.
DO	Tire deflection	in.
IW	Mass moment of inertia of tire, wheel, and brake	$ft\text{-}lbf\text{-}sec^2$

Table 2.–Definition of Simulator Parameters (Concluded)

Parameter	Definition	Unit
	Tire Parameters (Continued)	
PI	Tire operating inflation pressure	psi
PR	Tire rated inflation pressure	psi
RR	Tire rolling radius	ft
RT	Tire torque radius	ft
	Strut Parameters	
CO	Main gear vertical damping coefficient	lbf-sec/ft
CON	Nose gear vertical damping coefficient	lbf-sec/ft
CS	Main gear fore-aft damping coefficient	lbf-sec/ft
CT	Torsional Damping between strut and brake	lbf-ft-sec
IS	Mass moment of inertial of main gear strut	ft-lbf-sec^2
KO	Main gear vertical stiffness	lbf/ft
KON	Nose gear vertical stiffness	lbf/ft
KS	Main gear fore-aft stiffness	lbf/ft
L	Effective strut length	ft
MS	Effective mass of strut	lbf-sec^2/ft

Table 3.—Baseline Parameter Values Used in Airplane Simulation

Parameter	Unit	Airplane Model				
		727-200	737 Advanced	747-200	C-141A	F-4E
Airplane Parameters						
AM	ft^2	1560	980	5500	3228	530
CD		.293	.275	.18	.223	.32
CDD		.167	.194	.13	.115	.11
CL		.140	.242	.67	.262	.27
CLD		1.36	1.51	1.15	1.10	.27
FEO	lbf	2475	1200	9480	3600	1260
HB	ft	10.8	7.1	16.9	11.0	5.8
IYY	$ft\text{-}lb\text{-}sec^2$	2.75×10^6	1.22×10^6	2.21×10^7	4.62×10^6	1.09×10^5
KE	$lbf\text{-}sec/ft$	-6.37	2.0	17.1	-6.94	-4.9E
LA	ft	49.5	33.5	78.5	48.0	19.7
LB	ft	3.73	3.8	4.45	5.25	3.6
NB		2	2	4	4	1
NBA		4	4	16	8	2
NEN		2	2	2	2	2
NS		2	2	4	2	2
RHO	$lbf\text{-}sec^2/ft^4$	.00238	.00238	.00238	.00238	.00238
VI	ft/sec	195	173	219	200	256
VSTOP	ft/sec	24	24	24	24	24
WA	lbf	185000	85000	510000	260000	35000
Brake Parameters						
KP		1.25	1.25	1.25	1.25	1.25
MB	lbm	211	117	220	138	124
OMGP	rad/sec	14.8	17.0	33.0	20.0	29.7
PC	psi	65	150	300	200	200
TBO	ft-lbf/psi	16.5	5.83	10.0	13.6	3.50
TMAX	^0F	400	600	1000	650	1000
WN	Hz	40	60	40	40	40
ZETA		.707	.875	.707	.707	.707
Tire Parameters						
D	in	48.31	39.40	44.5	43.25	29.47
DO	in	3.5	3.25	3.5	2.9	1.70
IW	$ft\text{-}lbf\text{-}sec^2$	20.7	7.0	16.0	12.4	2.71
PI	psi	165	150	209	175	230
PR	psi	170	155	210	185	242
RR	ft	1.91	1.57	1.76	1.72	1.16
RT	ft	1.68	1.40	1.58	1.50	1.02
Strut Parameters						
CO	$lbf\text{-}sec/ft$	15340	15450	8000	7490	00
CON	$lbf\text{-}sec/ft$	1210	9640	8000	1680	1170
CS	$lbf\text{-}sec/ft$	1346	175	1272	200	200
CT	$lbf\text{-}ft\text{-}sec$	177	178	1000	200	200
IS	$ft\text{-}lbf\text{-}sec^2$	1.76	1.4	4.66	3.1	0.8
KO	lbf/ft	105900	533000	337000	107000	73000
KON	lbf/ft	42150	74800	92400	56000	39200
KS	lbf/ft	305000	153000	257000	1262000	163200
L	ft	5.82	5.17	10.8	4.4	3.74
MS	$lbf\ sec^2/ft$	44.88	29.28	181.2	80.0	12.75

SECTION V

SENSITIVITY STUDY TEST CONDITIONS

The sensitivity study involved changing a parameter or group of parameters to analyze its influence on stopping distance. Based on the factors listed in Table 1, a set of test conditions was formulated. The test conditions, as listed in Table 4, were performed on the analog-hardware simulator to analyze braking distance. Table 5 lists the parameters changed and the numerical value of the parameters associated with each test condition for the five aircraft.

A test outline was proposed to NASA, FAA, and USAF and, with their concurrence, nine sensitivity tests were formulated to analyze the sensitivity of the various aircraft systems to a parameter change. The tests were performed selectively at each test condition. The nine sensitivity tests have been divided into three major categories. The categories and the tests associated with each are as follows:

- Stability studies:

  Test 1–strut stability

- Performance studies:

  Test 2–touchdown dynamics

  Test 3–stabilized landing

  Test 4–mu steps

  Test 5–wet runway

- Hydraulic system studies:

  Test 6–frequency response

  Test 7–step response

  Test 8–antiskid valve characteristics

  Test 9–brake pressure and volume characteristics

A detailed description of the test procedure and sequence can be found in ASD-TR-74-41, Volume II, Section IX. The three major categories of sensitivity tests are briefly described below to point out their general significance.

Table 4.—Test Conditions

Baseline Study

Nominal values of all parameters

Parametric Studies

Airplane

1. Weight
   a. Maximum landing
   b. Minimum landing
2. Center of Gravity
   a. High
   b. Low
   c. Forward
   d. Aft
3. Brake application speed
   a. +10%
   b. +20%
4. Aerodynamics
   a. Spoiler or drag chute deployment – 1.0 sec after touchdown
   b. Spoiler or drag chute deployment – 2.0 sec after touchdown
   c. No spoilers or drag devices
   d. 60% effective spoilers
   e. 40% effective spoilers
   f. 120% engine idle thrust
   g. 80% engine idle thrust
5. Pilot technique
   a. 150% nominal pressure application rate
   b. 50% nominal pressure application rate
   c. Nominal rate at 2.0 sec from touchdown
   d. Nominal rate at 4.0 sec from touchdown
   e. 75% of full metered pressure
   f. 50% of full metered pressure

Runway and environmental system

1. Wind
   a. 10 knots
   b. 20 knots
   c. -10 knots

Table 4.—Test Conditions (Continued)

Parametric Studies (Continued)

Runway and environmental system (continued)

2. Air density
   a. Hot day (83°F – 28°C), high altitude (5000 ft)
   b. Cold day (-60°F – -51°C) sea level

3. Runway
   a. Roughness profile

Landing gear systems

1. Brake torque characteristics
   a. High fade brake – 80% MB (only 0.4 mu and greater)
   b. Low fade brake – 90% MB (only 0.4 mu and greater)
   c. Peaking to 150% of running
   d. No peaking
   e. Torque response breakpoint – 150% of nominal
   f. Torque response breakpoint – 50% of nominal
   g. Torque gain 120% of nominal
   h. Torque gain 80% of nominal
   i. Variable torque gain $T = f(p)^{0.5}$
   j. Linear torque gain $T = f(p)$

2. Tire
   a. Inflation pressure 120% of nominal
   b. Inflation pressure 80% of nominal
   c. 50% worn tire
   d. 80% worn tire
   e. Low tire heating
   f. Flat μ-σ peak

3. Strut
   a. Maximum strut frequency varying mass
   b. Minimum strut frequency varying mass
   c. Maximum strut frequency varying stiffness
   d. Minimum strut frequency varying stiffness
   e. Vertical stiffness 120% of nominal
   f. Vertical stiffness 80% of nominal
   g. Vertical damping 120% of nominal
   h. Vertical damping 80% of nominal

Table 4.—Test Conditions (Concluded)

Parametric studies (continued)
Hydraulic system
a. Decrease line diameter 50% (nearest diameter)
b. Increase line diameter 50% (nearest diameter)
c. Move dynamic breakpoint out 150% of nominal (line length change)
d. Move dynamic breakpoint in 50% of nominal (line length change)
e. Insert 20% restriction in return line
f. Increase brake volume by 10 cu in.
g. Increase brake p-v gain

Table 5.—Parameter Change Values

Test condition and parameter changed	Airplane model				
	727	737	747	C-141	F-4
Airplane Parameters					
1a Maximum Landing Weight					
WA	137900	103000	564000	300000	46000
VI	808	188	811	818	898
ITY x 10^{-6}	8.65	1.19	86.4	4.89	.113
1b Minimum Landing Weight					
WA	100000	70000	400000	180000	30000
VI	174	166	184	167	237
ITY x 10^{-6}	8.33	1.036	88.8	4.16	.1074
2a High Center of Gravity					
XB	•	7.68	•	•	•
2b Low Center of Gravity					
XB	•	6.89	•	•	•
3a Forward Center of Gravity					
% MAC	12	9	16	16.4	98
LA	47.6	31.86	76.0	49.9	19.3
LB	5.66	5.47	6.99	7.38	1.98
ITY x 10^{-6}	2.65	1.16	34	4.89	.1117
3d Aft Center of Gravity					
% MAC	34	33	33	31	31
LA	90.9	35.82	80.7	49.1	19.9
LB	8.35	7.11	8.85	4.13	1.44
ITY x 10^{-6}	3.07	1.18	38.9	5.14	.1071
3e Brakes on Speed - 10%					
VI	814	190.1	830	880	888
3h Brakes on Speed - 80%					
VI	834	807.6	841	840	308
4a Spoiler/Drag Device Deployment	1.0 Second After Touchdown				
4b Spoiler/Drag Device Deployment	2.0 Second After Touchdown				
4c No Spoiler/Drag Device					
CL	1.36	1.512	1.15	1.10	.87
CD	.167	.194	.1317	.1145	.11
4d 60% Effective Spoilers					
CL	.688	.768	.868	.597	.87
CD	.2186	.242	.1607	.179	.888
4e 40% Effective Spoilers					
CL	.878	1.003	.958	.761	.87
CD	.2014	.216	.151	.138	.198
4f 120% Engine Idle Thrust					
FNO	2970	1440	11375	4380	1510
KN	+5.1	2.4	20.5	-5.55	+4.0
4g 80% Engine Idle Thrust					
FNO	1980	960	7584	2880	1010
KN	+7.65	1.6	13.7	-8.33	+6.0
5a 150% Nominal Pressure Application Rate Rev-					
Time to Full Pressure (sec)	.2	.2	.2	•	.2
5b 50% Nominal Pressure Application Rate					
Time to Full Pressure (sec)	.6	.6	.6	.	.6
5c Nominal Pressure Rate at 2.0 Seconds From Touchdown	Delay Brake Pressure Application 2 Seconds				
5d Nominal Pressure Rate at 4.0 Seconds From Touchdown	Delay Brake Pressure Application 4 Seconds				
5e 75% of Full (Pilot) Metered Pressure					
5f 50% of Full (Pilot) Metered Pressure					
Runway and Environmental System					
1a 10 Knot Wind VW	16.8	16.8	16.8	16.8	16.8
1b 20 Knot Wind VW	33.7	33.7	33.7	33.7	33.7
1c -10 Knot Wind VW	-16.8	-16.8	-16.8	-16.8	-16.8
2a Wet Day RHO	.00189	.00186	.00189	.00189	.00189
2b Cold Day RHO	.00309	.00309	.00309	.00309	.00309
3a Rough Surface	Insert Runway Profile				

Table 5.—Parameter Change Values (Continued)

Test condition and parameter changed	Airplane model				
	727	727	747	C-141	F-4
Landing Gear Systems					
1a High Pedo Brake MB	169	93.6	176	110	99
1b Low Pedo Brake MB	190	109.3	198	131	111
1c Torque Peaking to 150% of Running KP	1.5	1.5	1.5	1.5	1.5
1d No Torque Peaking KP	1.0	1.0	1.0	1.0	1.0
1e Torque Response Break Point 150% Nominal MB	Infinity	Infinity	Infinity	Infinity	Infinity
1f Torque Response Break Point 50% Nominal MB	80	90	80	80	80
1g Torque Gain 120% of Nominal TMO	19.79	8.0	12.0	18.69	4.8
1h Torque Gain 80% of Nominal TMO	13.15	5.34	8.0	12.47	2.8
1i Variable Torque Gain $T=F(p)^{.5}$	Change Torque - Pressure Relation				
1j Linear Torque Gain $T=F(p)$	Change Torque - Pressure Relation				
2a Tire Inflation Pressure 120% of Nominal	Change Mu-Slip Curve				
2b Tire Inflation Pressure 80% of Nominal	Change Mu-Slip Curve				
2c 50% Worn Tire IW RT RR	19.89 1.66 1.87	6.41 1.35 1.53	14.8 1.938 1.77	11.44 1.46 1.68	2.28 .98 1.11
2d 80% Worn Tire IW RT RR	17.72 1.61 1.84	5.81 1.33 1.50	11.67 1.91 1.7	10.93 1.43 1.65	2.09 .75 1.09
2e Low Tire Heating	Change Mu-Slip Curve				
2f Flat u-s Peak	Change Mu-Slip Curve				
3a Maximum Strut Frequency Varying Mass Strut Frequency (cps) MS	18 24.1	15 14.4	10.5 59	24 55.-	20 10.1
3b Minimum Strut Frequency Varying Mass Strut Frequency (cps) MF	10 84.7	8 90.7	6 59 Rr=89000	15 142.0	16 16.9
3c Maximum Strut Frequency Varying Stiffness Strut Frequency (cps) KS	17 455000	13 260500	10.5 790000 MR=181.8	24 1819000	20 201000
3d Minimum Strut Frequency Varying Stiffness Strut Frequency (cps) KF	10 179000	8 74200	- -	13 710000	16 128800
3e Vertical Stiffness 120% of Nominal KO KOR	127080 50580	49600 19760	494400 110800	128200 67100	87600 47040
3f Vertical Stiffness 80% of Nominal KO KOR	84720 33720	42400 19840	269500 71800	85600 44800	58400 31360
3g Vertical Damping 120% Nominal CO COR	18400 1450	15990 11520	9600 9600	9000 2000	6120 1404
3h Vertical Damping 80% Nominal CO COR	12270 970	12170 7680	6400 6400	6000 1160	4080 936

Table 5.–Parameter Change Values (Concluded)

Test condition and parameter changed	Airplane model				
	727	737	747	C-141	F-4
Hydraulic system					
a. Decrease line diameter 50% Line diameter (in.)	0.250 0.250 hose	0.250 0.250 hose	*	0.250 0.250 hose	*
b. Increase line diameter 50% Line diameter (in.)	0.500 tube 0.500 hose	0.750 tube 0.500 hose	0.625 tube 0.500 hose	0.750 tube 0.500 hose	0.500 tube 0.500 hose
c. Move dynamic breakpoint out 150% of nominal (total line length from antiskid valve to brake)	4-ft hose	3-ft hose	10-ft hose	3-ft hose	4-ft hose
d. Move dynamic breakpoint in 50% of nominal (added line length from antiskid valve to brake)	10-ft tube	13-ft tube	15-ft tube	28-ft tube	40-ft tube
e. Insert 20% restriction in return line	Insert return line restriction				
f. Increase brake volume by 10 cu in.	Add 10 cu in. accumulator to brake				
g. Increase brake p-v gain	Replace brake with 10 cu in. accumulator				

*This test was not conducted. Further reduction in line diameter was deemed unreasonable.

1. STABILITY STUDIES

System stability is directly related to stopping performance. Severe instability can result in the loss of braking and can cause serious safety hazards. The study's purpose was to evaluate the ability of a brake control system to contribute to the stability of the gear.

2. PERFORMANCE STUDIES

The performance studies provide a measure of the performance capability of the brake system. The tests performed fall into two categories. The first defines the operation of the airplane under stable landing conditions. The second evaluates the ability of the brake system to adapt to the typical dynamic operating conditions encountered during an actual landing.

3. HYDRAULIC SYSTEM STUDIES

The hydraulic system studies measure the response of the antiskid valve, control box, and the actual brake hydraulic system. Specific tests were designed to define both the overall and component performance of the system. The results provide an insight into aircraft braking system performance and can be used to further improve some of the systems.

SECTION VI

TEST RESULTS

1. BASELINE

A baseline airplane was defined for each of the five aircraft studied. The baseline configuration is meant to represent a typical aircraft during its landing phase. The numerical values of the baseline parameters are listed in Table 3. The values, when used in the brake control simulation, establish a unique distance versus ground friction relation for each airplane.

Figure 9 relates the braking distance and peak available ground friction (peak available mu) for each of the five baseline airplanes. The data is associated with the braking segment only, so the distances shown represent only braked distances; approach, flare, and transition distances are excluded. For a skidding tire, the instantaneous coefficient of friction obtained at the tire-runway interface depends on the condition of the runway, aircraft characteristics, tire properties, and tire slippage. Thus, peak available mu (such as shown in Figure 9) is a computer input that defines the maximum value of friction available between the tire and ground during a test condition.

An ideal brake system should operate at the peak available friction value during the entire stop. However, the actual antiskid efficiencies realized are the result of component sizing and system characteristics and intergration. In addition, some compromises are necessary, so the system actually functions over a range of friction somewhat lower than the peak value. Since the actual antiskid system has been used in the brake control simulation the distances produced (Figure 9) reflect the efficiency of the braking system.

2. SENSITIVITY

The sensitivity study of the five airplanes involved changing a parameter, or group of parameters, and observing the effect on braking distance. The braking distance associated with a change was then compared to the baseline airplane distance at the same value of peak available mu. In this manner, the effect of a specific change could be analyzed quantitatively.

The braking data obtained from the brake control simulator represents an absolute distance. To facilitate the analysis of a parameter change, a normalized distance has been introduced. It is termed "baseline braking distance percentage." The use of a normalized distance allows the five airplanes to be compared simultaneously. The baseline braking distance percentage is the braking distance associated with a parameter change divided by the baseline braking distance at the same value of peak available mu; this quotient is then multiplied by 100% to obtain a percentage value.

Each airplane uses its own baseline distances as normalizing factors. Distances longer than baseline are greater than 100%, and shorter distances are reflected as less than 100%.

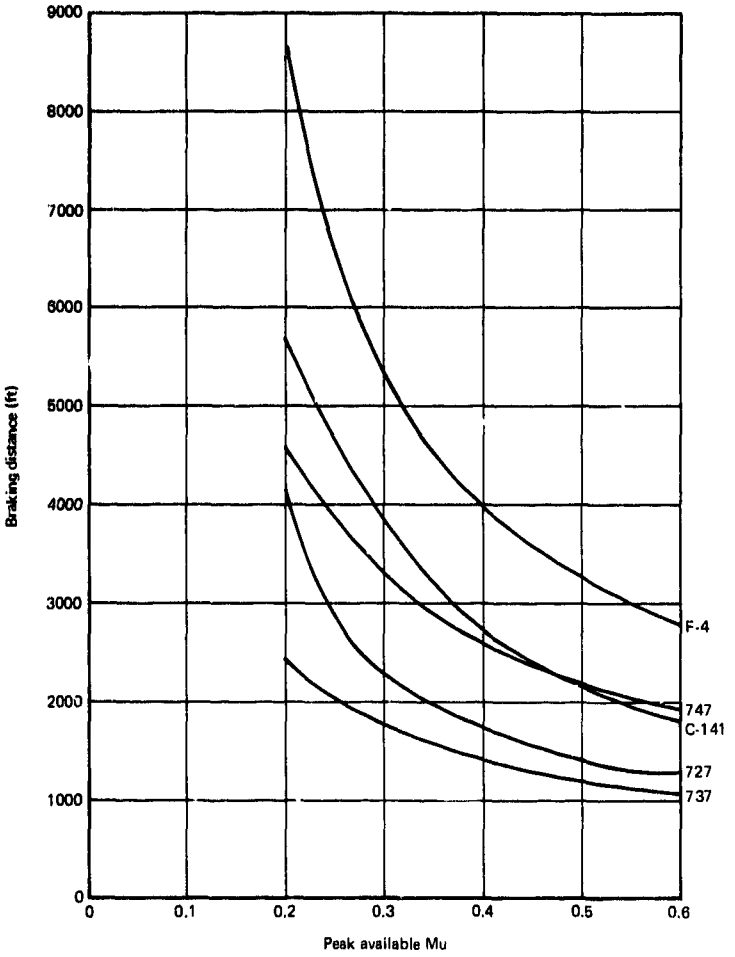

Figure 9.—Baseline Braking Distance vs Peak Available Mu

The braking distance results from the sensitivity study have been reduced to bar charts, Figure 10, Sheets 1 through 15. The test condition corresponding to each bar chart is given to the left and above the chart. On each graph, the baseline braking distance percentage for the five airplanes has been plotted for three values of peak available mu: 0.6, 0.4, and 0.2.

A brief analysis of the results follows. The raw data along with the associated performance indices can be found in ASD-TR-74-41, Volume II. Section X.

a. AIRPLANE FLIGHT CHARACTERISTICS

1. Landing Weight (1a and 1b, Sheet 1, Figure 10)

Three parameters were changed in these tests: landing weight, landing speed, and mass pitching moment. The landing speed was adjusted to reflect changes in stall speed resulting from variations in landing weight. The mass pitching moment was varied to reflect changes in load distribution. As shown in the bar charts, braking distance increases with an increase in gross weight. This results from the increased kinetic energy that must be dissipated during braking. The variation in distance is largely attributed to the increase in brake application speed. Additional tests indicated that the weight variation alone causes about a 3% variation in the baseline braking distance.

2. Center of Gravity

(a) High and Low Center of Gravity (2a and 2b, not diagramed).–High and low center of gravity tests were run on the Boeing 737. Initial digital computer studies showed this factor to be insignificant to braking distance, and actual tests with the 737 aircraft verified the prediction. As a result, these tests were deleted for the four remaining airplanes.

(b) Forward and Aft Center of Gravity (2c and 2d, Sheet 1, Figure 10).–Results show that aft location of center of gravity (CG) causes a decrease in braking distance. This results because more weight is placed on the main gear, increasing the available braking force. When analyzing CG location, steering requirements must also be considered. An increase in main gear load will result in loss of nose gear load and thus cornering capability. On wet runways, this situation warrants serious consideration, and some compromise is required.

The F-4 is the notable exception to the general trend. This airplane uses the Hydro-Aire Mark II system similar to the Boeing 727, though the choice of thresholds in the F-4 antiskid circuitry is different. As a consequence of this and system tuning, the F-4 antiskid system operates predominatly on the front side of the mu-slip curve. With more weight on the main gear, increased cycling of brake pressure occurs, which decreases system efficiency (mean effective pressure) and results in increased stopping distances. On the other hand, a forward CG location resulting in less weight on the main gear causes the system to cycle less often, thus increasing the system efficiency.

3. Brake Application Speed (3a and 3b, Sheet 2, Figure 10)

The brake application speed was varied to show the effect of a pilot making a "hot" landing. The results reflect the additional braking distance required to dissipate the increased kinetic

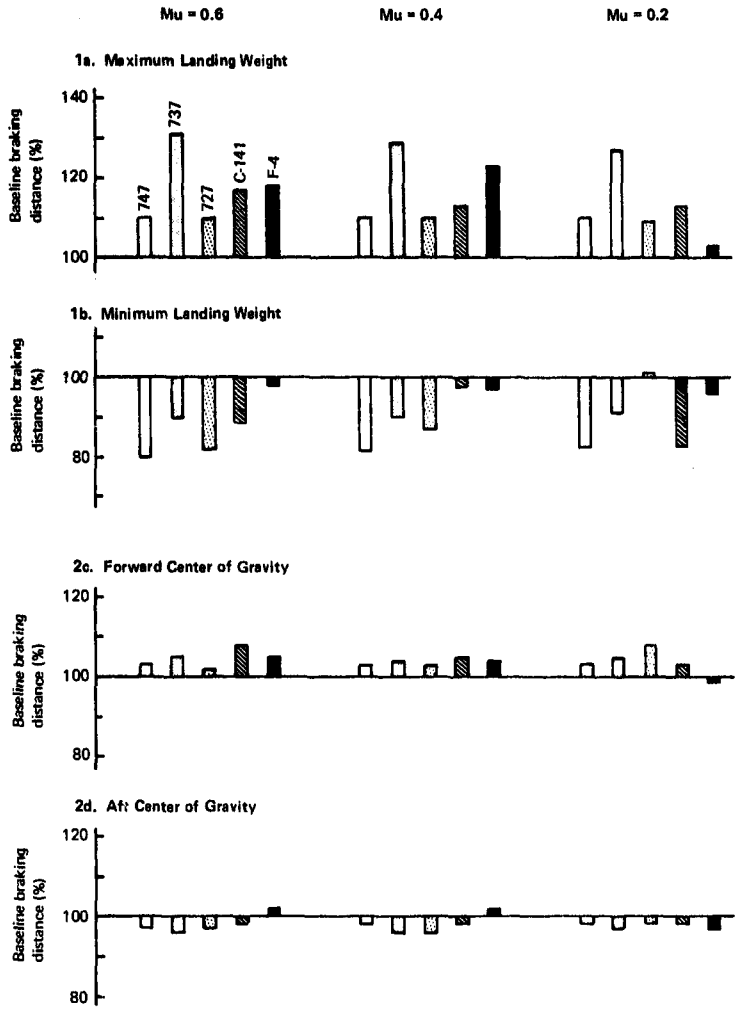

Figure 10.–Braking Distance Test Results (Sheet 1 of 15)

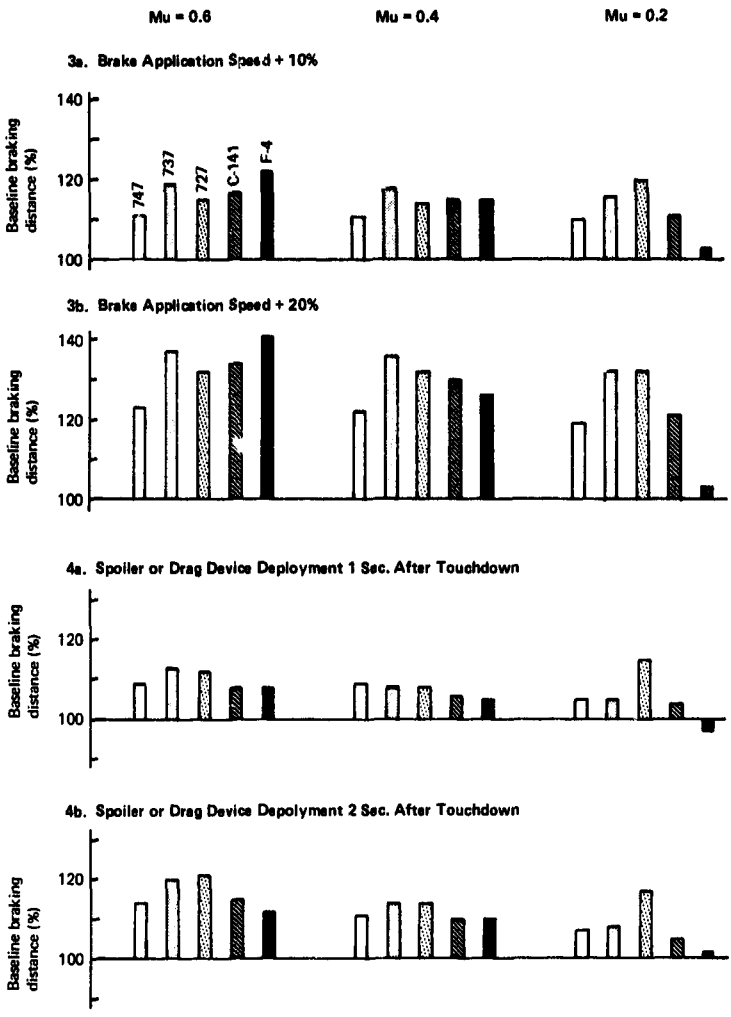

Figure 10.–Braking Distance Test Results (Sheet 2 of 15)

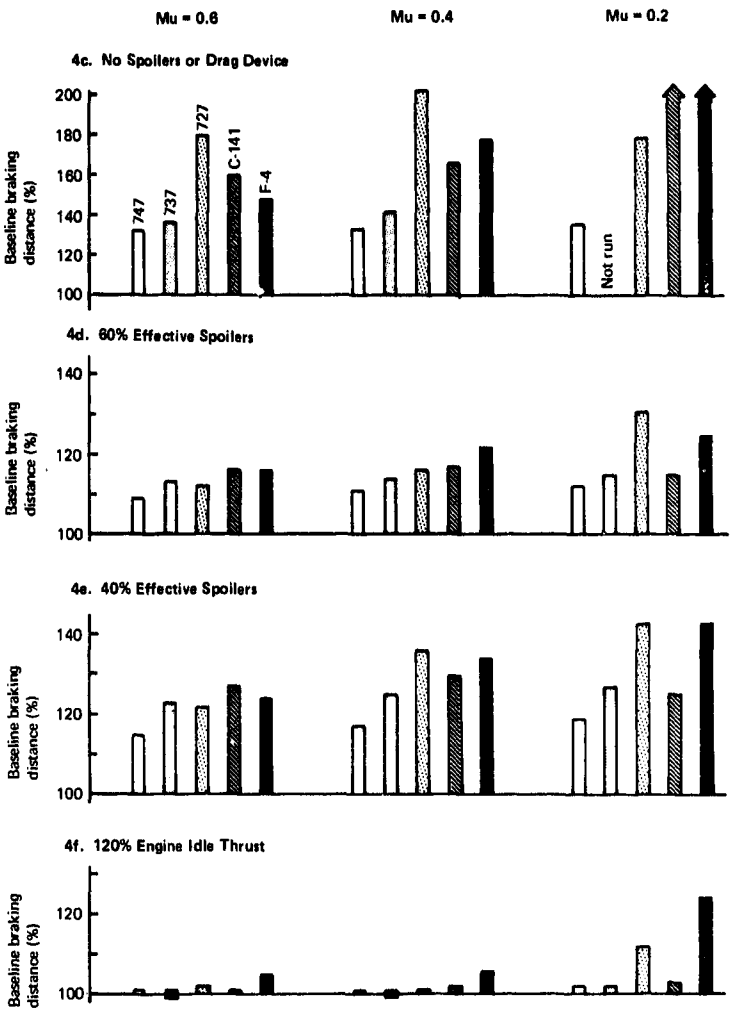

Figure 10.–Braking Distance Test Results (Sheet 3 of 15)

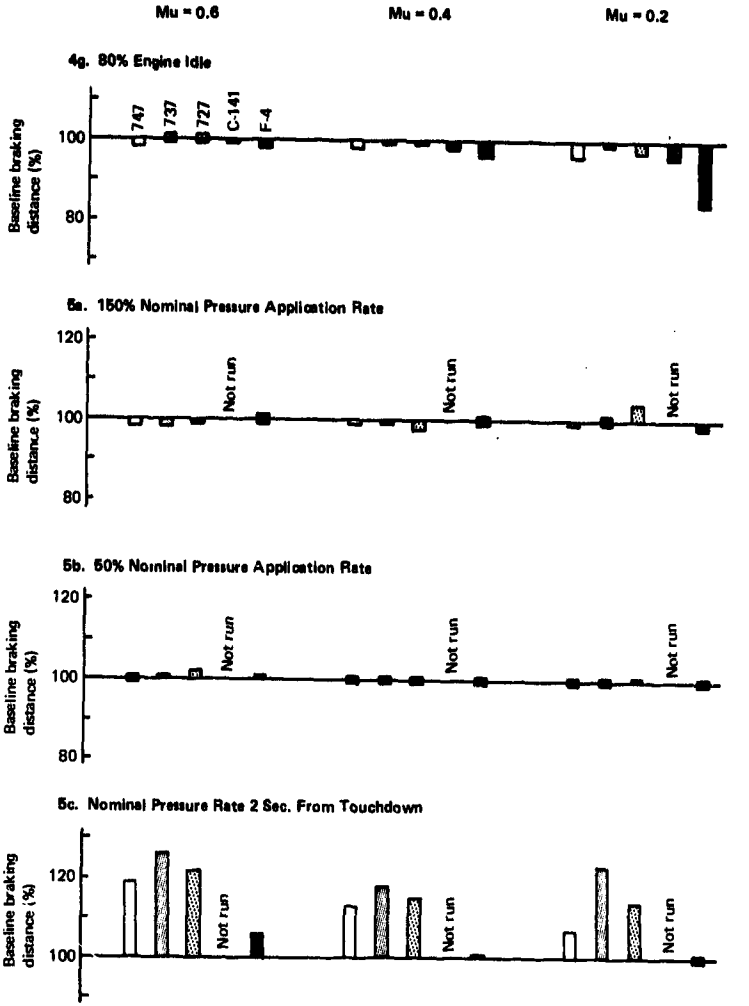

Figure 10.--Braking Distance Test Results (Sheet 4 of 15)

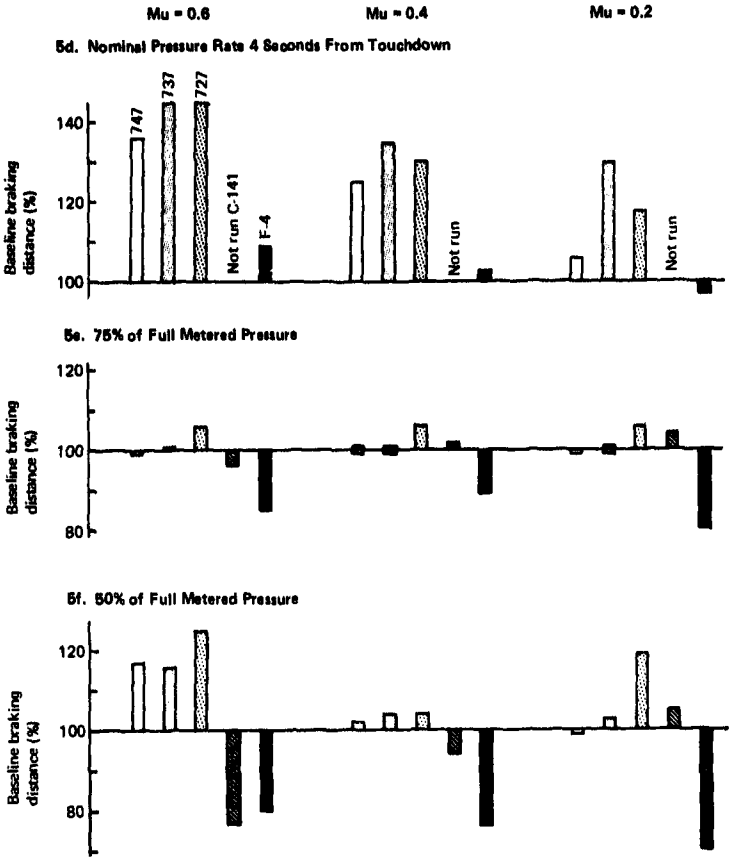

Figure 10.—Braking Distance Test Results (Sheet 5 of 15)

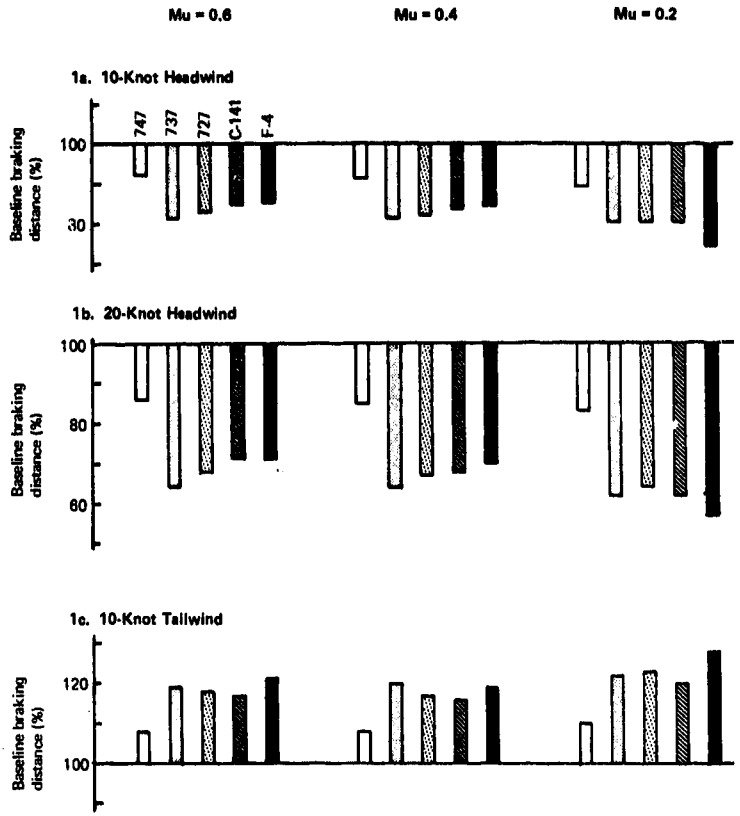

Figure 10.—Braking Distance Test Results (Sheet 6 of 15)

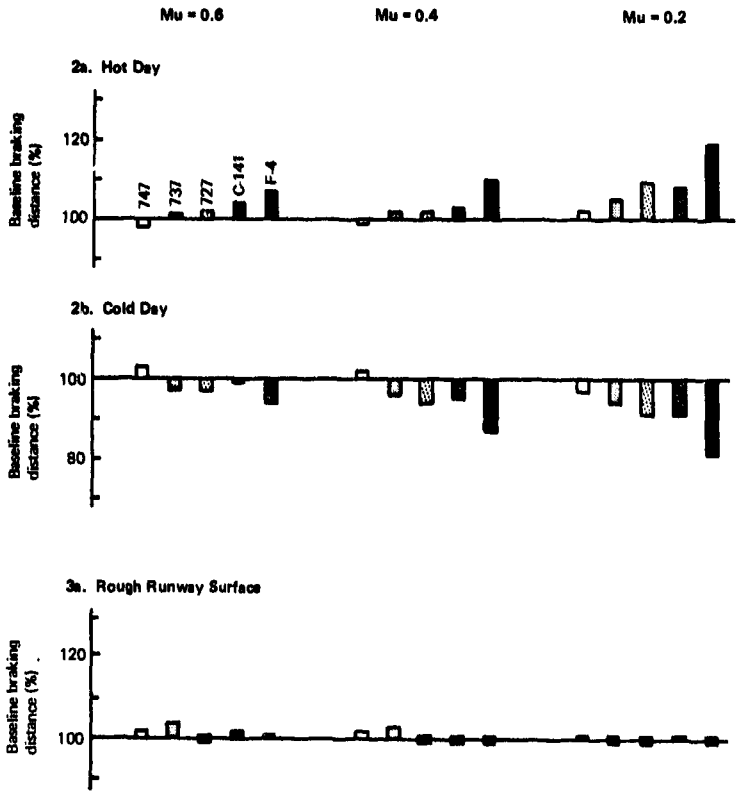

Figure 10.—Braking Distance Test Results (Sheet 7 of 15)

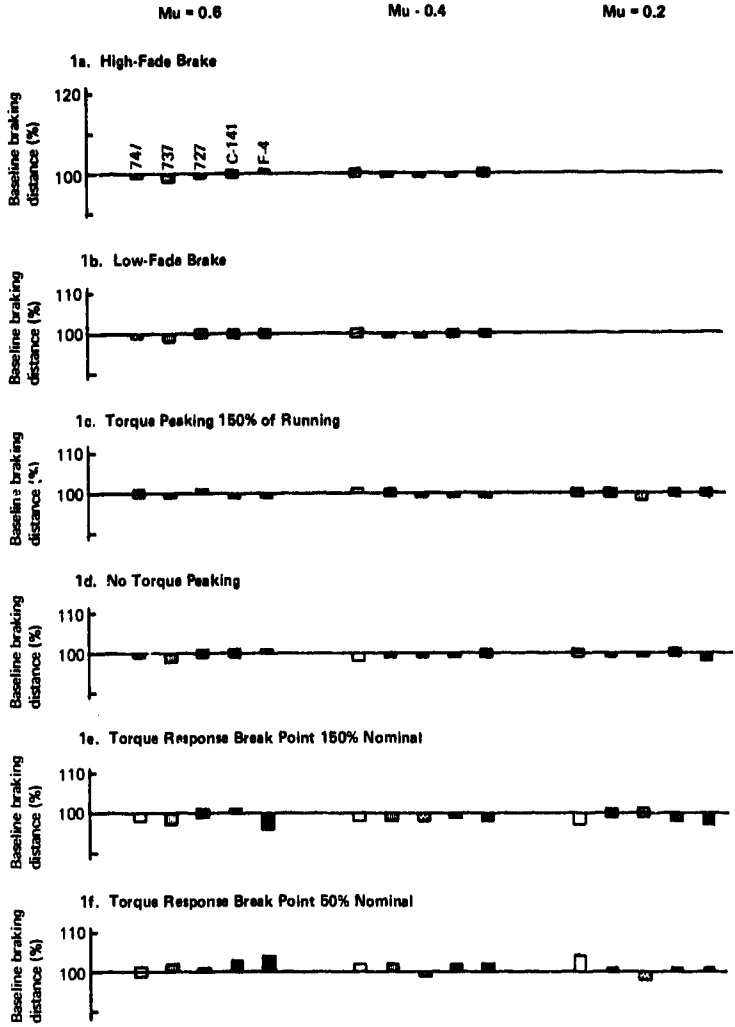

Figure 10.–Braking Distance Test Results (Sheet 8 of 15)

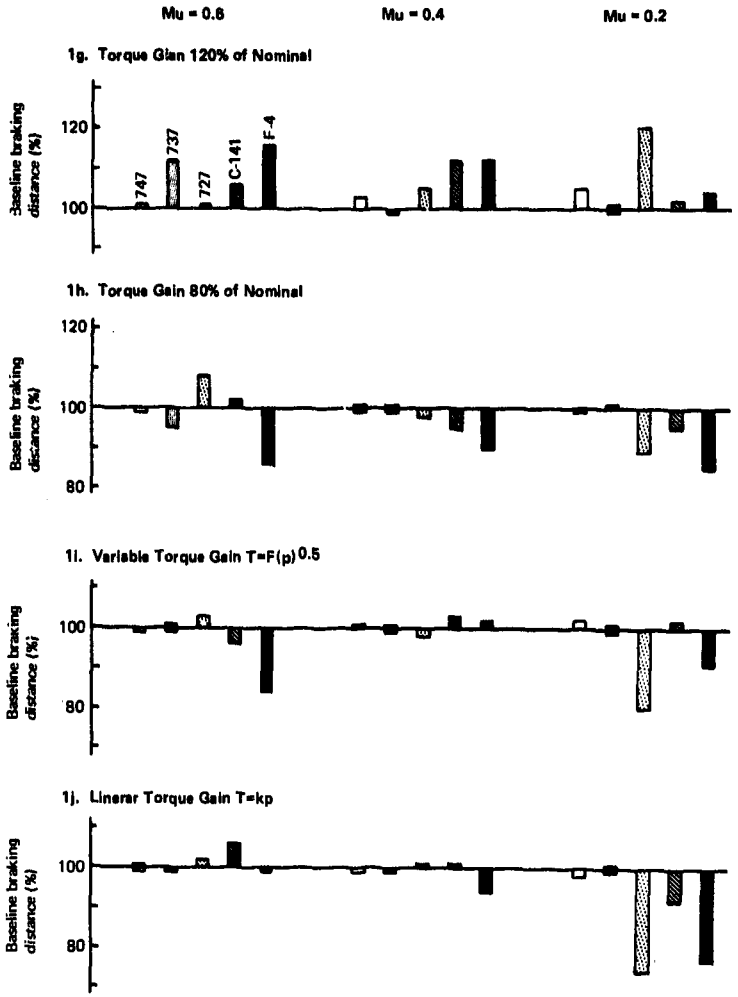

Figure 10.—Braking Distance Test Results (Sheet 9 of 15)

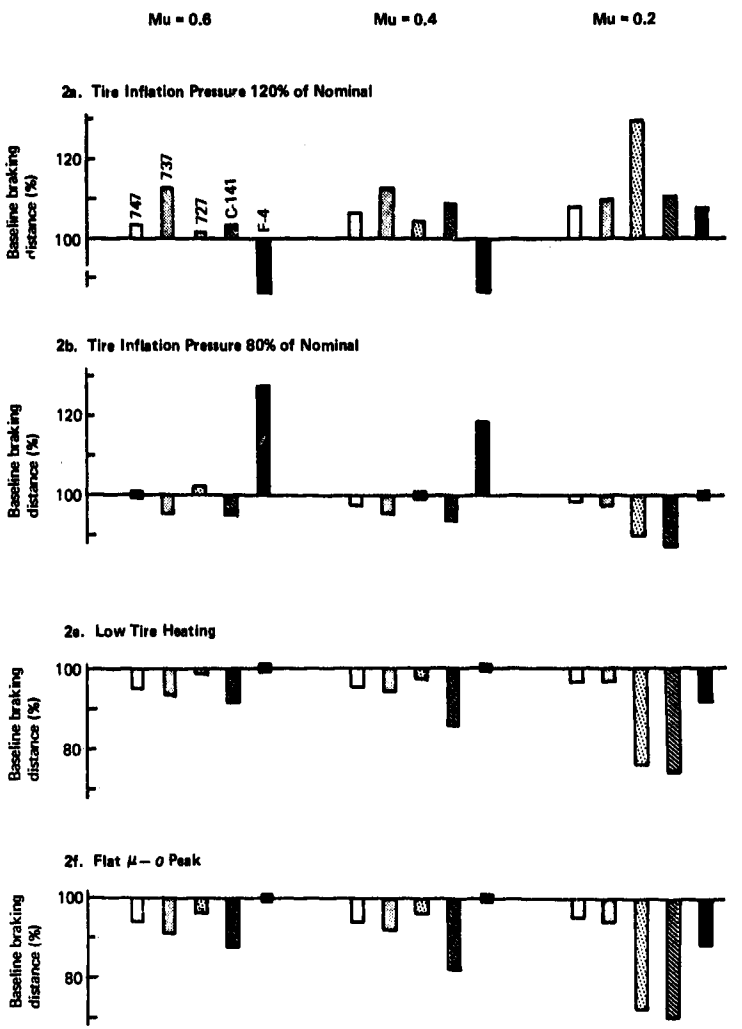

Figure 10.—Braking Distance Test Results (Sheet 10 of 15)

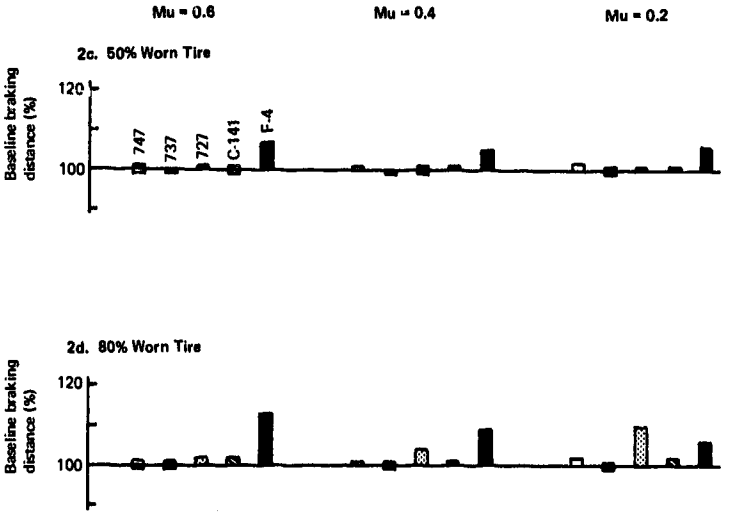

Figure 10.—Braking Distance Test Results (Sheet 11 of 15)

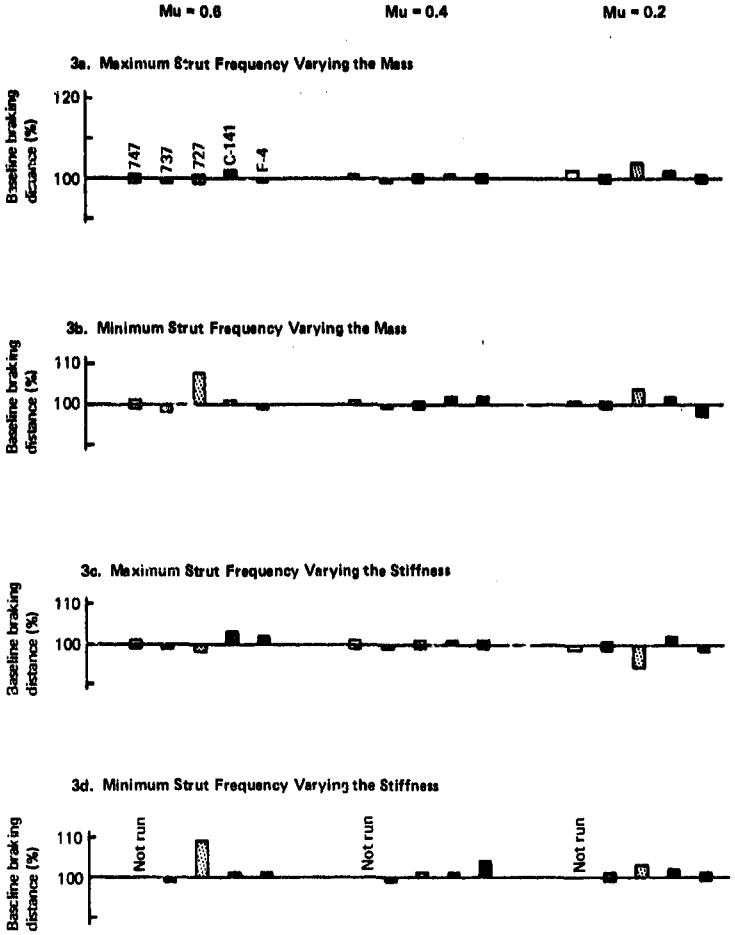

Figure 10 –Braking Distance Test Results (Sheet 12 of 15)

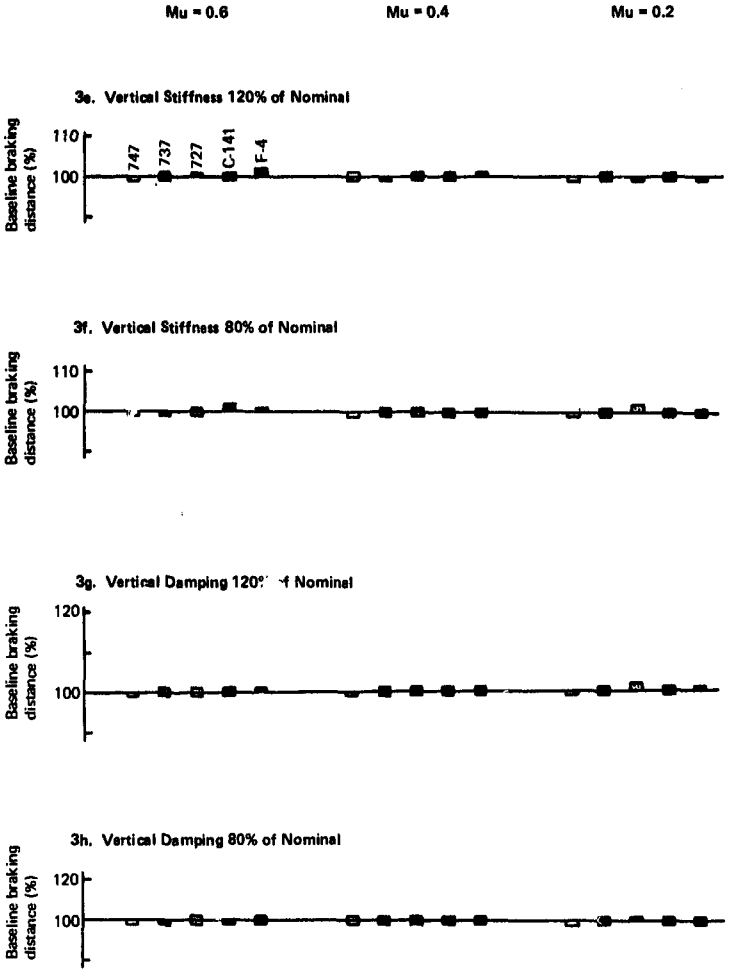

Figure 10.–Braking Distance Test Results (Sheet 13 of 15)

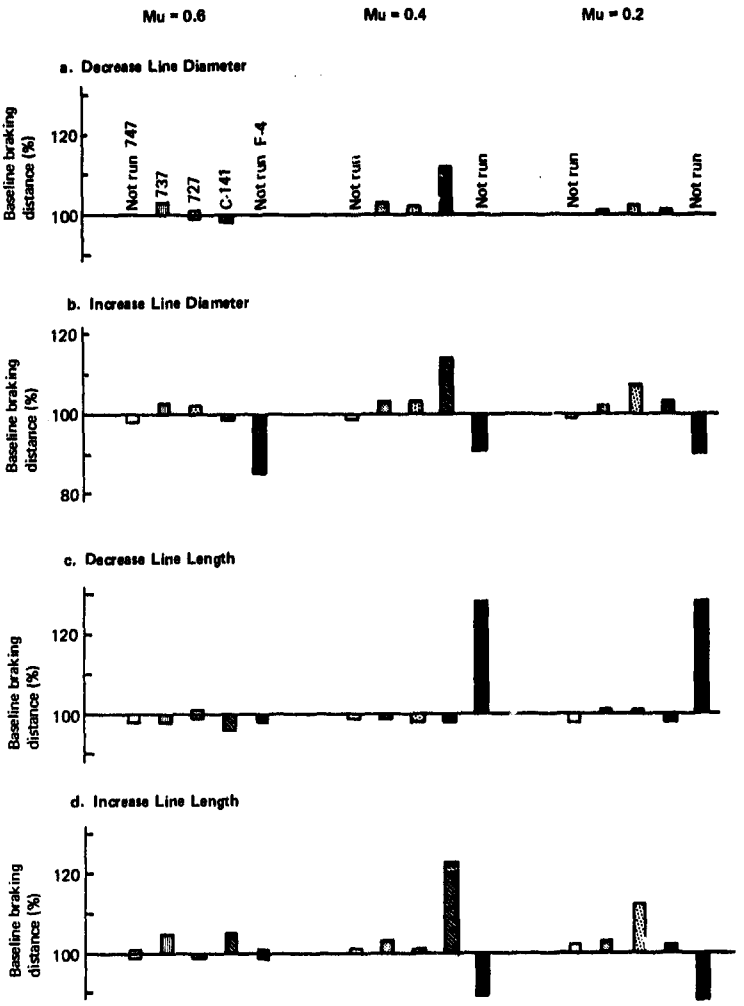

Figure 10.—Braking Distance Test Results (Sheet 14 of 15)

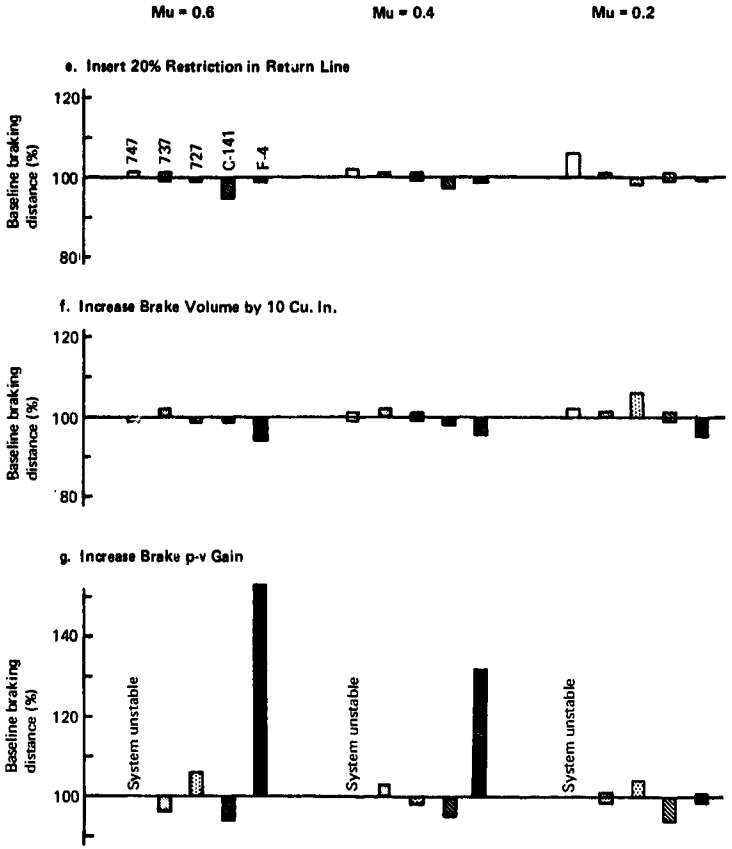

Figure 10.—Braking Distance Test Results (Sheet 15 of 15)

energy of the aircraft. The F-4 appears to operate quite differently at low ground friction values, largely because of its lift and drag characteristics. An increase in the landing speed of the F-4 results in a large increase in drag and a small decrease in main gear loading. At the low mu condition, the increased kinetic energy is nearly compensated by the increase in drag. Thus the braking distance shows only slight variations.

4. **Spoiler or Drag Chute Deployment** (4a and 4b, Sheet 2, Figure 10)

The general trend shown is that delaying spoiler application or drag chute deployment, is deterimental to braking performance. Significant braking force is lost during the period prior to spoiler deployment. From a braking performance standpoint, the pilot should spoil the lift as soon as possible.

5. **Spoiler or Drag Chute Effectiveness** (4c, 4d, and 4e, Sheet 3, Figure 10)

As shown, braking distance increases as the spoiler becomes less efficient. The increased distance results from: (1) loss of braking force due to an increase in life, and (2) loss of effective drag force due to lower drag coefficients. The graphs show the increasing effect of spoiler effectiveness at low mu conditions. This reflects the importance of spoilers during adverse weather.

6. **Engine Idle Thrust** (4f and 4g, Sheets 3 and 4, Figure 10)

Changes in the engine idle thrust value generally cause a change in braking distance of less than 3%. The F-4 is the exception; it has an unusually high ratio of idle thrust to weight. Thus a change in the idle thrust value causes a significant change in the kinetic energy to be dissipated during braking. This in turn directly affects the braking distance.

7. **Brake Pressure Application Rate** (5a and 5b, Sheet 4, Figure 10)

Distance variations resulting from a change in pressure application rate are a maximum of 4% and in general average about 1%. For the range of pressure application rates tested, it does not appear that the parameter has much effect.

8. **Delay of Brake Pressure Application** (5c and 5d, Sheets 4 and 5, Figure 10)

The delayed pressure application bar charts include both the actual braking distance and the added transition distance caused by the delay. As can be seen, the effect of delaying brakes simply causes an increase in total ground distance. This results from the loss of braking during the delay period and the small amount of speed lost during that time.

9. **Metered Pressure** (5e and 5f, Sheet 5, Figure 10)

The results from the metered pressure tests do not show a general distance trend. However, the variation of braking distance between the different aircraft is attributable to valve characteristics, torque limiting of the brake, and skid control adaptation to conditions. The Boeing 747, 737, and 727 show an increase in braking distance as the metered pressure is lowered. For these aircraft, the brake is pressure-limited and cannot develop sufficient

torque to initiate a skidding. The F-4 and C-141 show an opposite trend. At lower pressures, the dynamic response of these systems is slower, reducing the cycling of the antiskid system, increasing system efficiency, and reducing stopping distances.

b. RUNWAY AND ENVIRONMENTAL SYSTEM

1. **Wind** (1a, 1b, and 1c, Sheet 6, Figure 10)

The environmental parameter wind has quite a straightforward effect on braking distance. Headwinds (positive-knot values) reduce braking distance; tailwinds increase the distance.

2. **Hot and Cold Days** (1d and 1e, Sheet 7, Figure 10)

During these tests, the air density was varied to change the lift and drag forces on the airplane. On hot days, both lift and drag decrease; on cold days, they increase. The results show generally that drag has the greater effect on braking distance. On hot days, the distances are longer because of the decreased aerodynamic drag. The Boeing 747 is an exception; its lift-to-drag ratio is much greater than the other four airplanes, and the lift effect is more significant. During a hot day, lift decreases, placing more weight on the main gear. This increases the braking capability and decreases the braking distance. In operational situations, higher flap settings are selected to compenstate for this effect.

3. **Rough Surface** (3a, Sheet 7, Figure 10)

The addition of the rough runway surface has the effect of providing an additional perturbation to the vertical motion of the aircraft. This results in random main gear loading and tests the capability of a system to adapt to adverse runway surfaces. The data indicates that each system tested had no problem adapting to this surface condition. The power spectral density curve of the rough runway condition simulated is given in Appendix B.

c. LANDING GEAR SYSTEMS

1. **Brake Fade** (1a and 1b, Sheet 8, Figure 10)

During the high and low brake fade tests, the effective mass of the brake was lowered to initiate brake fade earlier in the braking segment. The largest variation in braking distance from this parameter change is 2%. In light of the 1% repeatability accuracy of the simulator, brake fade is not considered a significant variable in braking performance during landing rollout.

2. **Torque Peaking** (1c and 1d, Sheet 8, Figure 10)

The nominal value of torque during peaking was increased to 150% of running torque and decreased to no torque peaking. Peaking is a low-speed phenomenon that occurs during a deep skid and at the end of the braking segment. As a result, torque peaking has little or no effect on the actual braking distance.

3. **Torque Response Frequency** (1e and 1f, Sheet 8, Figure 10)

A change in the torque response frequency breakpoint effects the lag in the pressure-torque model. As predicted by theory and borne out by the data, movement of the breakpoint out to 150% of nominal reduces the system lag and allows faster response and shorter braking distances. Conversely, movement of the breakpoint inward increases the lag and lengthens the distance. This aspect of brake performance should be stressed to brake suppliers.

4. **Torque Gain** (1g, 1h, 1i, and 1j, Sheet 9, Figure 10)

During these four tests, the brake pressure-torque relationship was changed. The airplanes show a random degree of sensitivity to the changes. Little data is available on the actual pressure-torque relationship of brakes. The observed sensitivity simply points to the need for a better understanding of the torque gain of a brake.

5. **Mu-Slip Curve Variations** (2a, 2b, 2e, and 2f, Sheet 10, Figure 10)

Variations in the shape of the mu-slip curves were made to analyze how each antiskid system would react to changes in runway traction. The data shows significant sensitivity, which, however, is random. The randomness between the different aircraft results from the manner in which the antiskid system is implemented. Each system and the mu-slip curve variation is analyzed in depth in ASD-TR-7[illegible]-41, Volume II, Section VIII. The general conclusion to be made from these data is that the mu-slip curve shape influences stopping distance.

6. **Worn Tire** (2c and 2d, Sheet 11, Figure 10)

During the worn tire tests, the rolling radius, torque radius and wheel-tire inertia were changed. The change in braking distance averaged about 1% exclusive of the F-4. The F-4 is unusual because of its small main gear tire. The fixed change in torque radius (used for all airplanes) represents a large reduction in ground torque. This reduced torque has caused a significant increase in braking distance.

7. **Strut Frequency** (3a, 3b, 3c, and 3d, Sheet 12, Figure 10)

The natural frequency of the main gear was changed to check for the existance of coupling between the skid control box logic and gear motion. When coupling exists, a catastrophic gear failure may occur, or braking performance may be jeopardized. The 727 is the only aircraft where the braking distance was effected by greater than 2%. In this case, the coupling lowered the mean antiskid pressure level. This reduced the average brake torque throughout the run, which increased the braking distance.

8. Vertical Stiffness and Vertical Damping (3e, 3f, 3g, and 3h, Sheet 12, Figure 10

During these tests, the characteristics of the main and nose gear were changed. Such a change primarily effects the pitching motion of the aircraft and, to some extent, the tire load. The data shows braking distance to be insensitive to vertical gear stiffness and damping variations.

d. HYDRAULIC SYSTEMS

To realize the best possible stopping performance, each subsystem must be integrated into the total system. The hydraulic system is one such system that can be tuned to aid in obtaining optimum performance. These tests were designed to indicate how well the hydraulic system had been optimized. No attempt has been made to retune the antiskid system during these tests. Decreased braking performance may be reclaimed by retuning the antiskid control box.

1. Line Diameter (a and b, Sheet 14, Figure 10)

Line diameter tests reveal that, with the exception of the F-4, most of the systems have been properly implemented. The F-4 data shows that substantial performance can be gained by increasing the hydraulic line size. Decreased line diameter tests were not performed on the F-4 and 747 because the standard lines were 1/4-in. diameter, and further reduction was not deemed feasible.

2. Line Length (c and d, Sheet 14, Figure 10)

Changes in line length effect the frequency response gain and lag of the hydraulic system. Basic hydraulic analysis predicts that shorter lines decrease the gain and lag in the system; this will result in better performance. Excluding the F-4, the frequency response and braking distance showed the predicted trend. The F-4, however, exhibited a decrease in gain as line length increases, thus braking distance decreases as length increases. Further turning of the skid control system or use of a different skid control system and associated hardware could have shown different results. This, however, was not within the scope of these studies.

3. Restriction in Return Line (e, Sheet 15, Figure 10)

Except for isolated cases, braking distance was unaffected by hydraulic return line restructions.

4. Brake Volume Changes (f and g, Sheet 15, Figure 10)

The volume of the standard aircraft brake was changed, resulting in a modification of the pressure-volume curve of the brake. Increasing the brake volume decreases the brake gain. To increase the brake gain, the actual brake was replaced with a small accumulator. A varying degree of sensitivity was exhibited during these tests; however in general, only the increased gain case caused significant change. In the case of the 747, the change actually caused the system to be unstable, and the test could not be performed. Early simulator development is considered necessary to ensure proper brake characteristics. These characteristics can be incorporated in brake specifications. This procedure is routinely done during

the development of Boeing airplanes. The F-4 antiskid system was unable to accurately control the brake pressure. The result was increased cycling of the system and lowered performance. The instability of the 747 and the lower performance of the F-4 was caused by an increase in antiskid system gain (resulting from the brake change) without any tuning of the antiskid circuit. Due to proper tuning and hardware selection no stability problems exist in the Boeing 747.

e. COMPOSITE VARIATION OF PARAMETERS

During the braking sensitivity study, the baseline value of a parameter or group of related parameters was changed. The braking distance resulting from a change has been used as a measure of that parameter's effect on braking. Because nonlinear dynamic equations are involved, the effect of making composite parameter changes cannot be predicted by simple algebraic addition of the effect of each individual parameter. This aspect is stressed to discourage the use of data presented for purposes other than intended for this study.

SECTION VII

PARAMETER EVALUATION CRITERIA

1. PERFORMANCE INDICES

To evaluate the performance of a system, various normalized indices were developed. The use of such indices aids in the comparison of various systems.

The performance parameters used in evaluating each skid control system were:

- Airplane braking distance
- Braking distance efficiency
- Developed Mu efficiency
- Skid index
- Cornering index

With the exception of braking distance efficiency, these indices were calculated directly on the simulator and measured with a digital voltmeter. Braking distance efficiency was calculated from the results of the simulator and a digital computer program.

a. AIRPLANE BRAKING DISTANCE

Airplane braking distance, X_A, as measured on the analog computer is the distance the airplane travels from brake application to a low-velocity turn-off speed.

b. BRAKING DISTANCE EFFICIENCY

Braking distance efficiency, η_s, is the ratio of the perfect stop distance to the braked airplane distance.

$$\eta_s = X_p / X_A \times 100\%$$

where:

η_s = braking distance efficiency

X_p = perfect braking distance

X_A = airplane braking distance

The perfect braking distance is the distance required to stop the airplane if it is braked for the entire stop with maximum available braking force. This distance is determined by stopping a reference airplane that is identical to the braked airplane.

Braking distance efficiency indicates the degree to which the system meets its primary requirement of stopping the aircraft.

c. DEVELOPED MU EFFICIENCY

The developed mu efficiency is cumulative measure of the use of available mu. It is determined by dividing the time integral of developed mu by the time integral of available mu. This parameter is useful in evaluating system performance but can be misleading in that a high developed mu at high speed is more effective than a high developed mu at a low speed.

$$\eta_O = \frac{\int_o^T \mu_O \, dt}{\int_o^T \mu_A \, dt}$$

where:

η_O = developed mu efficiency

t = time

T = time to simulated stop

μ_O = developed mu

μ_A = available mu

d. SKID INDEX

The skid index is a measure of the tire wear produced by the brake control system. The index is defined as the integral of the product of sliding velocity and ground force divided and normalized by the integral of elapsed time. This parameter is also an indication of side force capability.

$$SI = \frac{\int_o^T V_S \cdot F_G \, dt}{\int_o^T dt}$$

where:

SI = skid index

V_S = sliding velocity

F_G = ground force

T = total time for the stop

e. CORNERING INDEX

The cornering index is a measure of the ability of the tire to sustain a side load. The instantaneous cornering index is defined as a function of tire slip. The total cornering index value is the summation of the instantaneous values throughout the stop.

$$CI = 100 \frac{\int_0^T (1 - \sigma)^n \, dt}{\int_0^T dt}$$

where: CI = cornering index, equal to zero for a wheel fully locked and 100 for a free-rolling wheel

σ = slip ratio

n = sensitivity coefficient (2.0)

T = total time for the stop

f. SYSTEM STABILITY

In addition to the five performance indices, a measure was made of the ability of an antiskid system to contribute to system stability. The criterion used to determine system stability was that the system is termed unstable if the main gear strut oscillations diverge. The stability of the system was measured by determining the damping ratio necessary to cause instability.

2. PARAMETER RATING SYSTEM

The final step in the sensitivity analysis of aircraft braking performance is to rate each parameter. To facilitate the rating of a parameter change the normalized distance "baseline braking distance percentage" was used. The use of this term allows the five airplanes to be analyzed as a group. In order to uniformly and quantitatively rate a parameter change, the following formula was used:

$$PRI = \frac{\sum_{i=1}^{n} \text{baseline braking distance percentage}_i - 100\%}{n}$$

PRI = parameter rating index
n = total number of data points for a particular parameter change
baseline braking distance percentage$_i$ = the baseline braking distance percentage value for the ith data point

The parameter rating index (PRI) as calculated above is the average percentage deviation from the baseline braking distance. Thus, the value of the PRI increases when a parameter change causes larger deviations from the baseline braking distance. The data used in the calculation of the PRI are given in ASD-TR-74-41, Volume II, Section XII. Also included are the final PRI values for the dry-stabilized landing conditions.

SECTION VIII

SIMULATOR-TO-AIRPLANE CORRELATION

Meaningful results from a simulator can be obtained only when correspondence to the modeled system can be demonstrated. The simulator used during this study is the culmination of considerable effort including model development, subsystem test and evaluation, correlation with airplane tests, and operational usage.

The analog computer models used in the simulator are expanded versions of those used in the Boeing Baseline Simulation (Ref. 1). A continuous improvement effort has been made to represent the dynamic system behavior more thoroughly as data has become available. Data used for model expansion and improvement has been derived from:

- Flight test results
- Dynamometer tests
- Contracts such as "Brake Sensitivity Analysis" and "Antiskid Performance Compatability and Improvement"
- In-house research
- Literature

The basic simulation has been used for system evaluation, tuning, and development on virtually all Boeing commercial jet transports. An integral part of its use has been a thorough verification that system performance on the computer matches that obtained during airplane flight tests.

Verification of simulator performance consists of comparing results with results from similar tests conducted on the airplane. In this study, the Boeing airplane performance data was readily available from in-house flight testing. Data from the Rain Tire test program was provided for the F-4. Limited data on the C-141A was available from the Combat Traction I program. The specific test conditions used for correlation are listed in Table 6. Conditions duplicating airplane weight, CG location, brake application speed, and others were run on the simulator and compared with these records. Key parameters were adjusted until the desired level of correspondence was obtained. The following items were considered in evaluating the correlation:

- Stopping distance
- Skidding pressure
- Number of skids
- Depth of skids

Table 6.—Correlation Tests

Aircraft	Test	Conditions
737	Test 29-35	Condition 1.20.05.001.1 100,500 lb 5.3% MAC 198 fps
	Test 75-3	
747	Test 11-8	Condition 1.20.052.003.5 486,100 lb 15% MAC 234 fps
	Test 23-16	
727	Test 181-16	Condition 3.15.49.2.5 123,000 lb 25% MAC 176 fps
	Run 50, Edwards AFB USAF/NASA/FAA Tests	112,000 lb 192 fps
C-141A	Combat traction final report	
F-4E	Rain tire program Run 4	35,476 lb 150 fps
	Rain tire program Run 23	33,636 lb 222 fps

- Rate in and out of skids
- General control

In addition, strut fore and aft and airplane pitching freqeuncies and damping ratios were checked when airplane data was available.

No attempt was made to exactly duplicate airplane stopping distance or measured parameter traces. Instead, emphasis was placed on producing the same control characteristics. Stopping distances were matched by adjusting the tire-to-ground friction coefficient. The other parameters were then checked and, if necessary, adjusted to the levels measured from flight test records. Correct skidding pressure levels are important because they relate brake characteristics, runway friction levels, and tire vertical loading. Similarly, data on the depth, rates in and out, and the number of skids ensure that the tire simulation is behaving as it should and that the ground force simulation is properly adjusted for the particular airplane.

In general, traces from the computer tend to be regular in nature and consistent. Flight test records, though, show the random effects produced by runway discontinuities, irregularities, and second-order effects. Overall, the simulator reproduces the predominant factors in the stop.

The following paragraphs briefly describe the correlation of each airplane.

1. 727

Portions of test 181-16 condition 3.15.49.2.5 are shown in Figure 11 along with an equivalent condition from the simulator. The control is characterized by multiple skids at the start followed by skids at essentially regular intervals. The skid rate is about once per second. Longer intervals occur after the initial cycling (more pronounced on some wheels than others). Between cycles, a fairly constant pressure increase occurs at a rate of about 250 psi/sec. Skidding pressures are about 1000 to 1200 psi. Both the flight test and simulators show these characteristics. The airplane braking distance was 1163 ft, and the distance obtained from the simulator was 1278 ft.

2. 737

The 737 simulator performance was compared against Boeing flight test 29-35 condition 1.20.05.001.1, which was a performance landing at a weight of 100,500 lb. The center of gravity was in a forward position (5.3% MAC), and brakes were applied at 198 fps. Portions of the wheel velocity and brake pressure traces from this test are shown in Figure 12 along with corresponding traces from the computer.

Analysis of the records showed the basic similarity between the airplane and the simulator. Skidding pressures during the flight test ranged from 2400 to 2800 psi on the left side of the airplane, while those on the right side ranged between 1800 and 2500 psi. The skidding pressures on the simulator ranged from 2100 to 2400 psi. At high speed, the skid depths on the airplane and the simulator are shallow (15 to 20% slip); at low speed, the skids become

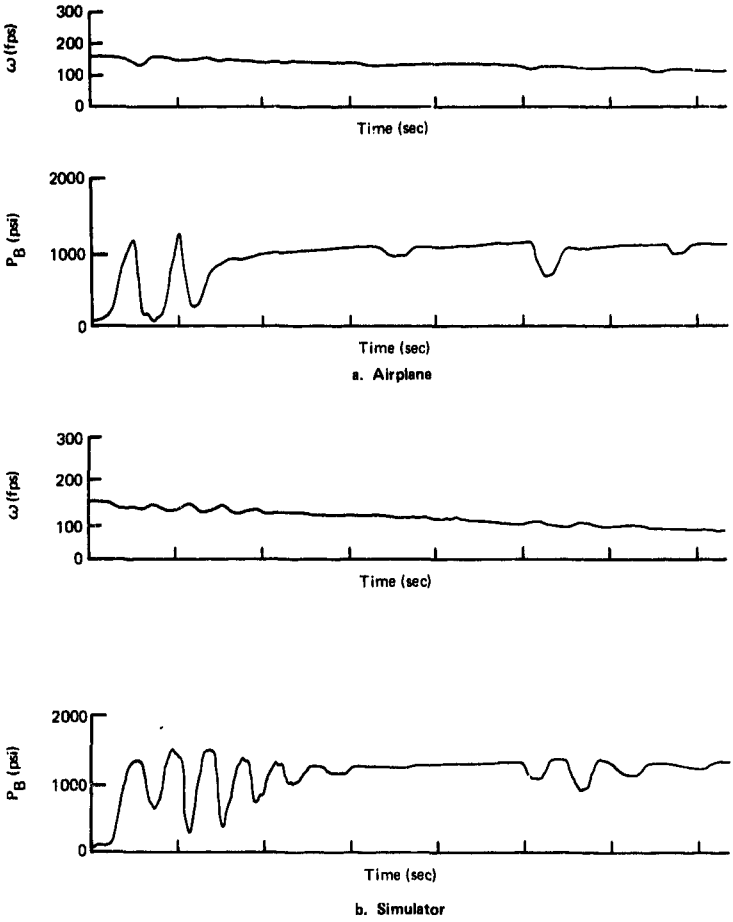

Figure 11.–727 Dry Runway

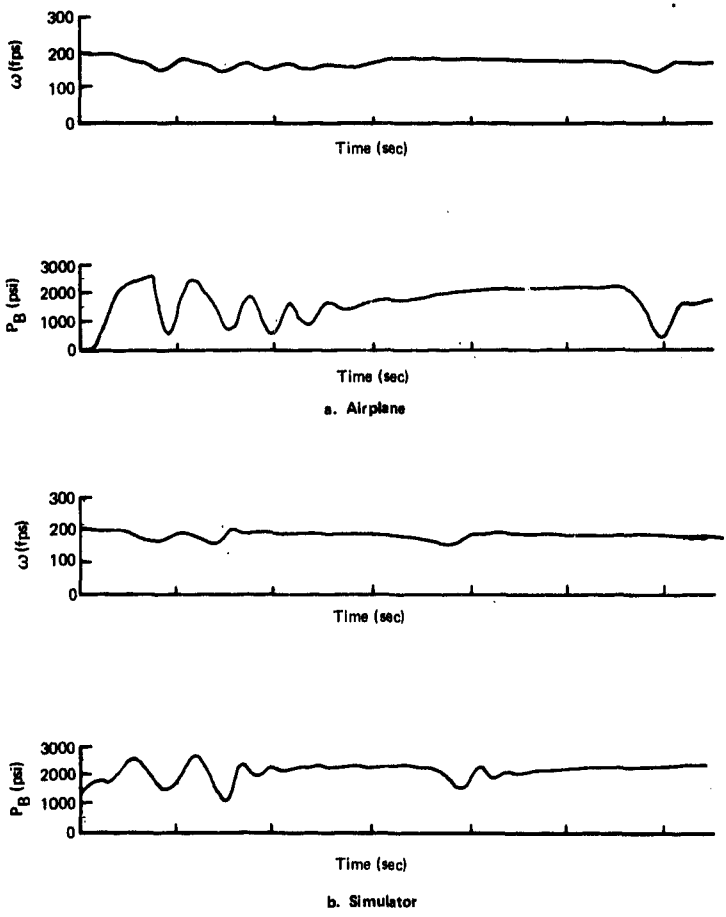

Figure 12.–737 Dry Runway

much deeper (70-80%). Rates into skids range from 400 to 600 fps^2 and rates out of skids, from 600 to 1200 fps^2 for both the airplane and the simulator. Stopping distances were also close, with 1387 ft on the computer compared to 1348 ft for the airplane.

3. 747

The 747 correlation runs were made using the basic 747 antiskid system. This system uses a 50-tooth wheel speed transducer; the sensitivity tests used the improved system, which has a 200-tooth transducer and incorporates other tuning changes. Extensive use of the simulator was made in developing the improved system from the basic. Detailed correlation of the simulation was made at that time.

For these tests, the simulator was compared against two flight test conditions. Test 11-8 condition 1.20.052.003.5 was a performance landing on a dry runway with an airplane weight of 486,100 lb. Test 23-16 was a stop made on a wet runway.

For Test 11-8 and the corresponding simulator run (Figure 13), the control is characterized by multiple skids at the beginning. Once control is established, skids occur at essentially regular intervals about 1 sec apart. At high speed, the skids are shallow, becoming deeper at low speed even to the point of temporary lockups. Likewise, the amount of pressure released during a skid increases until, at low speed, the pressure is reduced from zero during each skid. Skidding pressures are around 1500 psi at high speed, increasing to around 2200 psi at low speed. Stopping distance for the simulator and the airplane were identical at 2743 ft.

On a wet runway (Figure 14), the wheels begin a series of deep skids. During each skid, the brake is completely released and a long period elapses before the pressure starts to increase. As soon as the pressure starts increasing, the wheel goes into another skid. This pattern is repeated during most of the stop.

4. C-141A

The C-141A brake control system is unique among those tested and posed unique problems in simulator setup and correlation. The primary concern during simulator setup was t... wheel speed transducer. Unlike the other systems tested, the C-141A uses an AC generator to measure wheel velocity. The output of the generator is an AC voltage with an amplitude and frequency proportional to wheel velocity. The output is rectified and filtered in the control box to produce a DC voltage proportional to wheel velocity. The input to the box from the computer then had to produce the same amplitude and frequency as the transducer. (The other systems worked strictly on frequency content and were essentially insensitive to signal amplitude.)

To ensure correct simulation of the transducer, an aircraft transducer was set up on a test rig, and the output frequency and amplitude were determined as a function of velocity. This output was then produced as shown in Figure 15.

Flight test records for the C-141A were scarce. Those available were from the Combat Traction Flight Test program. A dry and a wet condition are shown in Figures 16 and 17. Because of the scale of the records, little quantitative data could be taken from them. They do, though, provide qualitative data on the general control of the system.

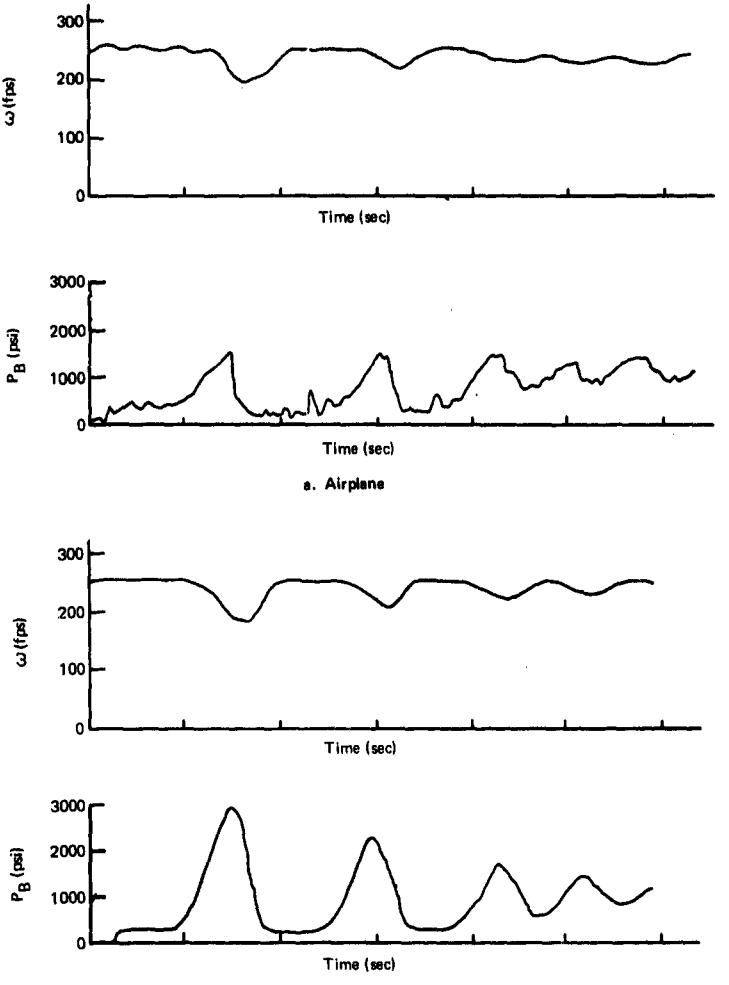

Figure 13.–747 Dry Runway

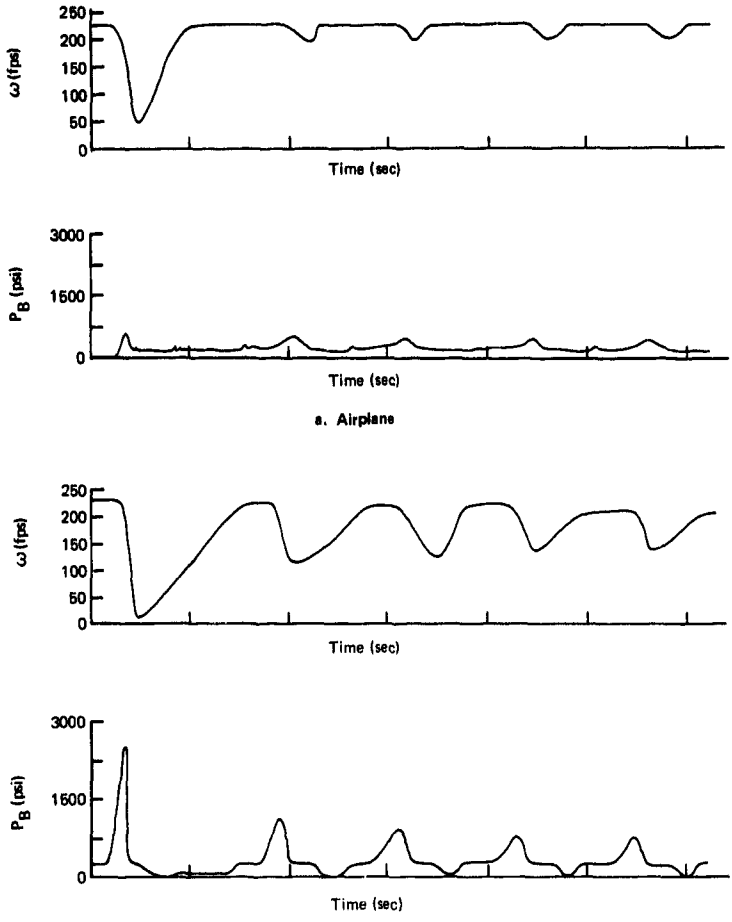

Figure 14.—747 Wet Runway

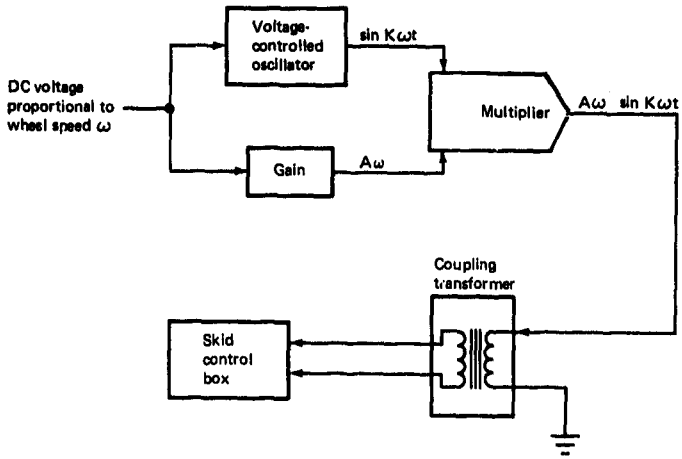

Figure 15.—C-141 Wheel Speed Transducer Simulation

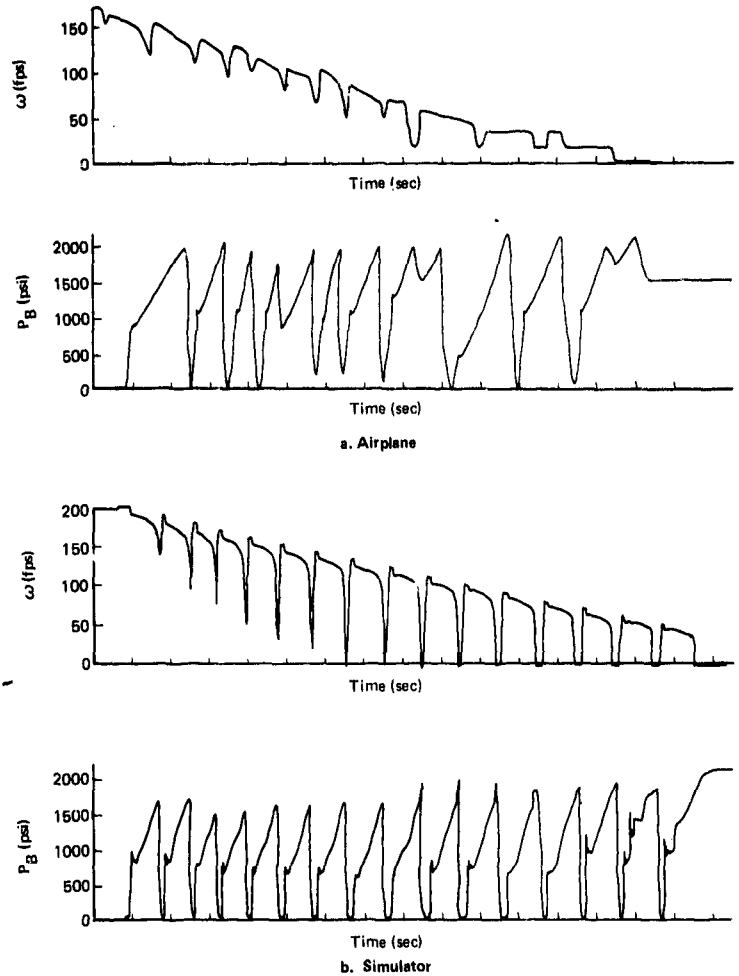

Figure 16.–C-141 Dry Runway

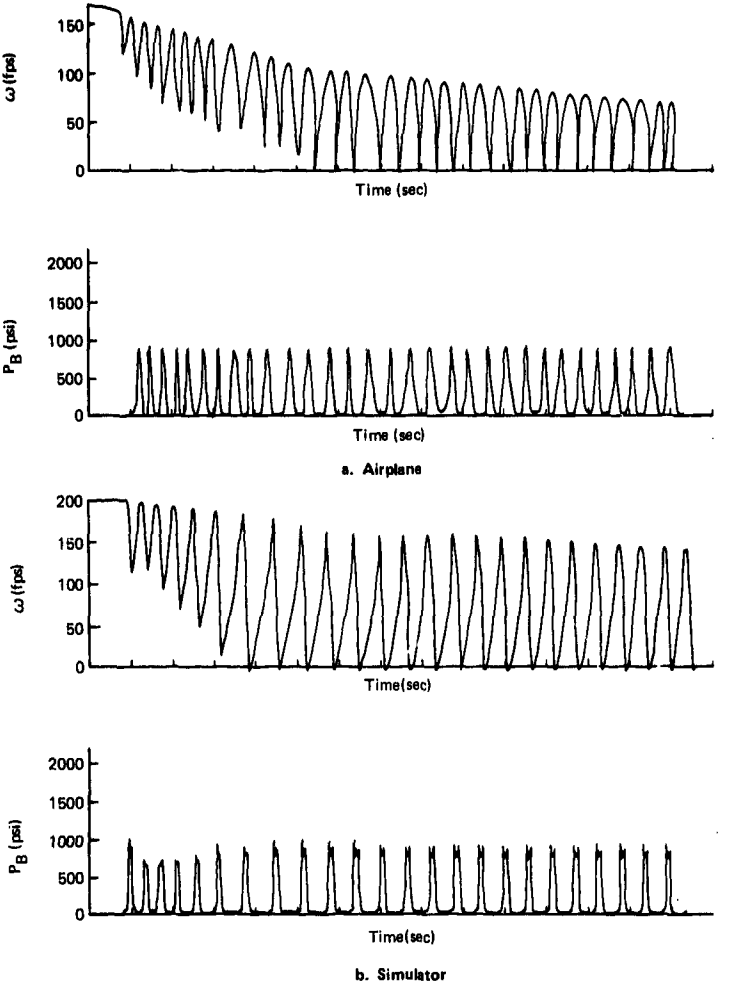

Figure 17.–C-141 Wet Runway

Considering the dry stop, the control is characterized by numerous full brake dumps (activation of the Step 2 solenoid) followed by a gradual pressure reapplication. The Step 1 solenoid (slower partial dump) actuates occasionally. The skidding rate is about one skid per second, and total stopping time is about 13 sec. The wheel speed traces show shallow skids at high speed and deep skids at low speed. The actual speed departures on the airplane were probably larger than the traces indicate, because the low transducer frequency requires a large amount of filtering.

A dry condition run on the simulator is also shown in Figure 16. As in the flight test record, the deep dumps predominate, accompanied by an occasional activation of the shallow dump. Skidding rate is about one skid per second. The wheel speed departures are much greater than those from the flight test, as expected. The trend of shallow skids at high speed and complete lockups at low speed is duplicated. The stopping distance for this condition was 1841 ft, compared to a handbook value of 1900 ft.

The wet runway landing (Figure 17) shows a continuous sequence of deep skids at a rate of about three skids per second. The control is characterized by a reapplication pressure higher than the runway can sustain. Hence, the wheel goes into a skid as soon as pressure is reapplied. Similarly, the simulator records show the same dump-fill pattern at about the same rate.

5. F-4

Control of the F-4 on a dry runway (Figure 18) is characterized by a large number of shallow skids. Most of the skids result in a short, partial dump of brake pressure. As speed decreases, the skids generally become deeper and fewer. Another prominent characteristic of this airplane is the gradual increase in skidding pressure as the speed decreases. The aircraft braking distance for this control was 3400 ft, while the simulator distance was 3278 ft.

On a wet runway, Run 23, the skids are much more definite, being deeper and of longer duration (Figure 19). Only one wheel on the airplane goes into a skid. This is caused by the paired wheel control used on the airplane. The brake pressure is operating in a dump-fill mode common to many systems on low mu surfaces. Equivalent conditions from the simulator show the same characteristics. The aircraft braking distance was 6221 ft, and the simulator distance was 5890 ft.

6. OPERATIONAL ANOMALIES

The basic correlation described in preceding paragraphs has been limited to the normal operation of brake control systems. Under certain conditions, a system does not operate normally. These anomalies exist only under extreme operating conditions.

Two anomalies will be discussed here as a further indication of the ability of the simulator to duplicate the behavior of the airplane.

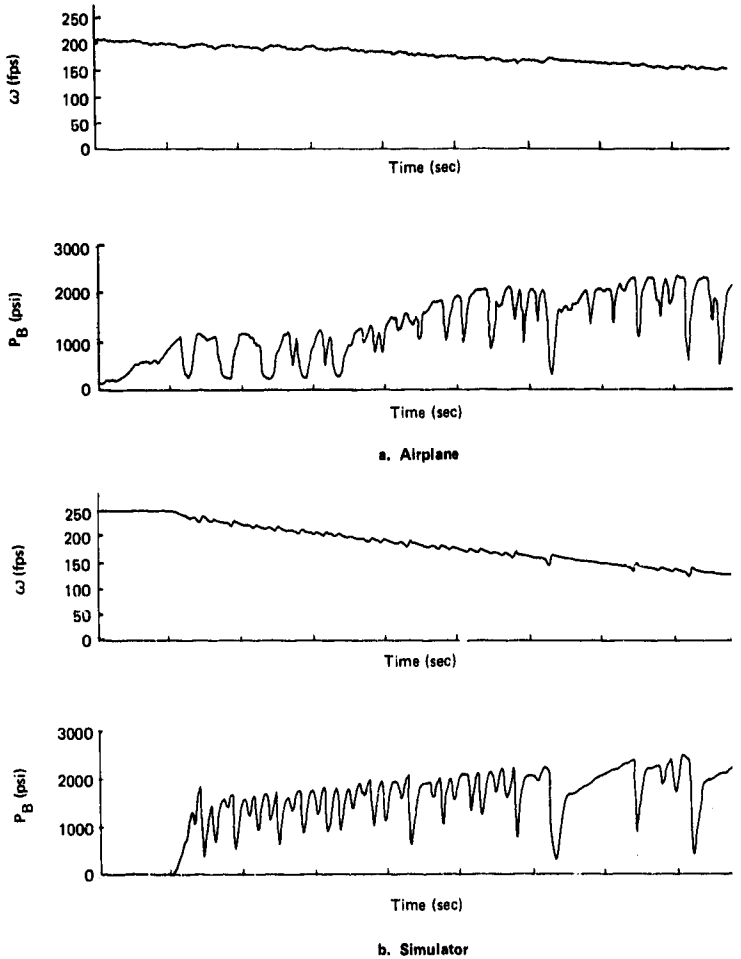

Figure 18.– F-4 Dry Runway

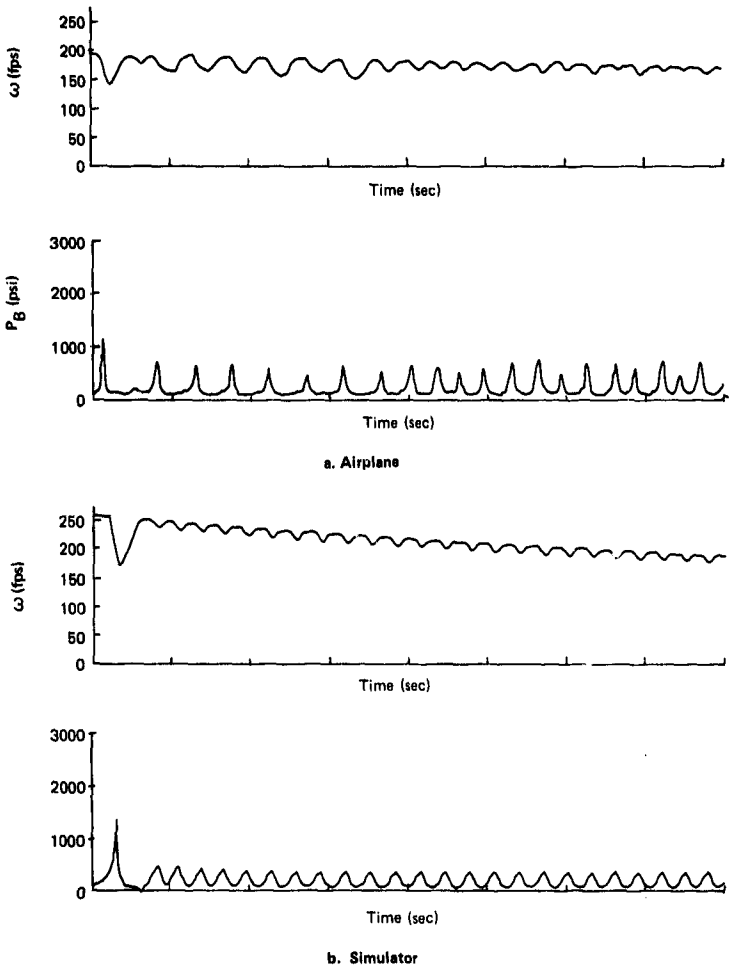

Figure 19.—F-4 Wet Runway

The first anomaly involves the operation of the locked-wheel protection device in the 727 Mark II antiskid system. Locked-wheel protection normally prevents complete wheel lock-ups. But if the pilot, on a runway with very low friction, meters full pressure to the brakes and the two paired wheels spin down together, the locked-wheel protection for those wheels can disarm and the wheels can lock. This was demonstrated during USAF/NASA/FAA testing at Edwards AFB. Figure 20 shows wheel velocities and brake pressures for the airplane and similar conditions on the simulator.

The second anomaly relates to a 737 landing at Rosewell, New Mexico, on a wet runway. The brakes were applied before full wheel spinup, causing the system to operate for an extended period of time in the high-slip region. Wheel velocity and brake pressure traces for this condition and a computer run are shown in Figure 21.

While these two cases show that the simulator will reproduce abnormal conditions, this study was primarily concerned with normal system operation. Abnormal conditions must be considered case by case because factors that may otherwise have only minor influence can become major.

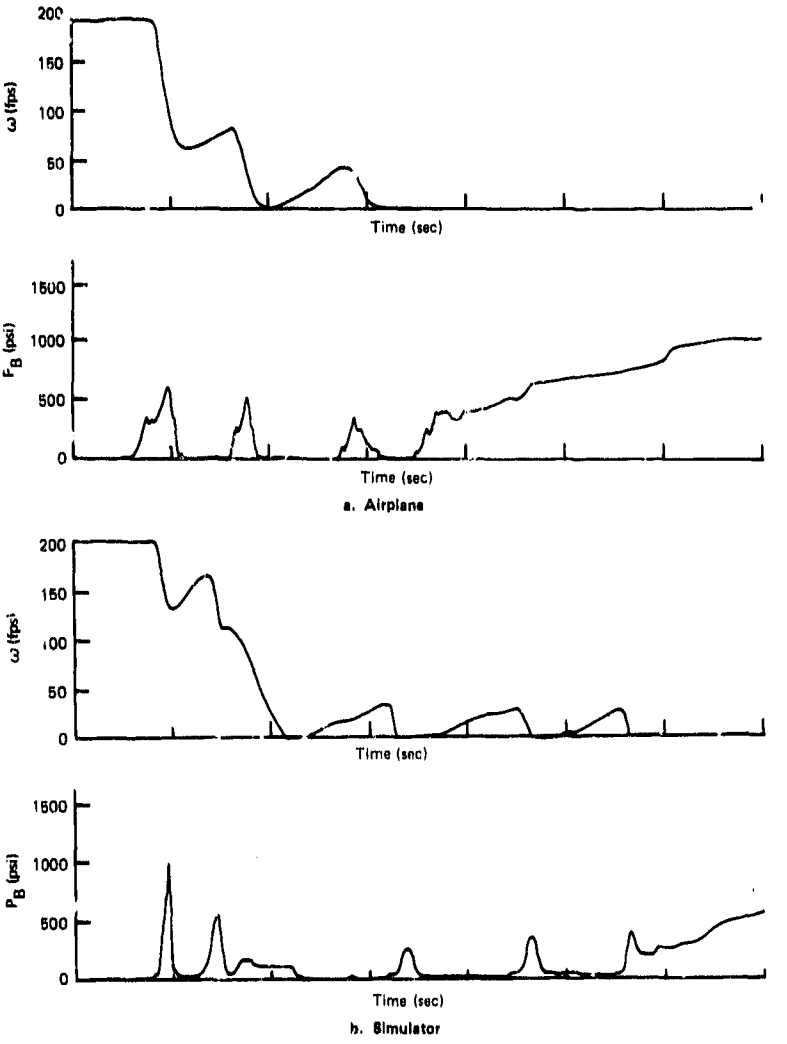

Figure 20.--727 Flooded Runway

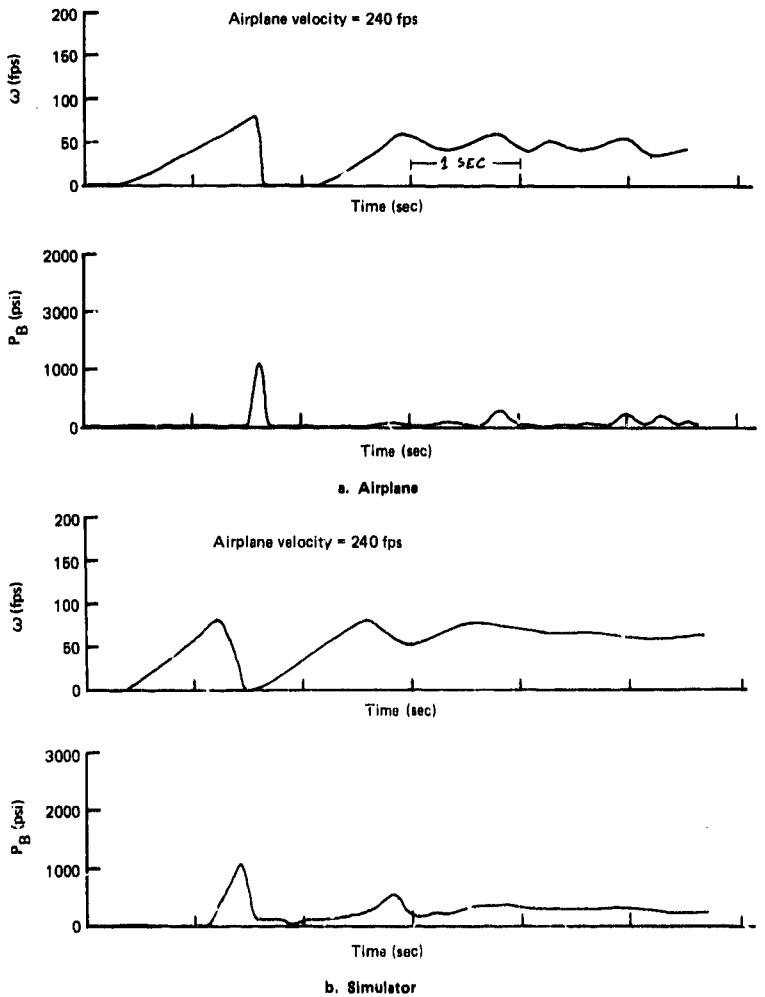

Figure 21.—737 Wet Runway Early Brake Application

SECTION IX

DETERMINATION OF SIGNIFICANT PARAMETERS

1. PARAMETER RATINGS

The parameter rating index (PRI) was used to rank the parameter changes according to their effect on braking distance. The value of the PRI is the average percentage deviation from the baseline braking distance. Thus, the larger the PRI, the greater impact the parameter has on airplane braking distance. Based on the PRI, the parameter changes have been arranged in numerical order, and the results are listed in Table 7. The table presents the average PRI for the five aircraft tested. The PRI for each airplane taken individually is listed in ASD-TR-74-41, Volume II, Section XII. Although the tire-ground friction coefficient (mu) is a predominant influence on airplane braking performance (see Figure 9), it is not included in Table 7 because the PRI rating methodology was used to determine variable significance for a range of mu values.

Table 7.—Parameter Rating

Rank	Test condition	Description	Performance rating index
1	4e.	No spoilers/drag devices	66.2
2	1a.	20 Knot wind	30.6
3	3b.	Brakes on Speed +20%	27.9
4	4a.	40% Effective Spoilers	27.3
5	5d.	Nominal Pressure Rate at 4.0 seconds	23.8
6	1c.	-10 Knot Wind	17.7
7	1a.	10 Knot Wind	16.7
8	4d.	60% Effective Spoilers	16.3
9	1e.	Maximum Landing Weight	15.5
10	3a.	Brakes on Speed + 10%	14.5
11	5d.	Nominal Pressure Rate at 2.0 seconds	13.6
12	5f.	50% of Full Metered Pressure	13.3
13	4b.	Spoiler Deployment at 2.0 seconds	12.0
14	1b.	Minimum Landing Weight	11.5
15	g.	Increase Brake p-v gain	10.1
16	2f.	Flat μ-s Peak	9.6
17	2a.	Tire Inflation Pressure 120% of Nominal	9.4
18	2c.	Low Tire Heating	8.0
19	4a.	Spoiler Deployment at 1.0 second	7.9
20	2b.	Tire Inflation Pressure 80% of Nominal	6.8
21	1g.	Torque Gain 120% of Nominal	6.7
22	2b.	Cold Day	6.1
23	d.	Move Dynamic Breakpoint In 10% of Nominal	5.4
24	1h.	Torque Gain 80% of Nominal	5.3
25	1j.	Linear Torque Gain T = f(p)	5.3
26	c.	Move Dynamic Breakpoint out 10% of Nominal	5.2
27	5e.	75% of Full Metered Pressure	5.2
28	b.	Increase Line Diameter 10%	5.1
29	2a.	Hot Day	4.8
30	4f.	1/2 of Engine Idle Thrust	4.1
31	1i.	Variable Torque Gain T = f(p)^2	4.1
32	3c.	Forward Center of Gravity	4.1
33	2d.	20% Worn Tire	4.0
34	4g.	1/4 of Engine Idle Thrust	3.9
35	a.	Decrease Line Diameter 10%	3.7
36	3d.	Aft Center of Gravity	3.6
37	f.	Increase Brake Volume by 50 in^3	3.2
38	5i.	Minimum Burst Frequency varying Stiffness	2.0
39	5h.	Minimum Burst Frequency varying Mass	1.9
40	1f.	Torque Breakpoint Breakpoint 50% of Nominal	1.9
41	1e.	Torque Breakpoint Breakpoint 150% of Nominal	1.8
42	2e.	50% Worn Tire	1.8
43	e.	Insert 50% Restriction in Return Line	1.7
44	5c.	Maximum Burst Frequency varying Stiffness	1.6
45	5a.	Post Nominal Pressure Application Rate	1.1
46	3e.	Aft Runway Center	1.1
47	3e.	High Center of Gravity	1.0
48	5g.	Maximum Burst Frequency varying Mass	1.0
49	1d.	No Torque Peaking	.9
50	1a.	High Brake Rate	.9
51	1c.	Torque Peaking 150% of Rounding	.9
52	1m.	Vertical Stiffness 150% of Nominal	.8
53	1f.	Vertical Stiffness 50% of Nominal	.8
54	1k.	Low Rate Brake	.8
55	i	50% Nominal Pressure Application Rate	.8
56		Vertical Damping 150% of Nominal	.8
57		Vertical Damping 50% of Nominal	.8
58	3b.	Low Center of Gravity	.8

2. SIGNIFICANT PARAMETERS

The second step in the rating of parameters was to determine which parameter changes have a significant effect on stopping distance. It was decided to consider all parameters having a PRI greater than 2.0 as being significant. A value of 2.0 represents a 2% change in the baseline braking distance. The repeatability of the analog-hardware simulation itself results in 1% variations.

Based on the above criterion, Table 7 has been reduced to peak available mu included. In addition, the parameter changes have been summarized by combining related tests under a general heading. The resulting list of parameters having significant effect on braking distance is given in Table 8.

The directional control impact of some of these variables was also assessed, but the data is not shown in the form of bar charts. The indices of directional performance measured during this program, although significant, are not the only contributing factors. Undue emphasis on these could lead to misunderstanding rather than clarification.

Generally, inefficient skid control systems display high skidding values, thus reducing cornering capability; a decrease in cornering coefficient significantly degrades directional control. True assessment of this aspect will require an in-depth study using steering and ground handling simulators. The reader is therefore cautioned regarding the use of cornering index as noted during the tests. See ASD-TR-74-41, Volume II, Section XII, for numerical values of the cornering index for all aircraft tested.

Table 8.—Reduced Significant Parameters

1.	Peak available ground friction
2.	Spoiler or drag device effectiveness
3.	Head or tailwind
4.	Brake application speed
5.	Brake pressure application rate
6.	Landing weight
7.	Metered pressure effectiveness
8.	Drag device deployment timing
9.	Mu-slip curve shapes:
	Tire inflation pressure
	Tire heating
	Flat μ-σ peak
	Peak μ percentage
10.	Ambient temperature
11.	Engine idle thrust
12.	Center-of-gravity location
13.	Brake pressure application timing

SECTION X

SELECTION OF PERTINENT PARAMETERS

Figure 22 is a flow chart where each block represents a major step of analysis in the formulation of the prediction equation and the resulting methodology.

Table 9 lists significant parameters after excluding the parameters that depend on pilot technique and are outside the scope of the present work. The following paragraphs present the reasoning for further refinement to the list.

Table 9.—Significant Parameters **

1.	Peak available mu
2.	Drag device effectiveness
3.	Head or tail wind
4.	Brake application speed
5.	Landing weight
6.	Air density
7.	Engine idle thrust
8.	Center-of-gravity location

** Excludes parameters dependent on pilot technique.*

1. BRAKE APPLICATION VELOCITY

If an airplane is loaded heavily, its landing speed increases. Because the maximum lift coefficient and wing area remain the same, the landing speed is a direct function of gross weight. Accordingly, for a lower landing weight, the landing speed decreases. So the landing weight of an airplane cannot be varied independent of the landing velocity. Because pilot techniques vary, however, the velocity can vary independent of weight.

One of the requirements of forming dimensionless groups is that each term or group be independent. Therefore, only velocity (but not weight and velocity) was chosen as a significant independent variable.

2. AERODYNAMIC LIFT AND DRAG

The same reasoning applies to the variation of lift and drag coefficients. One cannot be varied without varying the other, so the C_L/C_D ratio was chosen as an independent variable. The only exception if the F-4 where no spoilers and only a drag chute is employed for aerodynamic braking. The C_L thus remains constant. However, when C_D was considered as an independent variable (πterm) instead of C_L/C_D for the F-4, the prediction equation for

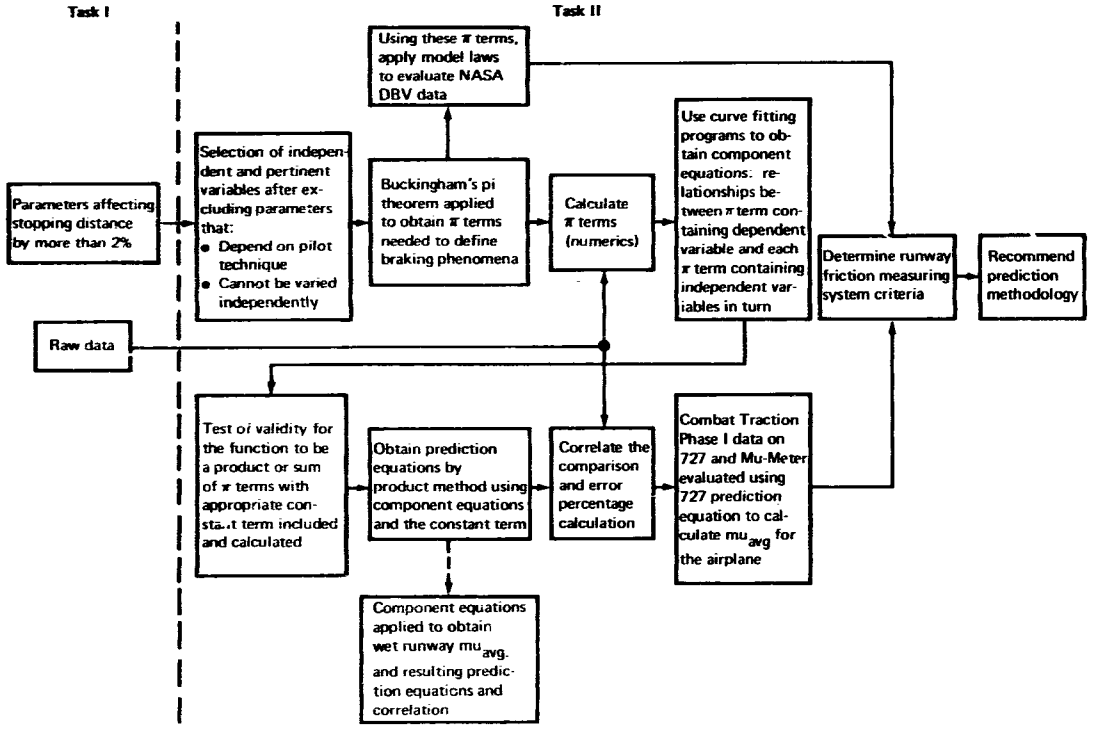

Figure 22.—Block Diagram for Task II Analysis

the model did not change in its accuracy or complexity. Thus, the C_L/C_D π term was used for F-4, as for the other airplanes studied.

3. WIND VELOCITY

Head and tail winds affect the air distance and transition distance as well as the braking distance. The analog simulation and dimensional analysis represent only the braking segment of the landing process. The question therefore was whether the wind velocity should be considered as an independent variable for the dimensional analysis.

The effect of brake application speed and that of the head and tail winds on the stopping distance was plotted and compared (Figures 23 and 24). In Figure 23, for example, curves have been drawn through 737 and C-141 data points; similar curves could be drawn for the other airplane data points. Since a single curve can describe the variation of both wind velocity and brake application speed, wind velocity need not be considered as an independent variable.

4. CENTER-OF-GRAVITY

The CG location effect considered in the analog simulation was of the form:

$$\Psi = \frac{\mu \cdot LA}{LA + LB + \mu \cdot HB}$$

where LA, LB, and HB are geometric distances (see Table 2), and μ is the coefficient of available friction. Because the CG variation of any correlation ground vehicle would be minimal, and because geometric similarity with an airplane would be almost impossible to achieve, it was decided to consider only the coefficient of available friction as the independent variable.

5. OTHER PARAMETERS

The remaining parameters (ρ and F_e) are independent variables and require no discussion. From the preceding paragraphs, it follows that the pertinent variables are:

- Braking distance (s)
- Available mu (μ)
- C_L/C_D ratio (C_L/C_D)
- Brake application speed (v)
- Air density (ρ)
- Engine idle thrust (F_e)

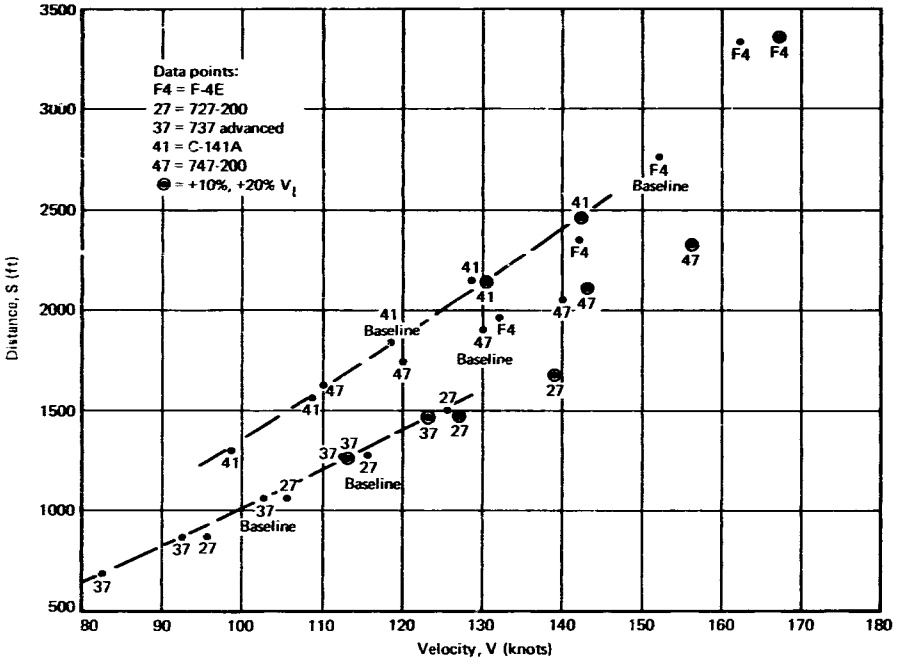

Figure 23.—Effect of Wind at $\pi_2 = 0.6$

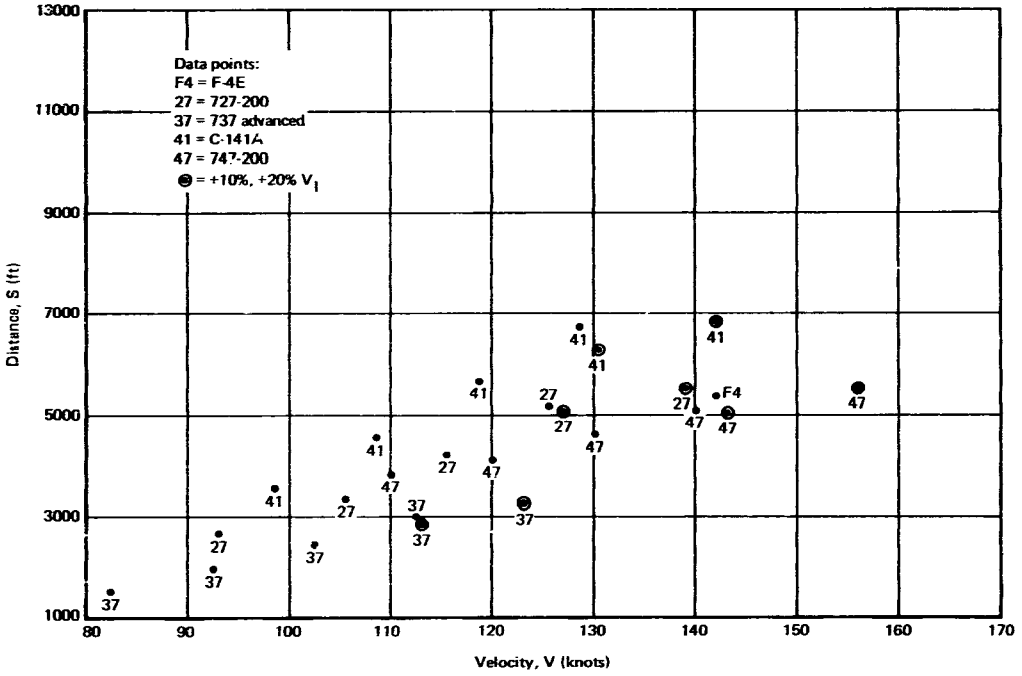

Figure 24.—Effect of Wind at $\pi_2 = 0.2$

SECTION XI

DEVELOPMENT OF PREDICTION MODEL

1. COMPONENT EQUATIONS

The first step in forming a prediction model is to identify the pertinent and independent variables. This step is by far the most important because the validity of the results depends on the correctness with which the pertinent factors are selected. For this study, as explained in Section X, this required the combining of some of the interdependent variables listed in Table 9. The list of resultant independent variables is shown in Table 10.

The second step is to express the secondary quantity (dependent variable) as a function of the primary quantities (independent variables), so that:

$$s = F\,(g, v, \rho, F_e, \mu, C_L/C_D) \tag{1}$$

where:

s = braking stop distance

g = acceleration caused by gravity

The dimensional matrix that can be formed for the fundamental units (mass, length, and time) of the seven parameters in Eq 1 is of rank 3, so that, according to Buckingham's π theorem, these would yield four independent π terms. By inspection and analysis, they can be written (sg/v^2), (μ), (C_L/C_D), and $(\rho v^6/F_e g^2)$. Thus:

$$(sg/v^2) = F\left(\mu, C_L/C_D, \rho v^6/F_e\, g^2\right) \tag{2}$$

or:

$$(\pi_1) = F\left(\pi_2, \pi_3, \pi_4\right) \tag{2a}$$

where:

$\pi_1 = sg/v^2$

$\pi_2 = \mu$

$\pi_3 = C_L/C_D$

$\pi_4 = \rho v^6/F_e\, g^2$

Appendix C shows the detailed analysis of arriving at Eq 2 and Eq 2a. The application of dimensional analysis, including the pi theorem, leads to a type of equation involving an unknown function, of which Eq 2 is an example. Before a prediction equation can be formulated, the nature of the function must be determined. This cannot be accomplished by dimensional analysis, but it can be done from analysis of laboratory observations.

Table 10.—Pertinent Independent Variables

Variable	Notation
Available mu	μ
Brake application speed	v
Drag device effectiveness	C_L/C_D
Engine thrust	F_e
Air density	ρ

The best procedure for evaluating a function is to arrange the observations so that all but one of the pi terms containing the independent variables in the function remain constant. Then the remaining independently variable pi term is varied to establish a relationship between it and the dependent variable (π_1 term). This procedure is repeated for each of the pi terms in the function; the resulting relationships between π_1 and the other individual pi terms are called component equations. Statistical curve fitting computer programs were used to generate the component equations (see Appendix D). A summary of the equations is listed in Table 11.

2. GENERALIZED FUNCTIONS

When the component equations have been determined, they are combined in a certain manner to give a general relationship. It is possible for some of the component equations to be combined by multiplication, while others require addition in the formation of the resultant prediction equation. In general, these two methods are adequate for the majority of engineering problems. For the stopping distance problem, the analysis showed that the prediction equation should be formed by multiplication. The necessary and sufficient conditions to be met for the function to be a product were developed and translated into tests of validity. All aspects of the development of prediction equations discussed in this paragraph are detailed in Appendix E. The major equations of interest are repeated in succeeding paragraphs.

When the component equations (see Table 11) are combined by multiplication, the prediction equation is of the form:

$$\pi_{1'} = (C)\,(\pi_1)_{\bar{3},\bar{4}}\,(\pi_1)_{\bar{2},\bar{4}}\,(\pi_1)_{\bar{2},\bar{3}} \tag{40}$$

where the bar denotes a constant (held) value.

The analysis shows that the value of the constant term C is of the form

$$C = \frac{1}{\left[F\,(\bar{\pi}_2, \bar{\pi}_3, \bar{\pi}_4)\right]^2} \tag{41}$$

Thus the prediction equation is of the form:

$$F\,(\pi_2, \pi_3, \pi_4) = \frac{F\,(\pi_2, \bar{\pi}_3, \bar{\pi}_4)\;F\,(\bar{\pi}_2, \pi_3, \bar{\pi}_4)\;F\,(\bar{\pi}_2, \bar{\pi}_3, \pi_4)}{\left[F\,(\bar{\pi}_2, \bar{\pi}_3, \bar{\pi}_4)\right]^2} \tag{42}$$

Table 11.—Summary of Component Equations

Airplane model	μ*	Equation	Eq No.
727	0.6	$(\pi_1) = 0.7048\ (\pi_2)^{-0.8196}$	(3)
		$(\pi_1) = 1.06869\ (\pi_3)^{[0.3125-0.3375\ \%\ SP]}$ **	(4)
		$(\pi_1) = 2.314\ (\pi_4)^{[-0.06836]}$	(5)
	0.4	$(\pi_1) = 0.7048\ (\pi_2)^{[-0.8196]}$	(3)
		$(\pi_1) = 1.4882\ (\pi_3)^{[0.3090-0.3070\ \%\ SP]}$	(6)
		$(\pi_1) = 4.2724\ (\pi_4)^{-0.09409}$	(7)
	0.2	$(\pi_1) = 0.5648\ (\pi_2)^{-1.125}$	(8)
		$(\pi_1) = 3.7262\ (\pi_3)^{[0.21596-0.13473\ \%\ SP]}$	(9)
		$(\pi_1) = 27.297\ (\pi_4)^{-0.1768}$	(10)
737	0.6	$(\pi_1) = 0.7716\ (\pi_2)^{-0.7647}$	(11)
		$(\pi_1) = 1.1593\ (\pi_3)^{[0.15663-0.018113\ \%\ SP]}$	(12)
		$(\pi_1) = 1.4078\ (\pi_4)^{-0.01951}$	(13)
	0.4	$(\pi_1) = 0.7716\ (\pi_2)^{0.7647}$	(11)
		$(\pi_1) = 1.5637\ (\pi_3)^{[0.16655-0.08663\ \%\ SP]}$	(14)
		$(\pi_1) = 2.1768\ (\pi_4)^{-0.0322}$	(15)
	0.2	$(\pi_1) = 0.7716\ (\pi_2)^{-0.7647}$	(11)
		$(\pi_1) = 2.6687\ (\pi_3)^{[0.16397-0.06279\ \%\ SP]}$	(16)
		$(\pi_1) = 4.8621\ (\pi_4)^{-0.05739}$	(17)
747	0.6	$(\pi_1) = 0.838\ (\pi_2)^{-0.815}$	(18)
		$(\pi_1) = 1.2214\ (\pi_3)^{[0.14803-0.11286\ \%\ SP]}$	(19)
		$(\pi_1) = 1.5162\ (\pi_4)^{-0.01676}$	(20)

* Value of μ used in the data set.

** % SP is the percentage of the spoiler configuration.

Table 11.—Summary of Component Equations (Continued)

Airplane model	μ^*	Equation	Eq No.
747 (Cont.)	0.4	$(\pi_1) = 0.838\ (\pi_2)^{-0.815}$	(18)
		$(\pi_1) = 1.5541\ (\pi_3)^{[0.18957-0.09193\ \%\ SP]}$	(21)
		$(\pi_1) = 2.3966\ (\pi_4)^{-0.03004}$	(22)
	0.2	$(\pi_1) = 0.838\ (\pi_2)^{-0.815}$	(18)
		$(\pi_1) = 2.5185\ (\pi_3)^{[0.2365-0.0818\ \%\ SP]}$	(23)
		$(\pi_1) = 5.4099\ (\pi_4)^{-0.05588}$	(24)
C-141	0.6	$(\pi_1) = 0.876\ (\pi_2)^{-1.0268}$	(25)
		$(\pi_1) = 1.462\ (\pi_3)^{[0.2134-0.13084\ \%\ SP]}$	(26)
		$(\pi_1) = 2.8835\ (\pi_4)^{-0.06129}$	(27)
	0.4	$(\pi_1) = 0.876\ (\pi_2)^{-1.0268}$	(25)
		$(\pi_1) = 2.1846\ (\pi_3)^{[0.23065-0.14819\ \%\ SP]}$	(28)
		$(\pi_1) = 5.6891\ (\pi_4)^{-.08694}$	(29)
	0.2	$(\pi_1) = 0.876\ (\pi_2)^{-1.0268}$	(25)
		$(\pi_1) = 4.51737\ (\pi_3)^{[0.21614-0.16567\ \%\ SP]}$	(30)
		$(\pi_1) = 21.6248\ (\pi_4)^{-0.14344}$	(31)
F-4	0.6	$(\pi_1) = 0.84575\ (\pi_2)^{-0.9239}$	(32)
		$(\pi_1) = 1.4699\ (\pi_3)^{+0.3636}$	(33)
		$(\pi_1) = 2.5323\ (\pi_4)^{-0.04408}$	(34)
	0.4	$(\pi_1) = 0.84575\ (\pi_2)^{-0.9239}$	(32)
		$(\pi_1) = 2.1615\ (\pi_3)^{[0.52698-+0.08287\ \%\ SP]}$	(35)
		$(\pi_1) = 5.8972\ (\pi_4)^{-0.07895}$	(36)

Table 11.—Summary of Component Equations (Concluded)

Airplane model	μ^*	Equation	Eq No.
F-4 (Cont.)	0.2	$(\pi_1) = 0.7337\ (\pi_2)^{-1.0694}$	(37)
		$(\pi_1) = 4.7285\ (\pi_3)^{+0.69738}$	(38)
		$(\pi_1) = 161.9648\ (\pi_4)^{-0.26017}$	(39)

The equations constituting a test for the validity of Eq 42 are shown to be (see Appendix E):

$$\frac{F\,(\bar{\pi}_2, \pi_3, \bar{\pi}_4)\;F\,(\bar{\pi}_2, \bar{\pi}_3, \pi_4)}{\left[F\,(\bar{\pi}_2, \bar{\pi}_3, \bar{\pi}_4)\right]^2} = \frac{F\,(\bar{\bar{\pi}}_2, \pi_3, \bar{\pi}_4)\;F\,(\bar{\bar{\pi}}_2, \bar{\pi}_3, \pi_4)}{\left[F\,(\bar{\bar{\pi}}_2, \bar{\pi}_3, \bar{\pi}_4)\right]^2} \tag{43}$$

or:

$$\frac{F\,(\pi_2, \bar{\pi}_3, \bar{\pi}_4)\;F\,(\bar{\pi}_2, \bar{\pi}_3, \pi_4)}{\left[F\,(\bar{\pi}_2, \bar{\pi}_3, \bar{\pi}_4)\right]^2} = \frac{F\,(\pi_2, \bar{\bar{\pi}}_3, \bar{\pi}_4)\;F\,(\bar{\pi}_2, \bar{\bar{\pi}}_3, \pi_4)}{\left[F\,(\bar{\pi}_2, \bar{\bar{\pi}}_3, \bar{\pi}_4)\right]^2} \tag{43a}$$

The values $\bar{\bar{\pi}}_2$ and $\bar{\bar{\pi}}_3$ are values of π_2 and π_3 held constant at some value other than $\bar{\pi}_2$ and $\bar{\pi}_3$. Thus from the observed data:

$\bar{\pi}_2 = 0.6$ — the primary set of data, for example

$\bar{\bar{\pi}}_2 = 0.4$, $\bar{\bar{\pi}}_2 = 0.2$ — supplementary sets of data

If the supplementary sets of data satisfy either Eq 43 or 43a, the general equation can be formed by multiplying the component equations together and dividing by the constant, as indicated in Eq 42.

This test was applied to all available data (component equations); the results are shown in table 12, clearly indicating the validity of the approach. Table E-1 contains the details of this calculation.

Another test of validity was to calculate the value of the constant term C of Eq 40. The test requires that any of the three component equations should yield an identical value for C. This test was also applied to all the test data; the results are shown in Table 13. Again, the accuracy achieved is satisfactory. Table E-2 contains details of this calculation.

The two validity tests were successful, thus permitting the writing of the prediction equations. A summary of all prediction equations is listed in Table 14. Equation 44 is a combination of Eq 3, 4, 5 and corresponding C. Equation 45 is a combination of Eq 3, 6, 7 and corresponding C, and so on.

Table 12.—Test of Validity for the Function To Be A Product

Airplane model	Value of function in Eq 43			Ideal value of function in Eq 43	Deviation percentage		
	L.H.S. $\bar{\pi}_2$ = 0.6	R.H.S. $\bar{\pi}_2$ = 0.4	R.H.S. $\bar{\pi}_2$ = 0.2		L.H.S. $\bar{\pi}_2$ = 0.6	R.H.S. $\bar{\pi}_2$ = 0.4	R.H.S. $\bar{\pi}_2$ = 0.2
727	1.006	0.997	1.037	1.0	+0.6	-0.3	+3.7
737	1.003	0.996	0.998	1.0	+0.3	-0.4	-0.2
747	1.008	1.002	0.996	1.0	+0.8	+0.2	-0.4
C-141	0.999	0.990	0.997	1.0	-0.1	-1.0	-0.3
F-4	1.010	0.994	0.985	1.0	+1.0	-0.5	-1.5

Table 13.–Test of Validity for Constant Term

Airplane model	$C = \left[1/F\,(\pi_2, \pi_3, \pi_4)\right]^2$			Ideal value of C	Average deviation (%)	Value of π_2
	Component equation used					
	π_1 vs π_2	π_1 vs π_3	π_1 vs π_4			
727	0.8711	0.8504	0.8607	0.8542	+0.8	0.6
	0.4484	0.4553	0.4484	0.4553	-1.0	0.4
	---	0.07935	---	0.07935	---	0.2
737	0.7695	0.7588	0.7665	0.7575	+1.0	0.6
	0.4141	0.4173	0.4208	0.4168	-0.1	0.4
	0.1435	0.1442	0.1440	0.1440	0	0.2
747	0.6190	0.6113	0.6075	0.6113	+0.2	0.6
	0.3199	0.3206	0.3174	0.3206	-0.4	0.4
	0.1033	0.1049	0.1043	0.1049	-0.7	0.2
C-141	0.4533	0.4533	0.4533	0.4533	0	0.6
	0.1982	0.2038	0.2044	0.2038	-0.8	0.4
	0.04773	0.04822	0.04834	0.04834	-0.5	0.2
F-4	0.5430	0.5228	0.5336	0.5414	-1.5	0.6
	0.2571	0.2624	0.2603	0.2624	-0.9	0.4
	---	0.05647	0.05426	0.0561	-1.2	0.2

Table 14.–Summary of Prediction Equations

Airplane model	μ*	Equation	Eq No.
727	0.6	$(\pi_1) = 1.5001\ (\pi_2)^{-0.8196}\ (\pi_3)^{[0.3125-0.3375\ \%\ SP]}\ (\pi_4)^{-0.06836}$	(44)
	0.4	$(\pi_1) = 2.0197\ (\pi_2)^{-0.8196}\ (\pi_3)^{[0.3090-0.30107\ \%\ SP]}\ (\pi_4)^{-0.0941}$	(45)
	0.2	$(\pi_1) = 4.558\ (\pi_2)^{-1.125}\ (\pi_3)^{[0.2159-0.1347\ \%\ SP]}\ (\pi_4)^{-0.1768}$	(46)
737	0.6	$(\pi_1) = 0.9632\ (\pi_2)^{-0.7647}\ (\pi_3)^{[0.1567-0.08113\ \%\ SP]}\ (\pi_4)^{-0.01951}$	(47)
	0.4	$(\pi_1) = 1.096\ (\pi_2)^{-0.7647}\ (\pi_3)^{[0.16655-0.08663\ \%\ SP]}\ (\pi_4)^{-0.03222}$	(48)
	0.2	$(\pi_1) = 1.4409\ (\pi_2)^{-0.7647}\ (\pi_3)^{[0.16397-0.06279\ \%\ SP]}\ (\pi_4)^{-0.05739}$	(49)
747	0.6	$(\pi_1) = 0.9539\ (\pi_2)^{-0.815}\ (\pi_3)^{[0.14803-0.11286\ \%\ SP]}\ (\pi_4)^{-0.01676}$	(50)
	0.4	$(\pi_1) = 0.9974\ (\pi_2)^{-0.815}\ (\pi_3)^{[0.18957-0.09193\ \%\ SP]}\ (\pi_4)^{-0.03004}$	(51)
	0.2	$(\pi_1) = 1.1897\ (\pi_2)^{-0.815}\ (\pi_3)^{[0.2365-0.0818\ \%\ SP]}\ (\pi_4)^{-0.05588}$	(52)
C-141	0.6	$(\pi_1) = 1.6814\ (\pi_2)^{-1.0268}\ (\pi_3)^{[0.21341-0.13084\ \%\ SP]}\ (\pi_4)^{-0.06129}$	(53)
	0.4	$(\pi_1) = 2.20115\ (\pi_2)^{-1.0268}\ (\pi_3)^{[0.23065-0.14819\ \%\ SP]}\ (\pi_4)^{-0.08694}$	(54)
	0.2	$(\pi_1) = 4.1160\ (\pi_2)^{-1.0268}\ (\pi_3)^{[0.21614-0.16567\ \%\ SP]}\ (\pi_4)^{-0.14344}$	(55)
F-4	0.6	$(\pi_1) = 1.6790\ (\pi_2)^{-0.9239}\ (\pi_3)^{-0.3636}\ (\pi_4)^{-0.04408}$	(56)
	0.4	$(\pi_1) = 2.80256\ (\pi_2)^{-0.9239}\ (\pi_3)^{[0.52698+0.08287\ \%\ SP]}\ (\pi_4)^{-0.07895}$	(57)
	0.2	$(\pi_1) = 31.52\ (\pi_2)^{-1.0694}\ (\pi_3)^{-0.69738}\ (\pi_4)^{-0.26017}$	(58)

* Value used to derive the equation.

SECTION XII

MODEL-TO-SIMULATOR CORRELATION

The prediction equations were next used to correlate back with the stopping distance data collected in the Task I simulation. A summary of errors in correlation is listed in Table 15.

The limitations (range of validity) of the prediction equations are:

- Equations 47 through 55 are applicable for μ values of 0.1 to 0.6.
- Equations 44, 45, 56, and 57 are applicable for μ values of 0.3 to 0.6
- Equations 45 and 58 are applicable for μ values of 0.1 to 0.2 only.

For a given airplane model, the three prediction equations are interchangeable, alternate solutions if their range of applicability and validity is common. Thus, Eq 45 and 58 are unique solutions and not interchangeable with their counterpart Eq 44 and 45, or 56 and 57. Some airplane systems need only one prediction equation to define the entire range of μ values tested on the simulator; others needed more than one equation. The reason for this can be comprehended by studying braking distance efficiency curves for the various systems as shown by Figure 25.

Braking distance efficiency, η_s, is defined as the ratio of the perfect braking distance to the braked airplane distance resulting from the simulation.

$$\eta_s = X_p/X_a \times 100\%$$

where:

η_s = braking distance efficiency

X_p = perfect braking distance

X_a = airplane braking distance

The perfect braking distance is the distance required to stop the airplane if it is braked for the entire stop with maximum available braking force. Braking distance efficiency indicates the degree to which the system meets its primary requirement of stopping the aircraft.

The skid control systems for the five subject airplanes encompass three generations of technology namely the old, intermediate, and an advanced type. A study of Figure 25 shows that the curves for the advanced technology system is nearly linear, sharp changes in slope appear in the curves for the old as well as the intermediate technology systems at μ values of 0.3. Piecemeal linearization is always required when writing mathematical relationships for curves of the type shown for the old and intermediate technology systems. That is why

Table 15.—Summary of Percentage Errors

Airplane model	Using equation	Applied to data at $\overline{\pi}_2$	Error range (%)
727	(44)	0.6	-2.9 to +4.8
		0.4	-5.0 to +3.5
	(45)	0.4	-4.8 to +1.9
		0.6	-4.9 to +5.0
	(46)	0.2	-4.9 to +3.7
737	(47)	0.6	-1.7 to +1.8
		0.4	-1.2 to +3.9
		0.2	-3.6 to +3.1
	(48)	0.6	-3.4 to +1.3
		0.4	-1.0 to +1.8
		0.2	-3.1 to +4.6
	(49)	0.6	-4.9 to +1.8
		0.4	-2.9 to +2.6
		0.2	-2.0 to +2.0
747	(50)	0.6	-1.7 to +2.0
		0.4	-1.3 to +2.5
		0.2	-1.8 to +4.8
	(51)	0.6	-3.2 to +0.9
		0.4	-1.8 to +1.6
		0.2	-1.6 to +3.9
	(52)	0.6	-5.0 to +2.4
		0.4	-3.9 to +2.3
		0.2	-1.1 to +2.6
C-141	(53)	0.6	-1.9 to +4.0
		0.4	-2.6 to +4.8
		0.2	-1.1 to +2.7
	(54)	0.6	-4.0 to +2.7
		0.4	-1.0 to +1.2
		0.2	-1.3 to +3.2
	(55)	0.6	-4.7 to +2.2
		0.4	-4.4 to +3.4
		0.2	-1.7 to +1.7
F-4	(56)	0.6	-2.9 to +0.7
		0.4	-5.6 to +5.0
	(57)	0.4	-5.4 to +5.4
		0.6	-6.7 to +7.3
	(58)	0.2	-1.7 to +3.3

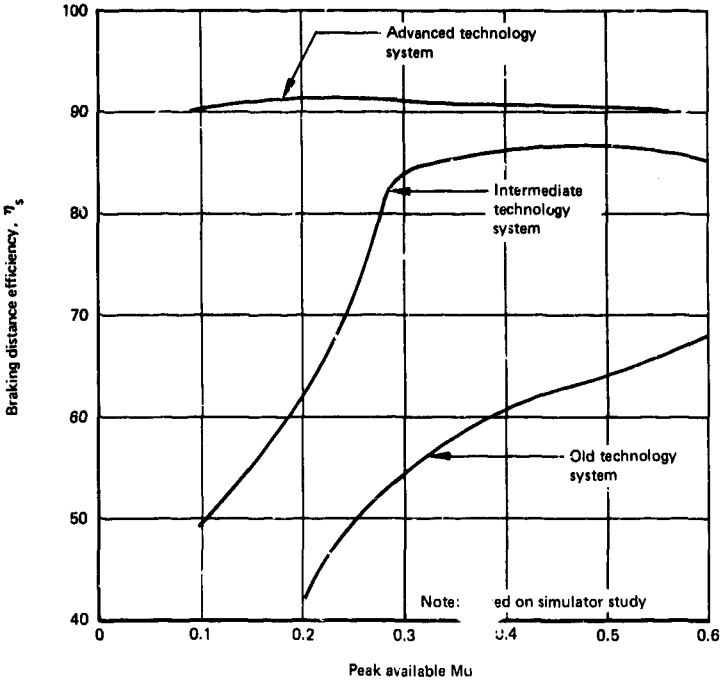

Figure 25.—Mu-Efficiency Curves

more than one prediction equation was necessary to treat these two cases. Performance deficiency of the old and intermediate systems at low μ values has led to the development of advanced systems.

The correlation data error summary (Table 15) indicates that, for almost all conditions, a prediction accuracy of ±5% can be achieved.

Even though in the correlation process, comparison was made between predicted and actual π_1 values, that is:

$$(sg/v^2)\text{pred vs } (sg/v^2)\text{actual}$$

it is tantamount to comparing the braking stop distances because both terms use identical g and v values, and the distance term s has no exponent. For example, from 727 correlation calculations:

$$(\pi_1)_{pred} = 1.078; (\pi_1)_{actual} = 1.082; \text{error percentage} = -0.4$$

$$(s)_{pred} = 1273 \text{ ft}; (s)_{actual} = 1278 \text{ ft}; \text{error percentage} = -0.4$$

SECTION XIII

MODEL-TO-SIMULATOR QUALITATIVE COMPARISON

1. PREDICTED MU FROM FLIGHT TEST DATA

The credibility of the simulator was established by comparing the simulator and airplane flight test data and showing that similar trends were obtained under identical conditions (see Section VIII). The credibility of the prediction model has been established by obtaining a ±5% correlation accuracy in predicting simulator stopping distances. The next logical step is to determine if the airplane flight test data could be correlated to the prediction model. The results of this exercise are shown in Table 16. From the type of information available on the flight test data (Table 16) the only parameter that could be calculated by the prediction equation was the friction coefficient. The predicted values, for both dry and wet runway conditions, appear reasonable.

2. WET-RUNWAY ANALYSIS

During Task I simulation testing, a wet runway was simulated so that the available ground mu was programmed to vary with speed. (See Figure 26). The mu values (end points) used were 0.05 at brake application speed and 0.5 at the end of the stop.

The average value of peak available mu for the braking system was unknown, so it was decided to use the component equations formed earlier (the π_1 versus π_2 relationships) to calculate peak available mu. Based on calculations for wet runways, prediction equations were generated for wet runway cases. With these prediction equations, a correlation prediction accuracy analysis was conducted as before and satisfactory results were obtained. The details of this analysis are reported in ASD-TR-74-41,Volume II, Section XVI. The results gave additional confidence to the selected methodology for forming prediction equations.

3. DATA VALIDITY

Yet another test of the prediction equations came about accidently. During the correlation process, in spite of excellent correlation an unusually high error would result for one or two conditions, even though there was close correlation between predicted and actual distances. This happened with three airplanes. When the raw data from Task I was rechecked, bookkeeping errors were discovered in the conditions that produced the anomalies. Thus the prediction equation was able to sort out the unusual cases that failed to fit the pattern, pointing out bad data.

Table 16.—Qualitative Comparison with Flight Test Data

Airplane	Condition No.	Flight test data			Calculated mu using prediction equation	Type of runway
		Application speed (fps)	Braking distance (ft)	$\frac{C_L}{C_D}$		
727	181-16 3.15.49.25	176	1163	0.553	0.549	Dry
737	29-35 1.20.65.001.1	198	1348	0.880	0.314	Dry
747	8-4 1.20.051.006	199	1841	3.722	0.489	Dry
747	.004	241	2552	3.722	0.526	Dry
F-4	Run 4	238	3400	0.846	0.422	Dry
F-4	Run 23	222	6221	0.846	0.24	Wet

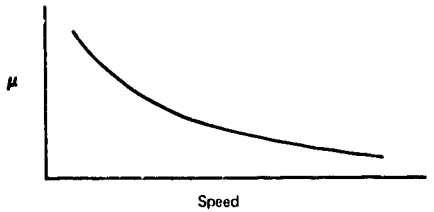

Figure 26.—Mu-Velocity Curve for Wet Runway

SECTION XIV

DETERMINATION OF VEHICLE CRITERIA

The formulation of the prediction equation has been accomplished with the use of dimensional analysis. In arriving at the equation, a complex dynamic process was duplicated with a hardware-analog brake control simulation. Comparison between actual airplane stops and the simulation indicated similar braking performance and established a high degree of confidence in this approach. The effect of parameter variations on stopping distance was then examined on the brake control simulator and compared to baseline data. Parameters that changed the stopping distance by more than 2% were considered significant and included in the dimensional analysis. The resulting prediction equation appears with the general format:

$$sg/v^2 = C(\mu)^{\alpha}(C_L/C_D)^{\beta}(\rho v^6/F_e g^2)^{\delta}$$

The equation has four different nondimensional terms. The dependent term represents a distance, s, which is normalized with the gravitational constant, g, and the aircraft velocity, v, relative to the ground at brake application. Head or tailwinds can affect the airplane velocity at touchdown and must be taken into consideration. In addition, pilot technique plays a major part in the determination of touchdown velocity. The dimensionless coefficient, μ, is the peak friction coefficient generated at the tire-runway interface under dynamic conditions of the braking process. For wet runway conditions, this "mu" can be obtained using the technique shown in ASD-TR-74-41, Volume II, Section XVI. The aerodynamic term, C_L/C_D, is a ratio of lift coefficient, C_L, and drag coefficient, C_D, of the airplane on the ground in braking configuration. Variations in these coefficients result from the use of different flap settings, spoilers, and drag devices. The last term, $\rho v^6/F_e g^2$, is a combination of runway, altitude, and temperature information as expressed in air density, ρ, and total engine idle thrust during braking. The exponents α, β and δ and the coefficient C result from the sensitivity study and the dimensional analysis. For each airplane, a unique coefficient and set of exponents exist.

The equation permits the calculation of the airplane stopping distance, assuming proper information of airplane and weather parameters and an accurate and meaningful measurement or prediction of the tire-runway friction coefficient. In turn, when the length of a specific runway is known, the safety margin for a landing and the last point for safe brake application can be determined. The most elusive value in the equation is an adequate value for the tire-runway friction coefficient. This is the peak value developed under the dynamic conditions of braking and is represented in the hardware-analog simulation with a friction slip curve. The dimensionless appearance of the prediction equation of similtude and the friction coefficient must be derived and measured for a similar process. Hence the following conditions must be observed.

Deceleration Process: The tire is deformed by shear forces in the braking process, and a shift in the footprint occurs.

Rotating Wheel: During the braking process, the wheel is controlled with an antiskid device that protects it from lockup and continuously hunts for the peak friction value.

Energy Absorbed in Brake: This implies that the major portion of the energy absorption is taking place in the brake. While braking can be realized with a locked wheel, the true dynamic process must be similar to that taking place on the braked airplane wheel.

Distance Generated: A measurable ground stopping distance must be available as a data point. Hence, braking should be continuous from the time of brake application until a full stop is reached.

Aircraft Tire: While similar in function, aircraft and automobile tires are different in construction. Notably, the inflation pressure of aircraft tires is much higher than in automotive tires, and the theoretical hydroplaning speed is directly affected. The footprint area of an automobile tire is rectangular with a constant width, while that of the airplane tire is elliptical.

Design criteria for a ground vehicle used in the prediction process must consider the above factors. Dynamic similtude could be obtained with the use of a model airplane with a brake system similar to those of existing systems. This would result in a complex and costly approach; in many cases, it would not be practical to fly the model. It appears that the most desirable approach would involve a vehicle that demonstrates dynamic similarity in the braking process. This could be a ground vehicle equipped with airplane tires (Type VII) and a suitable antiskid system. The vehicle could be used in predicting a meaningful tire-runway friction coefficient as shown in Figure 27. The approach outlined here is similar to that used in arriving at the airplane prediction equation. Simulation of the vehicle and its brake control system would permit a sensitivity study to define a stopping distance prediction equation based on the most important parameters. Most likely, the equation would be in a similar format as that developed for the airplanes. Rearrangement of the equation results in the formulation of the ground friction coefficient. Vehicle use will require the measurement of stopping distance and brake application speed. Combination of this data with all other required parameters will result in the calculation of the dynamic ground friction coefficient. The criteria are established in reference to the developed airplane prediction equation and the dynamic process it describes. Other desirable characteristics for such a ground vehicle are ease of maintenance, safe and simple operation, and a data collection system with minimum complexity. The last of these requirements appears to be met by existing ground vehicles such as the Diagonally Braked Vehicle (DBV) and the Mu-Meter. However, dynamic similarity of the tires used is absent. The DBV is a standard automobile that allows the full lockup of one front and one rear wheel. Stopping distances are measured and compared for different runway conditions. The Mu-Meter is a trailer that derives the friction coefficient through a side force measurement between two yawed tires. The vehicle is towed at constant, speed and the measurement of friction coefficient is continuous. Neither vehicle duplicates the requirements implied by the prediction equation. More details and a dimensional analysis of both ground vehicles is given in Appendix F.

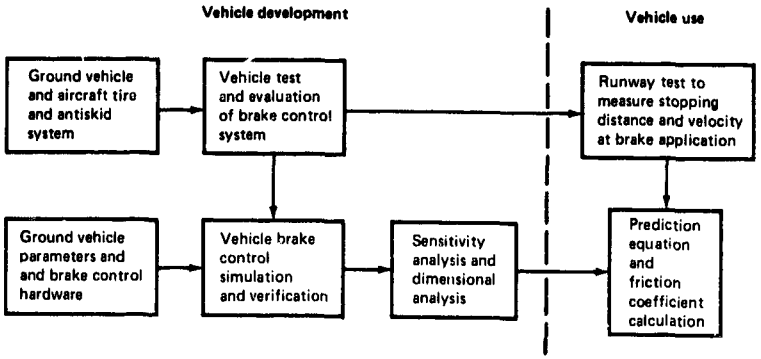

Figure 27.—Recommended Ground Vehicle Criteria

SECTION XV

EVALUATION OF DBV AND MU-METER

For the prediction equations to be operationally meaningful, it is necessary to accurately measure ground friction (available mu). Two ground vehicles--NASA Diagonally Braked Vehicle (DBV) and British Mu-Meter--have been tested extensively with varying degrees of aircraft-to-vehicle correlation accuracy (Refs. 2 through 8). Both vehicles have qualitative merit, but neither has the quantitative correlation capability required for the prediction equations.

To close the gap between the results of ground vehicles and aircraft measurements, the physical and operational reasons for the differences were investigated. Existing ground vehicles use relatively low pressure, light motor vehicle tires, while all aircraft tires are high pressure. Figure 28 and Table 17 compare an aircraft tire and a light motor vehicle tire. To expect a good correlation between the two tire-vehicle combinations without accounting for all the differences shown is not prudent. Thus, no existing ground vehicle meets the most fundamental and important requirement established herein of using a proper tire.

By applying model laws to the pi terms developed earlier, certain model design conditions can be identified. Subscripts m denote quantities relating to the model, and subscripts p denote quantities relating to the prototype. Sufficient conditions for the equality of μ_m and μ_p are (see Appendix F):

$$(C_L/C_D)_m = (C_L/C_D)_p \tag{59}$$

$$v_m = (\lambda)^{1/6} v_p \tag{60}$$

$$s_m = (\lambda)^6 s_p \tag{61}$$

where: $\lambda = W_m/W_p$, which is the weight scale ratio.

For reasons explained in Appendix F, no ground vehicle can satisfy Eq 59. When such is the case, that is, when a model fails to satisfy one or more of the design conditions, it becomes a distorted model. This can be properly accounted for by introducing the so-called prediction and distortion factors into the prediction equation. For example, for the current problem, the distortion factor is of the form (see Appendix F for detailed analysis):

$$\delta = a^{-[C_3 - C_4 \% SP]} \tag{62}$$

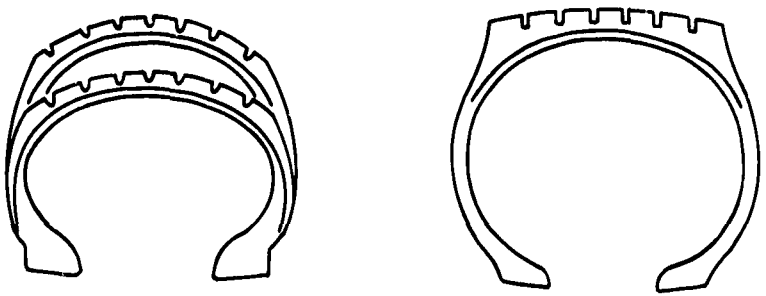

Normal and low-profile aircraft tire sections

Light motor vehicle tire section

Figure 28.—Comparison of Tire Sections

Table 17.—Comparison of Aircraft and Automotive Tires

Parameter	Airplane tire	Ground vehicle tire	Remarks
Tire footprint	Elliptical	Rectangular	Aircraft tire is primarily a torodial carcass with small additional tread rubber. Automotive tires use heavy tread, particularly in the shoulder region (Ref. 9).
Tire thread design	Natural rubber base	Synthetic rubber base	Synthetic rubber base materials can produce significantly higher μ on wet runways (Ref. 10).
Tire tread design	● Light tread ● High stiffness ● High aspect ratio	● Heavy tread ● Low stiffness ● Low aspect ratio	High mileage life and absorption of road surface shocks are criteria for automotive tire. Prevention of excessive loading of the runway surface is major criterion for aircraft tires (Ref. 11).
Tire deflection range	30 to 35%	12%	Deflection is defined as percentage of the height of the crown above the wheel rim (Ref. 11).
Hydroplaning inception speed (V_{cr})	● $V_{cr} = 9\sqrt{psi}$ ● Reversion possible for all tires	● $V_{cr} = K\sqrt{psi}$ for constant deflections. ● Reversion possible only if pi $>$ 50 psi and v $>$ 60 mph	Tire stiffness can be a factor in determing the hydroplaning inception speeds for smaller size (model) tires (Ref. 12).

where:

δ = prediction factor

α = distortion factor

and C_3, C_4 are exponents determined experimentally. See Table F-1 for a list of distortion factors to be used with various prediction equations derived.

When these criteria are applied to the NASA DBV, it fails to satisfy Eq 59, and no compensation was made during correlation analysis for the model distortion. When the criteria in Eqs 60 and 61 are applied to the baseline conditions of Tasks I and II, the results are as shown in Table 18.

Table 18 shows that with vehicle weight held constant, a different velocity is necessary each time a different condition is being run. Similarly v_m could be held constant and W_m would become a variable. In the case of DBV, however, both the weight and velocity were constants at 5200 lb and 60 mph, thus violating model laws. This situation could be corrected by running the vehicle tests for a range of speeds at constant weights and establishing a relationship between vehicle speed and distance under various runway conditions.

A slightly different approach was tried in evaluating the mu-meter to apply the model theory to its data. Only the NASA Wallops airport data of Ref. 3 was evaluated. Table F-2 shows the raw data taken from Ref. 3. Since the data shows the mu-meter average friction reading for each run and the corresponding stopping distance used by the 727, it was decided to calculate the average friction (μ) used by the airplane by applying the prediction equation for the model 727 arrived at earlier so that the two friction readings could be compared. The details of calculating π terms are shown in Table F-3, and the comparison is shown in Table 19 and plotted in Figure 29.

The comparison clearly indicates the randomness of the data and the missing quantitativeness. Another interesting point is observed by comparing runs 13 and 17. Both runs were conducted on section A-G of the runway, run 13 under wet conditions (water 0.01 in. deep) and run 17 under dry conditions. The mu-meter indicated a higher friction reading for run 13 than for 17, while the resulting airplane tire mu was closer to anticipated values.

The mu-meter is a continuous-recording trailer that measures the side force generated between the test surface and two pneumatic tires that are set at a fixed toe-out angle of 7.5 degrees to the line of drag. The available side load thus recorded is reported as a measure of the surface friction.

The above statement implies a few broad assumptions that may not be true for actual aircraft tire operation. For example:

- At a 7.5-degree yaw angle, the tire may not have reached the maximum and limiting tire-runway friction condition on a dry runway.

Table 18.—DBV Correlation Requirements

Airplane	V_p (mph)	S_p (ft)	V_m (mph)*	S_m (ft)
727	133.0	1278	78.3	443
737	118.0	1068	74.0	421
747	149.3	1905	69.5	413
C-141	136.4	1841	71.0	500
F-4	174.5	2766	127.0	1465

*W_m = 5200 lb = W_{DBV}

Table 19.—Mu-Meter Correlation Requirements

Run No.	Airplane average friction, calculated	Mu-meter average friction reading	$\frac{\text{Mu-meter } \mu_{avg}}{\text{Airplane } \mu_{avg}}$	Surface condition
10	0.518	0.810	1.564	Dry
11	0.524	0.810	1.546	Dry
13	0.391	0.766	1.959	Wet
14	0.439	0.760	1.731	Dry
17	0.454	0.760	1.674	Dry
18	0.304	0.674	2.217	Wet
21A	0.318	0.718	2.258	Wet

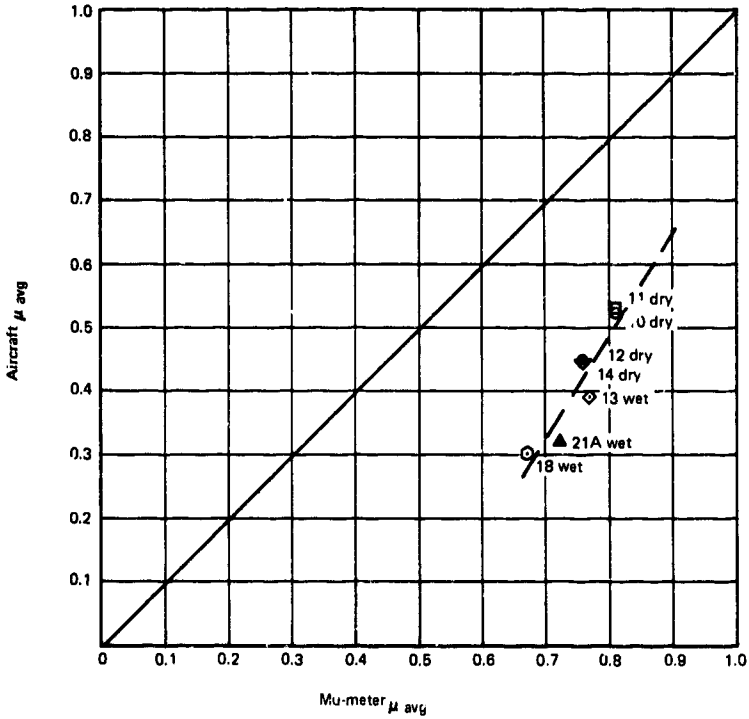

Figure 29.—Mu-Meter Evaluation

- Experimental data on tire cornering on wet runways show that the cornering coefficient reaches a maximum value at a critical yaw angle and then decreases with further increase in yaw angle. Thus, if the critical yaw angle is different than 7.5 degrees, the mu-meter reading will underestimate peak μ cornering.

In summary, Figures 28 and 29 and Tables 17 and 18, and 19 clearly show the inadequacy of the existing ground vehicles in meeting the previously developed criteria.

SECTION XVI

CONCLUSIONS AND RECOMMENDATIONS

1. CONCLUSIONS

The following conclusions have been arrived at from the analysis of the available data gathered during this program.

- A dimensional analysis technique can successfully express braking phenomena in the form of a mathematical (model) equation.
- Experimental data from an airplane braking distance sensitivity study are needed to determine the constants and exponents in the model equation leading to a prediction model equation.
- With the proper information of airplane and weather parameters and an accurate and meaningful measurement of the tire-runway friction coefficient, airplane braking distances can be predicted within reasonable tolerances.
- The most important requirements for a vehicle to accurately measure tire-runway interface friction are the selection of a proper tire, (preferably an aircraft type of tire) and a faithful reproduction of the interface dynamics, such as the use of a skid control system.
- Existing ground vehicles (DBV and mu-meter) fail to meet the criteria described herein and are distorted or dissimilar models.

2. RECOMMENDATIONS

If a suitable ground vehicle were available, a method to predict stopping distance could be outlined as shown in Figure 30. The ground vehicle is operated on the runway to measure brake application speed and stopping distance. Based on an earlier prediction equation, a ground friction coefficient can be calculated using the vehicle parameters and runway test data as an input. It is anticipated that the resulting ground friction coefficient cannot be directly applied to the airplane prediction equation unless some data on tire correlation is applied. Because the size and power of a ground vehicle are limited, the test tire should be a small aircraft tire. Because aircraft tires of many sizes are being used, a scaling factor must be applied to relate aircraft tire performance from the size on the test vehicle to other sizes. It appears that this body of data must still be generated.

Weather conditions can change rapidly, and a repeated and frequent prediction of the tire-runway friction coefficient may not always be practical. For instance, a short but heavy thundershower may change a dry runway to a flooded one. A correction factor for water accumulation on the runway would eliminate the need for an immediate new ground vehicle

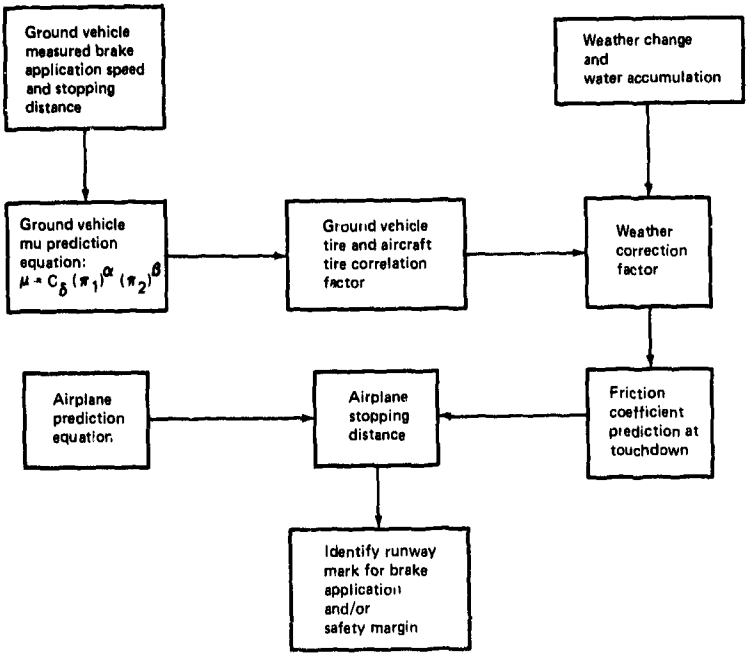

Figure 30.– Recommended Prediction Methodology

friction measurement. It is anticipated that in some circumstances, such as snow, ice and slush, a weather correction factor could be obtained only through a direct ground friction measurement by the vehicle. The runway friction coefficient could then be used in the prediction equation along with the specific airplane parameters to calculate the stopping distance. By a comparison to available runway lengths, a safety margin and brake application point on the runway can be established. Finally, the prediction model approach needs to be verified on additional aircraft, especially fighter types, to extend the application base.

REFERENCES

1. Amberg Robert L., *Baseline Simulation for Evaluation of Brake Antiskid Systems,* Boeing Document D6-58384-3TN, 1969

2. "Equipment, Procedures and Services; Runway Surface Conditions Including Snow, Slush, Ice and Water," ICAO, *Aerodrome Manual,* Part 5, Chapter 2, Montreal, 1964

3. Horne, W.B., et al., "Traction Measurements of Several Runways Under Wet and Dry Conditions with a Boeing 727, a Diagonal-Braked Vehicle, and a MU-Meter," LWP-1016, December 1971

4. Horne, W.B., et al., "Traction Measurements of Several Runways Under Wet and Dry Condition with a Douglas DC-9, a Diagonal-Braked Vehicle, and a MU-Meter," LWP 1051, September 1972

5. Yager, T.J., et al., "A Comparison of Aircraft and Ground Vehicle Stopping Performance on Dry, Wet, Flooded, Slush-Snow, and Ice-Covered Runways." NASA Technical Note D-6098, November, 1970

6. Horne, W.B., and J.A. Tanner, "Joint NASA-British Ministry of Technology Skid Correlation Study–Results from American Vehicles," *Pavement Ground and Traction Studies,* the proceedings of a conference held at Langley Research Center, Hampton, Virginia, U.S.A., Paper 23, NASA SP-5073, November 1968

7. Sugg, R.W., "Joint NASA-British Ministry of Technology Skid Correction Study–Results from British Vehicles," *ibid,* Paper 24, November 1968

8. Wyrick, D.R., "Model L-1011-1 (Base Aircraft) Landing Performance Report for FAA Evaluation of Concorde SST, Special Condition 25-43-EU-12, Report No. LR26267, January 1974

9. Clark, Samuel K., Editor, "Mechanics of Pneumatic Tires," National Bureau of Standards Monograph 122, 1971

10. "Frictional and Retardation Forces on Aircraft Tires, Part 1: Introduction," R.A.E. Engineering Sciences Data Unit Item No. 71025, August 1972

11. Hadekel, R., "The Mechanical Characteristics of Pneumatic Tires," Ministry of Supply S&T Memorandum 10/52, November 1952

12. Albert, B.J., SAE Paper No. 680140, Auto. Engr. Cong., Detroit, Michigan 1968

13. Murphy, Glenn C., *Similitude in Engineering,* The Ronald Press Co., New York, 1950

14. Baker, W. E., and J.S. Wilfred, *Similarity Methods in Engineering Dynamic Theory and Practice of Scale Modeling*, Spartan Books, 1973

15. *CTS Statistical Package (STAT-PK)*, Boeing Computer Services (BCS), 1974

APPENDIX A

CALCULATION OF APPROACH, FLARE, AND TRANSITION DISTANCES

Approach, flare and transition distances were calculated with the aid of a digital program. The equations used in the program along with the assumptions required are listed in succeeding paragraphs. Figure A-1 helps to define the significant variables involved.

1. Approach Distance

Approach distance was calculated as:

$$SA = 57.30H/\gamma$$

where:

SA = approach distance in feet
H = height above threshold in feet
γ = glide slope in degrees.

This equation assumes no speed loss during the approach and that γ is a small angle (for example, $\tan \gamma = \gamma$).

2. Flare Distance

To calculate flare distance, a constant centripetal acceleration has been assumed to exist during the flare. This assumption results in:

$$SF = 0.000271\ V^2\gamma/n\text{-}1$$

where:

SF = flare distance in feet
V = approach speed in feet per second
γ = glide slope in degrees
n = flare load factor $> 1.0 = \dfrac{\text{centripetal acceleration}}{\text{gravitational acceleration}}$

3. Transition Distance

During the transition segment, the pilot may initiate various actions that can affect the aerodynamics of the aircraft. To account for such actions, the digital program used a time-dependent step integration routine to calculate transition distance. The basic procedure involves two steps. During any one time period, an aircraft deceleration is first calculated. Based on this deceleration and the initial aircraft speed at the start of the time period, a final aircraft speed is calculated. The distance is then computed from the initial and final velocities over the known time interval. This procedure is repeated until braking is initiated. The applicable equations are:

$$a = (FE - FD - FB)/M$$

$$VF = VI - (a \cdot T)$$

$$DS = 0.5\,(VI + VF)\,T$$

$$ST = \Sigma\, DS$$

where:

- a = aircraft deceleration
- FE = aircraft thrust
- FD = aircraft drag force
- FB = aircraft braking (rolling friction) force
- M = aircraft mass
- T = time interval
- VI = initial aircraft velocity
- VF = final aircraft velocity
- DS = distance traveled during a time interval
- ST = total transition distance

Airplane thrust, drag, and braking forces are a function of vehicle velocity. Thus, deceleration changes throughout the transition segment.

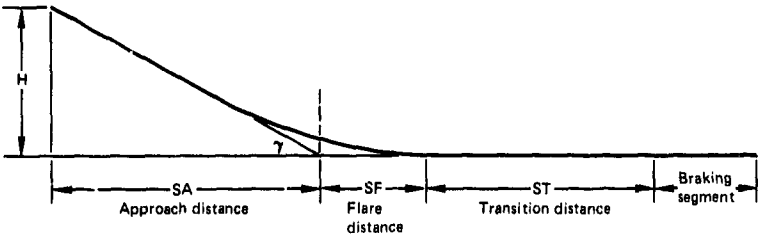

Figure A-1.—Air and Transition Distances

APPENDIX B

BOEING BRAKE CONTROL SIMULATION

The simulator is an analog-hardware system. The aircraft dynamics are simulated using analog computer equipment. Wherever possible, actual aircraft components are used instead of simulation. This approach is used to provide a more accurate simulator, particularly in areas where nonlinearities and complicated dynamics exist. An added benefit of reduced computer requirements is also realized.

The simulation can be divided into six sections:

- Hardware
- Airplane dynamics
- Strut dynamics
- Wheel dynamics
- Brake torque simulation
- Ground force simulation

The relationships and interactions between these elements are shown in a detailed block diagram of the simulation (Figure B-1). The detailed mathematical models are developed in Ref. 1.

1. Hardware

The hardware portion of the simulation consists of the brake system hydraulics, skid control card or box, skid control valve, instrumentation, and signal conditioning equipment. The hydraulic portion of the simulator includes all hydraulic components that can influence brake system performance. The actual hydraulic system mockup typically includes the pilot's metering valve, antiskid valves, accumulators, pumps, supply and return lines, reservoir, and the brakes. In this way, the hydraulic system characteristics, including any nonlinearity, are accurately simulated. Actual antiskid control circuit cards are used in the simulator to ensure that the overall function, nonlinearities, component characteristics, and system tolerances are accurately reproduced. Unless these components are reproduced precisely, the usefulness of the results can be seriously jeopardized. The signal conditioning portion requires that a DC voltage proportional to wheel speed (from the computer) be converted to a frequency-modulated signal. The FM signal is the input to the control box. Brake pressure is monitored and becomes an input to the computer for use in the brake torque simulation.

2. Airplane Dynamics

A three-degree-of-freedom model is used to simulate airplane dynamics. The model includes the vertical and pitching degrees of freedom in addition to the horizontal degree of freedom (braked airplane). The vertical and pitching modes are used to account for dynamic changes in the vertical reaction between the tire and runway. The braked airplane simulation includes the effects of aerodynamic forces, engine thrust, and ground force.

3. Strut Dynamics

The strut, a very important aspect of the simulation, is modeled with a two degree of freedom system. The model accounts for the fore and aft deflection of the axle centerline and the torsional deflection of the end of the strut. The effects of the strut motion on the ground force, airplane dynamics and measured wheel velocity are also included.

Special attention is given to modeling the natural frequency and the damping of the gear. This is done by determining an effective strut mass and fore-aft stiffness which yields a natural gear frequency which is compatible with airplane records.

4. Wheel Dynamics

The wheel dynamics simulation uses the ground force and the brake torque to develop a wheel velocity. The simulation of ground force and brake torque are carried out by separate models as described in the paragraphs below. Data used in this portion of the simulation of the tire and wheel was obtained directly from the tire manufacturers' published data.

5. Brake Torque Simulation

Although the actual brake is used for the hydraulic load, the brake does not serve as a torque producing element in the simulator. The signal generated by the brake pressure transducer is used as an input signal to the brake torque simulation which includes torque gain, dynamic response retractor spring deadband, torque peaking and brake fade. The model used in the brake simulation is the result of extensive research including both full scale brake testing (dynamometer and airplane) and small scale brake lining evaluation. Some of the dynamometer brake tests were carried out under two recent funded Air Force contracts (F33615-73-C-3017 and F33615-72-C-1015).

6. Ground Force Simulation

The ground force simulation is used to develop the horizontal force acting between the tire and ground. The method used is based on an experimentally determine ' relationship between the ground friction coefficient and the percent slip of the tire, o. Tire heating effects are also considered in the model.

The effects of a wet or contaminated runway are also reproduced in the wheel and tire/ground force portion of the simulation. The significance of vehicle velocity on the friction coefficient and the path clearing effect of the forward tire of truck type landing gear are considered. Data from Boeing flight tests and from NASA/AF/FAA tests was used in developing this portion of the simulation.

7. Nonlinear Relationships

Several nonlinear relationships were used in the aircraft simulation. These relationships required special implementation on the computer. The nonlinear functions used were:

- Wet runway curve
- Touchdown profile
- Brake torque-pressure relation for two conditions:
  - $T = f(p)^{0.5}$
  - $T = f(p)^{0.73}$
- Mu-slip curves
- Power spectral density curve of rough runway test

The actual relationships used are documented in Figures B-2 through B-6. In addition, each relationship is briefly described in the following paragraphs.

(a) Wet Runway Curve.—The friction coefficient obtained between the tire and ground on a wet runway is a function of aircraft velocity (Figure B-2). Characteristically, friction increases as airplane speed decreases. The wet coefficient of friction was produced on the simulator by subtracting a velocity-dependent function (Figure B-2) from the maximum value of friction available on the wet surface.

(b) Touchdown Profile.—The touchdown profile as implemented on the simulator is a time-dependent function that modifies the main gear load (Figure B-3). The function was modeled after typical bounce conditions seen during commercial aircraft landings.

(c) Nonlinear Torque Gain Curves.—The static torque-pressure curve of a typical aircraft brake is a nonlinear function (Figure B-4). The curve shape is dependent on brake design and the physical properties of the brake lining. The actual curves used were based on data produced during dynamometer brake tests.

(d) Mu-Slip Curve Variations.—The baseline mu-slip curve used during the sensitivity study represents the curve commonly accepted throughout the aircraft industry (Figure B-5). The four other curves were derived to test antiskid system reaction to changes in the mu-slip relationship.

(e) Power Spectral Density Curve of Rough Runway.—The power spectral density (PSD) curve of the rough runway test condition is a statistical description of the Kennedy Airport runway surface (Figure B-6). The area beneath the PSD curve is the square of the rms value of runway rouginess, where roughness is a measure of the runway vertical profile. The shape of the PSD curve indicates the wavelength of a particular roughness.

8. Recorded Data

In addition to the performance indices, the following data was recorded on an eight-channel pen recorder:

- Braked wheel speed (two wheels)
- Brake pressure (two brakes)
- Strut displacement
- Valve signal (two wheels)

The variables are required to properly assess system capabilities. For various tests. the following were recorded to facilitate analysis:

- Supply pressure
- Return pressure
- Metered pressure
- Brake torque
- Ground force
- Vertical displacement of airplane CG

The ground force model was monitored on the oscilloscope to observe the control system operation. This was necessary to initiate some stability tests.

9. Test Equipment

A variety of test equipment and recording devices were required during the study. The equipment used throughout the testing included:

- Brush chart recorder
- Digital voltmeter
- Weston Boon shaft function analyzer

- Oscilloscope
- X-Y plotter
- Wavetek function generator
- Pressure transducers and associated devices

Each piece of test equipment was calibrated before testing began and as required thereafter. The brush chart recorder was used for indication only and was not calibrated.

The pressure transducers are identified in Table B-1.

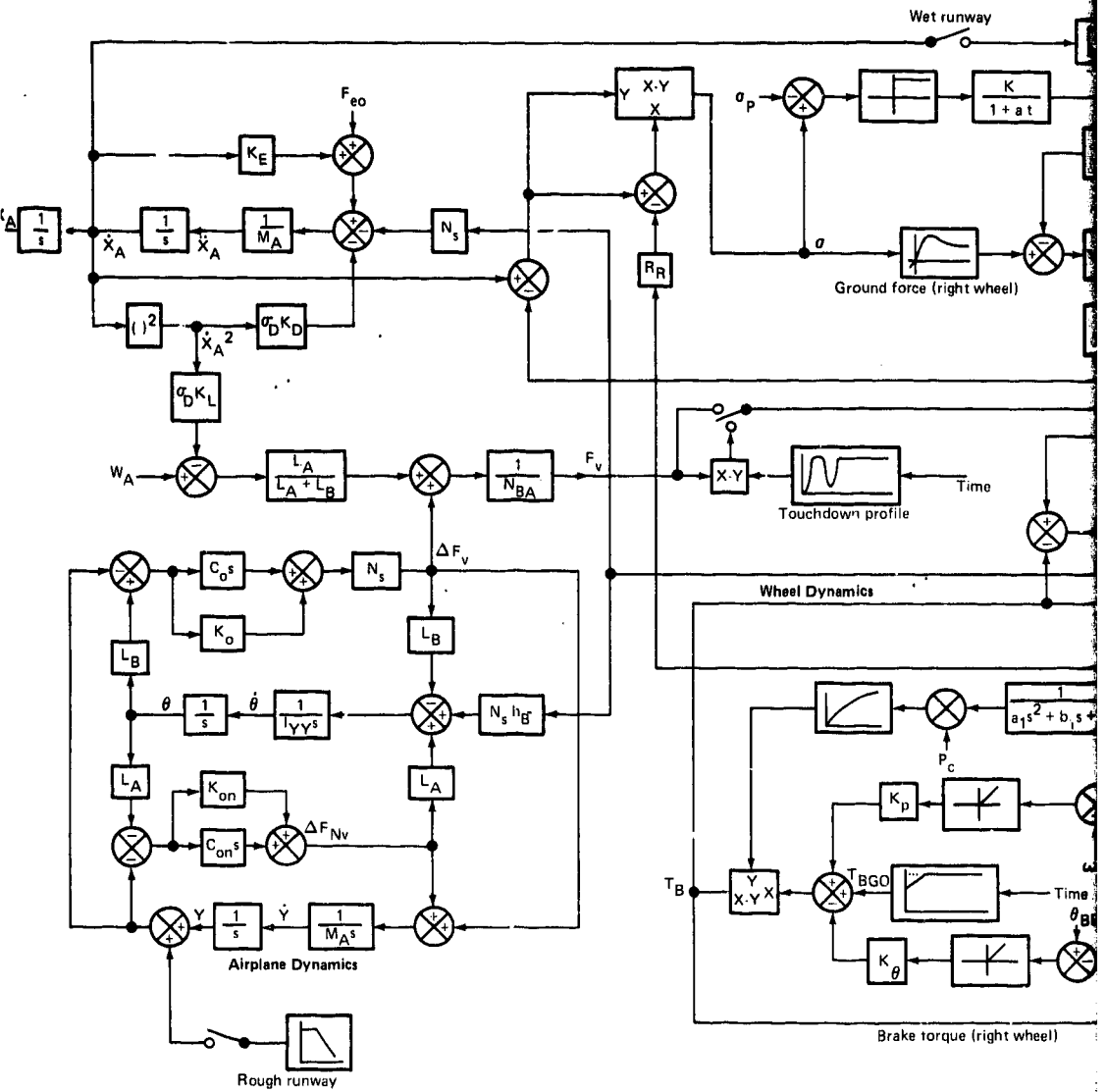
Wet runway
F_{eo}
K_E
$\frac{1}{s}$
$\frac{1}{s}$
$\frac{1}{M_A}$
N_s
$\dot{X}_A$
$\dot{X}_A$
$\dot{X}_A^2$
$()^2$
$\sigma_D K_D$
$\sigma_D K_L$
W_A
$\frac{L_A}{L_A + L_B}$
$\frac{1}{N_{BA}}$
F_v
ΔF_v
$C_o s$
K_o
N_s
L_B
L_B
θ
$\frac{1}{s}$
$\dot{\theta}$
$\frac{1}{I_{YY} s}$
$N_s h_B$
L_A
L_A
K_{on}
$C_{on} s$
ΔF_{Nv}
Y
$\frac{1}{s}$
$\dot{Y}$
$\frac{1}{M_A s}$
Airplane Dynamics
Rough runway
Y X·Y X
R_R
σ_p
$\frac{K}{1 + a t}$
σ
Ground force (right wheel)
X·Y
Time
Touchdown profile
Wheel Dynamics
$\frac{1}{a_1 s^2 + b_1 s +}$
P_c
K_p
T_B
Y X·Y X
T_{BGO}
Time
θ_B
K_θ
Brake torque (right wheel)

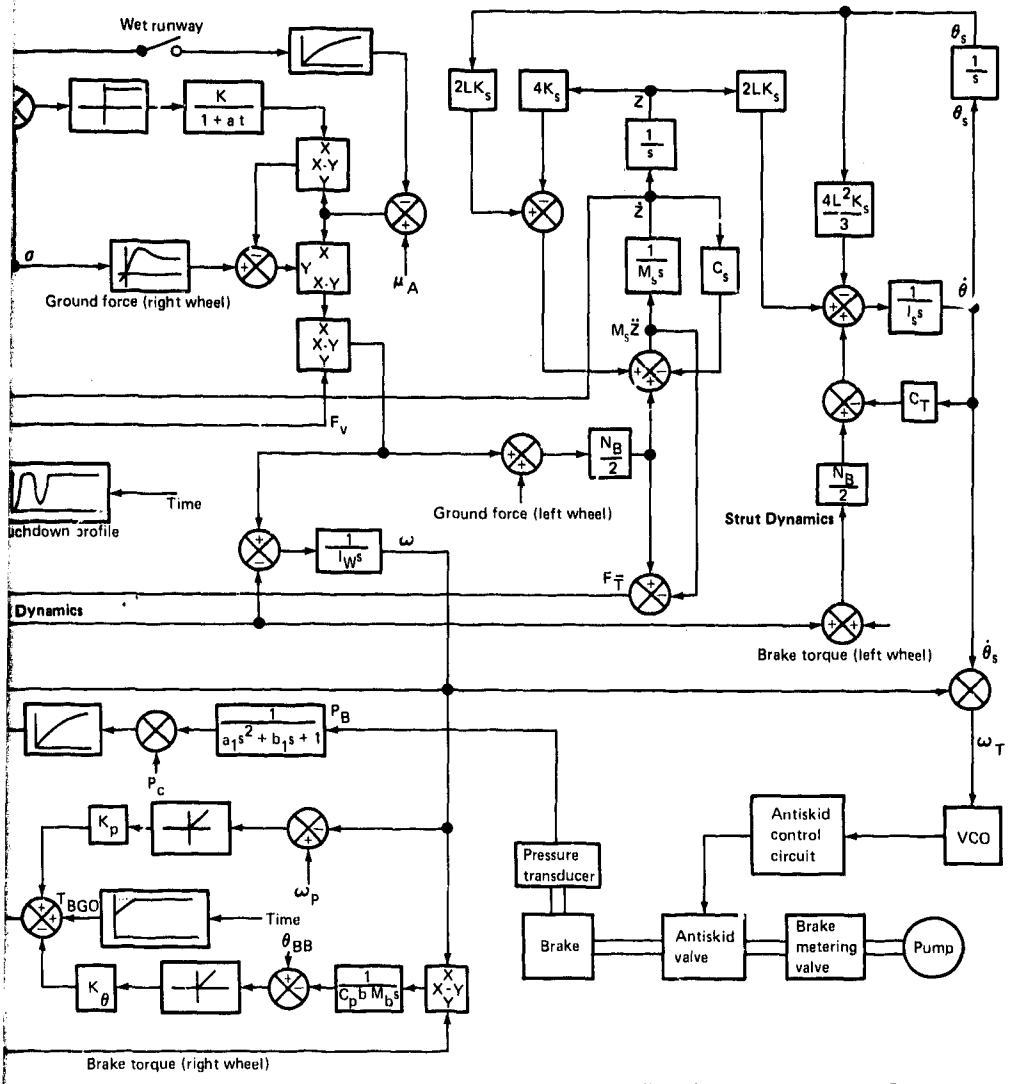

Figure B-1.—Block Diagram of Boeing Brake Control Simulator

$$\mu_{wet} = \mu_{maximum\ available} - K\mu_{WC}$$

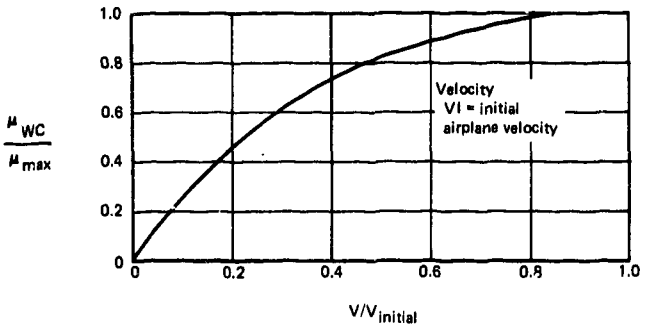

Figure B-2.—Wet Runway Curve

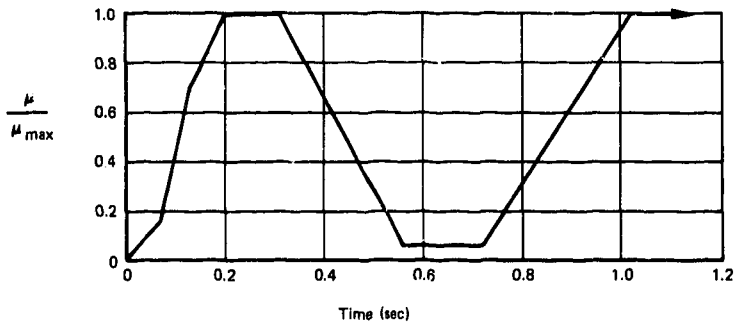

Figure B-3.—Touchdown Profile

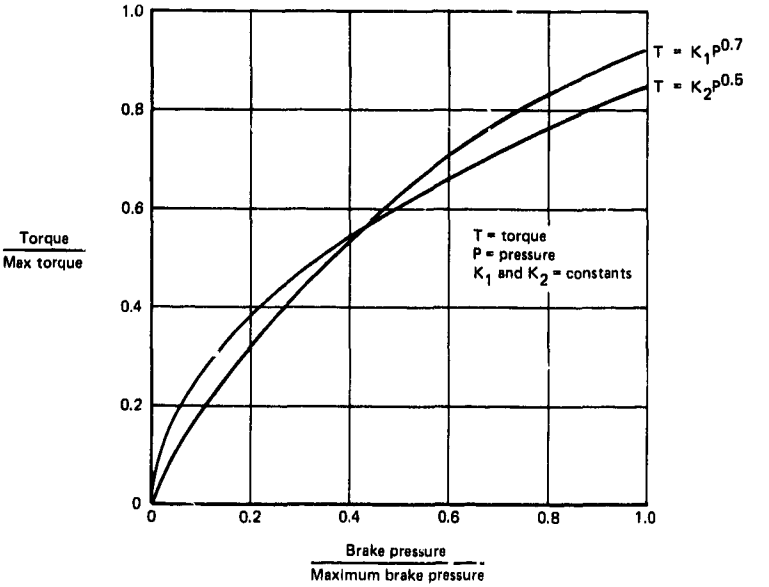

Figure B-4.—Nonlinear Torque Gain Curves

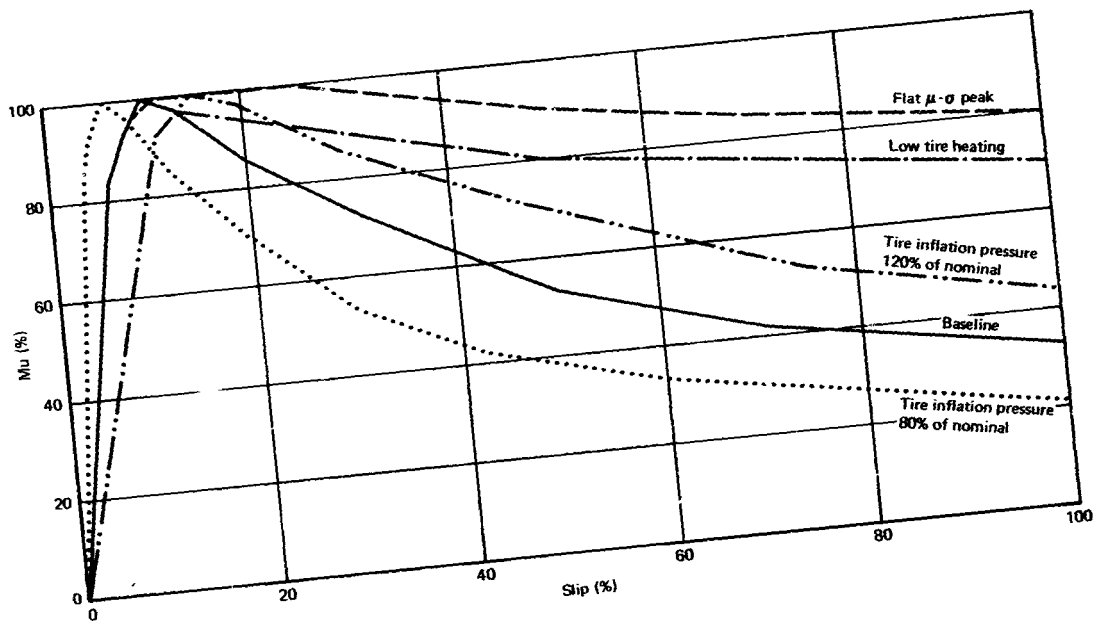

Figure B-5.–Percentage of Peak Available Mu vs Percentage of Slip

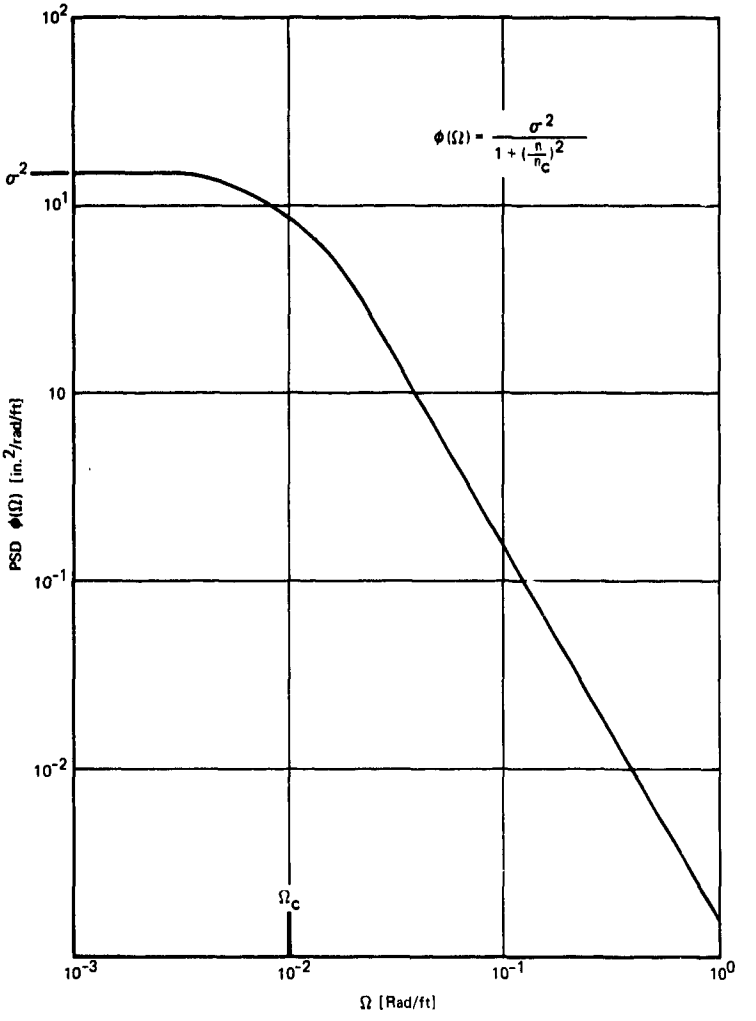

Figure B-6.—Reduced Frequency Power Spectral Density Curve of Rough Runway Simulation

Table B-1.—Pressure Transducer Information

Airplane	Transducer location	Transducer model	Manufacturer	Serial No.	Pressure range (psi)	Maximum voltage (volts)	Transducer resistance (ohms)
727	Right brake	390	Standard	11657	0-3000	10	350
	Left brake	100	Standard	7510	0-3000	10	500
	Metered pressure	355	Standard	9391	0-3000	10	350
	Return pressure	300-27	Standard	8963	0-3000	10	350
737	Right brake	APT111-5M	Dynisco	12955	0-5000	5	– – –
	Left brake	PT135-5M	Dynisco	41655	0-5000	10	– – –
	Metered pressure	PT135-5M	Dynisco	40331	0-5000	10	– – –
	Return pressure	PT135-5M	Dynisco	42112	0-5000	10	– – –
747	Right brake	355	Standard	10685	0-3000	12	350
	Left brake	355	Standard	14451	0-3500	10	350
	Metered pressure	PT135-5M	Dynisco	31629	0-3000	10	– – –
	Return pressure	PA140TCf -1M-350	Standard	1192	0-1000	5	– – –
C-141	Right brake	300-27	Standard	8905	0-3000	10	350
	Left brake	300-27	Standard	8127	0-3000	10	350
	Metered pressure	300-27	Standard	8125	0-3000	10	350
	Return pressure	PT114-50	Dynisco	11721	0-500	10	– – –
F-4	Right brake	100	Standard	7511	0-3000	10	350
	Left brake	APT111-5M	Dynisco	12932	0-5000	5	– – –
	Metered pressure	APT111-5M	Dynisco	12951	0-5000	5	– – –
	Return pressure	PA707TC -200-350	Standard	10409	0-200	7	– – –

APPENDIX C

DIMENSIONAL ANALYSIS TECHNIQUE

Dimensional analysis differs from other types of analysis in that it is based solely on the relationships that must exist among the pertinent variables because of their dimensions rather than the laws of physics and classical mathematical derivation. In itself, dimensional analysis gives qualitative rather than quantitative relationships, but when combined with experimental procedures, it may be made to supply quantitative results and accurate prediction equations.

1. Form of Dimensional Equations

In general, any measurable quantity a (a secondary quantity) may be expressed in terms of the appropriate quantities a_i (called primary quantities) that affect the magnitude of the secondary quantity. The general relationship between a and the primary quantities may be written as:

$$a = f(a_1, a_2, a_3, \ldots\ldots a_n) \tag{C-1}$$

in which a is the number denoting the magnitude of the secondary quantity. Therefore, a_1, a_2, a_3, $\ldots\ldots a_n$ are the numbers denoting the magnitude of the significant primary quantities involved.

The general solution (nature of the function) from Eq C-1 can be shown to be:

$$a = C_a a_1^{C_1} a_2^{C_2} a_3^{C_3} \ldots\ldots a_n^{C_n} \tag{C-2}$$

in which the secondary quantity is expressed as a dimensionless coefficient (C_a) multiplied by the product of the pertinent primary quantities, each raised to the appropriate power. Thus, any measurable phenomenon can be evaluated by Eq C-2 in terms of the factors causing it. The nature of coefficient C_a must be determined experimentally.

2. Development of Prediction Equations

Development of prediction equations and related material has been strictly based on procedures described in Ref. 13. As a result, Ref. 13 material has been freely used and quoted as such.

Two general methods are available for developing prediction equations. One method consists of establishing, by careful observation and measurement, the effect of the pertinent variables upon the quantity to be predicted. The other method consists of applying the natural laws pertinent to the problem to develop relationships among the significant variables. The natural laws used in this method are simply generalizations of reliable information assembled through observation and measurement. The first method is usually referred to as the experimental method, the second as the analytical method. However, each involves analysis, and each is basically dependent upon experimental findings. Often, it is necessary to develop prediction equations for phenomena to which the usual analytical procedures are not well adapted.

The first step of determining the pertinent variables is described in Section X. The second step is to express the secondary quantity as a function of the primary quantities, that is:

$$s = f(g, v, \rho, F_e, \mu, C_L/C_D) \tag{a}$$

Next, a relationship is developed among the variables by dimensional analysis, leading to an expression of the form:

$$s = C\, g^{C_1}\, v^{C_2}\, \rho^{C_3}\, F_e^{C_4}\, \mu^{C_5}\, (C_L/C_D)^{C_6} \tag{b}$$

The determination of the prediction equation for s, from Eq b, would involve the evaluation of seven unknowns (C, C_1, C_2, C_3, C_4, C_5, and C_6) but the number of unknowns can be reduced with the aid of dimensional analysis. The dimensional equation corresponding to Eq b is:

$$L = \left(LT^{-2}\right)^{C_1} \left(LT^{-1}\right)^{C_2} \left(ML^{-3}\right)^{C_3} \left(MLT^{-2}\right)^{C_4} \tag{c}$$

The variables μ and C_L/C_D are dimensionless. Equation c can be resolved into three component auxiliary equations:

$$\text{for M:} \quad 0 = C_3 + C_4 \tag{d}$$

$$\text{for L:} \quad 1 = C_1 + C_2 - 3C_3 + C_4 \tag{e}$$

$$\text{for T:} \quad 0 = -2C_1 - C_2 - 2C_4 \tag{f}$$

There are now four unknowns and three equations: hence three of the unknowns may be expressed in terms of the one remaining unknown. Several combinations are possible; one such combination is to express C_1, C_2, and C_4 in terms of C_3. From Eq d, e, and f:

$$C_1 = -1 - 2C_3 \tag{g}$$

$$C_2 = 2 + 6C_3 \tag{h}$$

$$C_4 = -C_3 \tag{i}$$

If these values are substituted into Eq b, the result is:

$$s = C\left(g^{-1 - 2C_3}\right)\left(v^{2 + 6C_3}\right)\left(\rho^{C_3}\right)\left(F_e^{-C_3}\right) \tag{j}$$

This may be consolidated to:

$$s = C_a \frac{v^2}{g} \left(\rho \frac{v^6}{F_e g^2}\right)^{C_3} (\mu)^{C_5} \left(C_L/C_D\right)^{C_6} \tag{k}$$

The original equation involving seven unknowns has been reduced to an equation involving only four unknowns, which represents considerable simplification. Several forms of the reduced equation are possible, dependent on which exponents are retained. Other possible forms are:

$$s = C_\beta \sqrt{\frac{F_e}{v^2 \rho}} \left(\frac{F_e g^2}{\rho v^6} \right)^{\frac{1}{2} C_1} (\mu)^{C_5} \left(C_L / C_D \right)^{C_6} \tag{l}$$

$$s = C_\gamma \sqrt[3]{\frac{F_e g}{\rho}} \left(\frac{\rho g^2 v^6}{F_e} \right)^{1/6\, C_2} (\mu)^{C_5} \left(C_L / C_D \right)^{C_6} \tag{m}$$

In each case, the quantities in parentheses are dimensionless. The coefficients C_α, C_β, and C_γ are dimensionless and are functions of the dimensionless groups:

$$C_\alpha = (\phi) \left(\frac{v^6 \rho}{F_e g^2}, \mu, C_L / C_D \right) \tag{C-3}$$

From this it follows that Eq k can be written:

$$\left(\frac{sg}{v^2} \right) = F \left(\mu, C_L / C_D, \frac{\rho v^6}{F_e g^2} \right) \tag{C-4}$$

Equation C-4 is a simplified form, involving an unknown function of three variables instead of the seven unknowns of Eq b. Each term in Eq C-4 is dimensionless.

Thus the term C_α is seen to be a function of dimensionless groups of the variables influencing the phenomenon. The dimensionless groups, which are known as pi terms, may be designated as π_i. Hence, Eq C-4 can be written in the general terms:

$$\pi_1 = F (\pi_2, \pi_3, \ldots\ldots \pi_k) \tag{C-5}$$

in which k denotes the total number of dimensionless groups affecting the phenomenon. The number of dimensionless groups, or pi terms, required to express a phenomenon can be determined from the Buckingham pi theorem.

3. The Buckingham Pi Theorem

This section has been developed based on Ref. 14 material. The Buckingham pi theorem, which is the basis of nondimensional analyses, asserts that any complete physical relationship can be expressed in terms of a set of independent dimensionless products composed of the relevant physical parameters. Bridgman's more mathematical statement of the pi theorem says, "If the equation $F(a_1, a_2, a_3, \ldots\ldots a_n) = 0$ is complete, the solution has the form $f(\pi_1, \pi_2, \ldots\ldots \pi_{n-k}) = 0$, where the π terms are independent products of the parameters a_1, a_2, etc., and are dimensionless in the fundamental dimensions." The number of pi terms in the solution equation is less than the number of parameters by a factor k. Usually k equals the number of fundamental dimensions; however, under certain circumstances, k can be less.

4. Statement of Dimensional Homogeneity

Because pi terms are products or quotients of the original parameters, and because these products or quotients are of zero dimension, we can write a general dimensional equation expressing this fact. The most general grouping of the parameters entering the current problem, for example, must combine in such a way that the dimensions of the product are zero; that is:

$$s^{C_1}\, g^{C_2}\, v^{C_3}\, \rho^{C_4}\, F_e^{C_5}\, \mu^{C_6} \left(C_L/C_D\right)^{C_7} \stackrel{d}{=} M^0 L^0 T^0 \qquad \text{(C-6)}$$

Equation C-6 is called an equation of dimensional homogeneity. The symbol $\stackrel{d}{=}$ means "dimensionally equal to." The symbols M, L, and T are the three fundamental dimensions in the physical system of mass, length, and time respectively. Equation C-6 implies that the product of all pi terms, each of which is singularly nondimensional of its own accord, will also be of zero dimension when expressed in the fundamental units of measure.

5. Determination of Pi Terms

The easiest and most orderly procedure for developing pi terms from a list of variables is as follows: The seven parameters needed to define the problem are summarized in Table C-1, where their fundamental dimensions are also presented in the mass (M), length (L), and time (T) system. The list of parameters to be manipulated can be reduced from seven to five by writing, by inspection, two pi terms that are already nondimensional quantities.

$$\pi_1 = \mu \text{ and } \pi_2 = C_L/C_D$$

Next we arrange the remaining five quantities in a matrix with their fundamental dimensions. Across the top of the array we write the variables, and down the left side we write the fundamental dimensions, in this case M, L, and T. Under each variable, we write the powers to which each dimension is raised in each variable.

	C_1	C_2	C_3	C_4	C_5
	s	g	v	ρ	F_e
M	0	0	0	1	1
L	1	1	1	-3	1
T	0	-2	-1	0	-2

We now apply the matrix algebra theorem, which states that "from a matrix there will be a number of independent equations equal to the rank of the matrix"; the rank of the matrix is defined to be the order of the highest-order determinant of the matrix that differs from zero. Because in dimensional analysis there always exists more columns than rows and columns, we can select numerous combinations of different columns from the matrix and combine them into determinants. Some of the determinants from our matrix are:

$$\begin{vmatrix} 0 & 0 & 0 \\ 1 & 1 & 1 \\ 0 & -2 & -1 \end{vmatrix} \quad \begin{vmatrix} 0 & 0 & 1 \\ 1 & 1 & -3 \\ -2 & -1 & 0 \end{vmatrix} \quad \begin{vmatrix} 0 & 1 & 1 \\ 1 & -3 & 1 \\ -1 & 0 & -2 \end{vmatrix} \quad \begin{vmatrix} 0 & 1 \\ 1 & 1 \end{vmatrix} \quad \begin{vmatrix} 1 & 0 \\ -3 & 1 \end{vmatrix} \quad \begin{vmatrix} 1 & -3 \\ 0 & 0 \end{vmatrix}$$

(a) (b) (c)

The order of a determinant is the number of columns or rows in the determinant. The first three determinants are third-order determinants, and the last three are second-order determinants. Although the determinant of (a) equals zero, the determinant of (b) equals +1.0 and is, therefore, not zero. This observation means that the rank of our matrix is 3 and that the total number of dimensionless products in a complete set is equal to the total number of variables minus the rank of their dimensional product or minus the number of independent equations. Thus we have 5-3, or 2 more π terms. Our three equations can be written by inspection from the preceding matrix as:

$$C_4 + C_5 = 0 \qquad \text{(C-7a)}$$

$$C_1 + C_2 + C_3 \cdot 3C_4 + C_5 = 0 \qquad \text{(C-7b)}$$

$$-2C_2 - C_3 - 2C_5 = 0 \qquad \text{(C-7c)}$$

Solving in terms of C_2, and C_3, and C_5 we get:

$$C_2 = C_1 - 2C_4 \tag{C-8a}$$

$$C_3 = 6C_4 - 2C_1 \tag{C-8b}$$

$$C_5 = -C_4 \tag{C-8c}$$

Substitution for C_2, C_3, and C_5 in a statement of dimensional homogeneity gives:

$$s^{C_1}\, g^{C_1 - 2C_4}\, v^{6C_4 - 2C_1}\, \rho^{C_4}\, F_e^{-C_4} = M^0L^0T^0$$

Collection of exponents with the same coefficient gives:

$$\left(\frac{sg}{v^2}\right)^{C_1} \left(\frac{v^6 \rho}{F_e g^2}\right)^{C_4} = M^0L^0T^0$$

These two nondimensional quantities are the additional pi terms. Rearrangement of the two pi terms obtained algebraically, together with the two pi terms written by inspection, gives:

$$\pi_1 = (sg/v^2)$$

$$\pi_2 = (\mu)$$

$$\pi_3 = \left(C_L/C_D\right)$$

$$\pi_4 = \left(\rho v^6/F_e g^2\right)$$

This result yields the functional relationship that:

$$\left(sg/v^2\right) = F\left(\mu, C_L/C_D, \rho v^6/F_e g^2\right) \tag{C-9}$$

This equation is identical in form with Eq C-4 solely because of the selection of the group of exponents in terms of which the independent equations were solved. Actually, pi terms can be multiplied to form new groups of pi terms. They can be inverted; they can be squared, or their square roots can be taken. Such manipulations are proper and are usually performed to create a more convenient ratio of physical phenomena. Most often, one isolates the dependent variable in a single pi term.

Table C-1.—Parameters for Braking Stop Distance Model

Parameter	Symbol	Fundamental dimension
Braking distance	s	L
Acceleration of gravity	g	L/T^2
Brake application speed	v	L/T
Air density	ρ	M/L^3
Forward thrust	F_e	ML/T^2
Coefficient of friction	μ	– – –
$\frac{\text{Coefficient of lift}}{\text{Coefficient of drag}}$ ratio	C_L/C_D	– – –

APPENDIX D

FORMULATION OF COMPONENT EQUATIONS

When the experimental data had been arranged as described in Appendix C, relationships between π_1, the term containing the dependent variable, and π_2, π_3 and π_4 in turn, the terms with independent variables, were obtained using statistical curve fitting programs. The relationships between π_1 and other individual π terms are called component equations.

Plots were prepared of π_1 vs π_2, π_1 vs π_3, and π_1 vs π_4 for all airplanes using data from ASD-TR-74-41, Volume II, Section XIII. An example of these plots is shown (for 737 data) in Figure D-1. This helped determine the general form of relationship that could exist between π_1 and π_2, π_1 and π_3, and so on; e.g. the π_1 vs π_2 data plotted as a straight line on the log-log paper and therefore should have a relationship of the form

$$y = Ax^B \qquad \text{(a)}$$

where A is a constant and B is a polynomial. Logarithms of both sides in Eq a give:

$$\ln(y) = \ln A + B \ln x$$

or:

$$\ln(\pi_1) = \ln A + B \ln(\pi_2)$$

which is the equation for a straight line. Thus, with π_1 and π_2 as inputs and the desired output in the form of Eq a, two computations were necessary, namely a log transformation and a determination of the constants, the latter requiring polynomial regression.

1. Polynomial Regression

Polynomial regression is a statistical technique for finding the coefficients in a functional relationship between a dependent variable (y) and a single independent variable (x). Powers of an independent variable are generated to calculate polynomials of successively increasing degree. If there is no reduction in the residual sum of squares between two successive degrees of polynomials, the calculation will be terminated before completing the analysis for the highest degree polynomial specified. This essentially is a method to establish minimum error in the solution.

The component equations for π_1 vs π_2 and π_1 vs π_4 were determined in the fashion just described.The curvature of the π_1 vs π_3 plots (Figure D-1) indicates that a straight line relationship such as Eq a would not yield the desired accuracy. Thus, it was necessary to use multiple linear regression in addition to the log transformation.

2. Multiple Linear Regression

This is a statistical technique for analyzing a relationship between a dependent variable (y) and a set of independent variables ($x_1, x_2, \ldots\ldots x_n$). Least-squares methods are used to estimate the coefficients in a linear relationship. The analysis showed that the relationship will be of the form:

$$y = Ax_1^{(B - Cx_2)}$$

where x_2 was found to be % spoiler (configuration).

Thus an intermediate calculation was necessary between log transformation and multiple regression to determine the product (spoiler percentage) $\ln(\pi_3)$. A flow chart (Figure D-2) depicting the formulation of component equations follows Figure D-1.

The curve fitting computer programs were used from BCS-STATPK, Ref. 15.

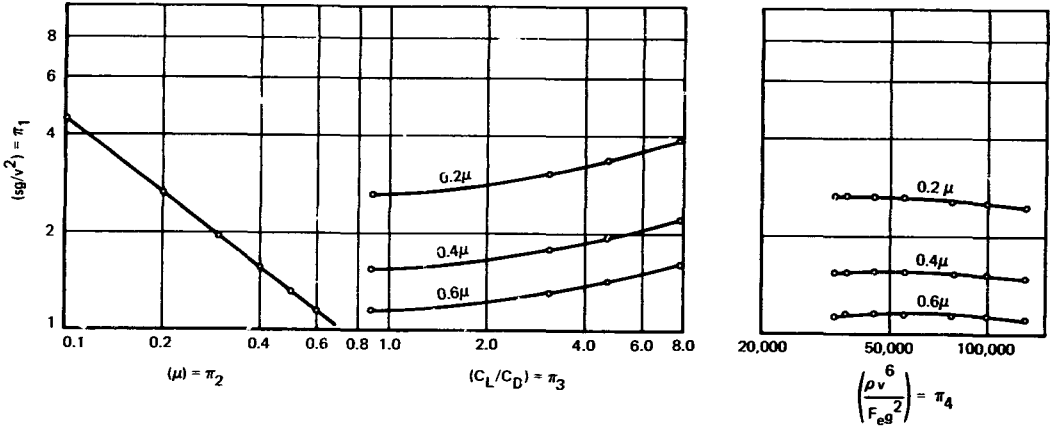

Figure D-1.—Plots of π_1 vs π_2, π_3, and π_4 (737 Data)

$X = \pi_2$ or π_3 or π_4 —the independent variable

$Y = \pi_1$ —the dependent variable

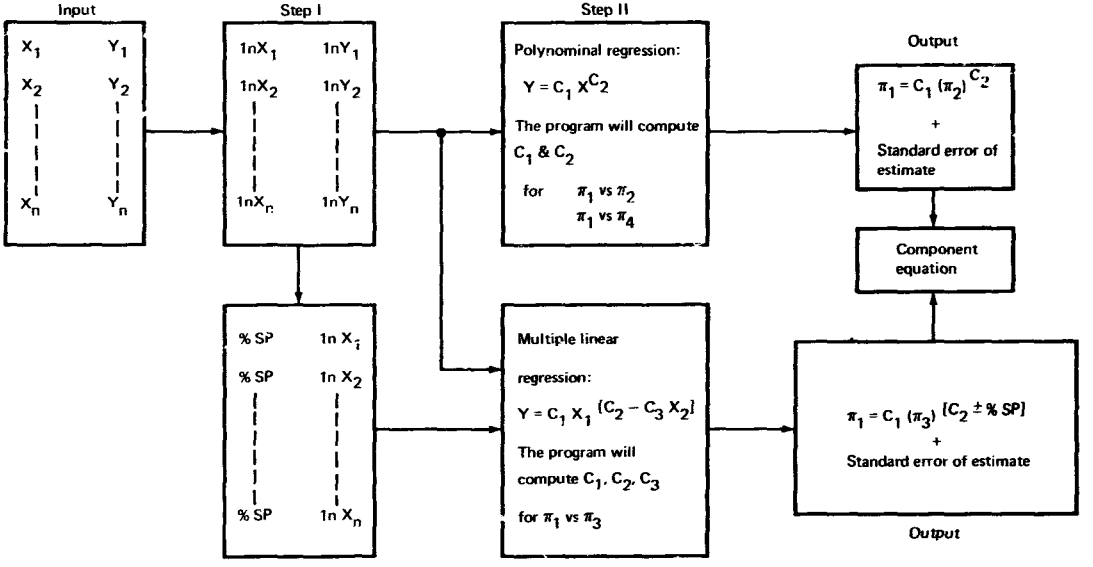

Figure D-2.—Equation Flow Chart

APPENDIX E

FORMULATION OF GENERALIZED FUNCTIONS

1. Determination of Functions

As pointed out in section XI, the component equations representing relationships between π_1 and the other individual pi terms are combined to give a general relationship. This combination is not always simple, but under certain conditions it may be reasonably direct. The function on the right-hand side of the general equation:

$$\pi_1 = F(\pi_2, \pi_3, \pi_4, \ldots\ldots \pi_k) \tag{E-1}$$

may denote any combination of the pi terms. We will now determine the conditions necessary or sufficient for certain simple combinations to exist.

2. Conditions for Function to be a Product

If four pi terms are involved in a phenomenon (as in the current situation):

$$\pi_1 = F(\pi_2, \pi_3, \pi_4) \tag{E-2}$$

experiments would be carried out varying π_2 and holding π_3 and π_4 constant. From a plot of π_1 against π_2, the relationship:

$$(\pi_1)\,\bar{3}, \bar{4} = f_1(\pi_2, \bar{\pi}_3, \bar{\pi}_4) \tag{E-3}$$

in which the bar denotes constant values, could be established. From another set of experiments, with both π_2 and π_4 constant and π_3 variable:

$$(\pi_1)\,\bar{2}, \bar{4} = f_2(\bar{\pi}_2, \pi_3, \bar{\pi}_4) \tag{E-3a}$$

may be established. Similarly, the relationship:

$$(\pi_1)\,\bar{2}, \bar{3} = f_3(\bar{\pi}_2, \bar{\pi}_3, \pi_4) \tag{E-3b}$$

could be established. Equations such as E-3, 3-3a, and E-3b, determined by holding all but one of the pi terms in the function constant, are called component equations.

Under certain conditions, the component equations can be combined to form the general prediction equation by multiplication. For example:

$$\pi_1 = C(\pi_1)\,\bar{3}, \bar{4}\,(\pi_1)\,\bar{2}, \bar{4}\,(\pi_1)\,\bar{2}, \bar{3} \tag{E-3c}$$

To establish those conditions, we first determine the constant C in Eq E-3c by assuming that the component equations are simply multiplied to form the general equation:

$$F(\pi_2, \pi_3, \pi_4) = f_1(\pi_2, \bar{\pi}_3, \bar{\pi}_4) f_2(\bar{\pi}_2, \pi_3, \bar{\pi}_4) f_3(\bar{\pi}_2, \bar{\pi}_3, \pi_4) \quad \text{(E-4)}$$

If this is true, the first set of tests, with π_3 and π_4 constant, will give:

$$F(\pi_2, \bar{\pi}_3, \bar{\pi}_4) = f_1(\pi_2, \bar{\pi}_3, \bar{\pi}_4) f_2(\bar{\pi}_2, \bar{\pi}_3, \bar{\pi}_4) f_3(\bar{\pi}_2, \bar{\pi}_3, \bar{\pi}_4) \quad \text{(E-4a)}$$

from which:

$$f_1(\pi_2, \bar{\pi}_3, \bar{\pi}_4) = \frac{F(\pi_2, \bar{\pi}_3, \bar{\pi}_4)}{f_2(\bar{\pi}_2, \bar{\pi}_3, \bar{\pi}_4) f_3(\bar{\pi}_2, \bar{\pi}_3, \bar{\pi}_4)} \quad \text{(E-4b)}$$

The second set of tests, with π_2 and π_4 constant, gives from Eq E-4:

$$F(\bar{\pi}_2, \pi_3, \bar{\pi}_4) = f_1(\bar{\pi}_2, \bar{\pi}_3, \bar{\pi}_4) f_2(\bar{\pi}_2, \pi_3, \bar{\pi}_4) f_3(\bar{\pi}_2, \bar{\pi}_3, \bar{\pi}_4) \quad \text{(E-4c)}$$

from which:

$$f_2(\bar{\pi}_2, \pi_3, \bar{\pi}_4) = \frac{F(\bar{\pi}_2, \pi_3, \bar{\pi}_4)}{f_1(\bar{\pi}_2, \bar{\pi}_3, \bar{\pi}_4) f_3(\bar{\pi}_2, \bar{\pi}_3, \bar{\pi}_4)} \quad \text{(E-4d)}$$

The third set of tests, with π_2 and π_3 constant, gives, from Eq E-4:

$$F(\bar{\pi}_2, \bar{\pi}_3, \pi_4) = f_1(\bar{\pi}_2, \bar{\pi}_3, \bar{\pi}_4) f_2(\bar{\pi}_2, \bar{\pi}_3, \bar{\pi}_4) f_3(\bar{\pi}_2, \bar{\pi}_3, \pi_4) \quad \text{(E-4e)}$$

from which:

$$f_3(\bar{\pi}_2, \bar{\pi}_3, \pi_4) = \frac{F(\bar{\pi}_2, \bar{\pi}_3, \pi_4)}{f_1(\bar{\pi}_2, \bar{\pi}_3, \bar{\pi}_4) f_2(\bar{\pi}_2, \bar{\pi}_3, \bar{\pi}_4)} \quad \text{(E-4f)}$$

values of $f_1(\pi_2, \bar{\pi}_3, \bar{\pi}_4)$, $f_2(\bar{\pi}_2, \pi_3, \bar{\pi}_4)$, and $f_3(\bar{\pi}_2, \bar{\pi}_3, \pi_4)$ from Eqs e-4b, e-4d and e-4f are substituted into Eq E-4 to give:

$$F(\pi_2, \pi_3, \pi_4) = \frac{F(\pi_2, \bar{\pi}_3, \bar{\pi}_4) F(\bar{\pi}_2, \pi_3, \bar{\pi}_4) F(\bar{\pi}_2, \bar{\pi}_3, \pi_4)}{\left[f_1(\bar{\pi}_2, \bar{\pi}_3, \bar{\pi}_4) f_2(\bar{\pi}_2, \bar{\pi}_3, \bar{\pi}_4) f_3(\bar{\pi}_2, \bar{\pi}_3, \bar{\pi}_4)\right]^2} \quad \text{(E-4g)}$$

However, the denominator of Eq E-4g is found from Eq E-4 with all π_2, π_3, and π_4 constant:

$$F\ (\bar{\pi}_2, \bar{\pi}_3, \bar{\pi}_4) = f_1\ (\bar{\pi}_2, \bar{\pi}_3, \bar{\pi}_4)\ f_2\ (\bar{\pi}_2, \bar{\pi}_3, \bar{\pi}_4)\ f_3\ (\bar{\pi}_2, \bar{\pi}_3, \bar{\pi}_4) \qquad \text{(E-4h)}$$

Hence:

$$F\ (\pi_2, \pi_3, \pi_4) = \frac{F\ (\pi_2, \bar{\pi}_3, \bar{\pi}_4)\ F\ (\bar{\pi}_2, \pi_3, \bar{\pi}_4)\ F\ (\bar{\pi}_2, \bar{\pi}_3, \pi_4)}{\left[F\ (\bar{\pi}_2, \bar{\pi}_3, \bar{\pi}_4)\right]^2} \qquad \text{(E-4i)}$$

In addition to giving the value of C in Eq E-3c as $1/|F(\bar{\pi}_2, \bar{\pi}_3, \bar{\pi}_4)|^2$ Eq E-4i indicates that the three component equations must have the same form.

A test for the validity of combining the component equations as a product may now be developed by assuming that a fourth component equation is determined from a fourth set of data in which one of the pi terms is held constant at a different value than in the preceding set of data. For example, the general Eq E-4i was determined by holding π_2 constant at a value of $\bar{\pi}_2$, but if valid, it could also have been determined from a set of data in which $\pi_2 = \bar{\bar{\pi}}_2$. Then:

$$F\ (\pi_2, \pi_3, \pi_4) = \frac{F\ (\pi_2, \bar{\pi}_3, \bar{\pi}_4)\ F\ (\bar{\bar{\pi}}_2, \pi_3, \bar{\pi}_4)\ F\ (\bar{\bar{\pi}}_2, \bar{\pi}_3, \bar{\pi}_4)}{\left[F\ (\bar{\bar{\pi}}_2, \bar{\pi}_3, \bar{\pi}_4)\right]^2} \qquad \text{(E-5)}$$

The right-hand side of Eq E-4i must equal the right-hand side of Eq E-5. Hence:

$$\frac{F\ (\bar{\pi}_2, \pi_3, \bar{\pi}_4)\ F\ (\bar{\pi}_2, \bar{\pi}_3, \pi_4)}{\left[F\ (\bar{\pi}_2, \bar{\pi}_3, \bar{\pi}_4)\right]^2} = \frac{F\ (\bar{\bar{\pi}}_2, \pi_3, \bar{\pi}_4)\ F\ (\bar{\bar{\pi}}_2, \bar{\pi}_3, \pi_4)}{\left[F\ (\bar{\bar{\pi}}_2, \bar{\pi}_3, \bar{\pi}_4)\right]^2} \qquad \text{(E-6)}$$

Similarly, if π_3 had been held constant at a different value, $\bar{\bar{\pi}}_3$:

$$\frac{F\ (\pi_2, \bar{\pi}_3, \bar{\pi}_4)\ F\ (\bar{\pi}_2, \bar{\pi}_3, \pi_4)}{\left[F\ (\bar{\pi}_2, \bar{\pi}_3, \bar{\pi}_4)\right]^2} = \frac{F\ (\pi_2, \bar{\bar{\pi}}_3, \bar{\pi}_4)\ F\ (\bar{\pi}_2, \bar{\bar{\pi}}_3, \pi_4)}{\left[F\ (\bar{\pi}_2, \bar{\bar{\pi}}_3, \bar{\pi}_4)\right]^2} \qquad \text{E-6a)}$$

Equations E-6 and E-6a constitute a test for the validity of Eq E-4i. That is, if the supplementary sets of data satisfy either Eq E-6 or E-6a, the general equation may be formed by multiplying the component equations together and dividing by the constant, as indicated in Eq E-4i.

Thus, if the general equation for a system involving k pi terms formed by multiplication of the component equations, it may be shown that the form is:

$$\pi_1 = \frac{F\ (\pi_2, \bar{\pi}_3, \bar{\pi}_4, \ldots \bar{\pi}_k)\ F\ (\bar{\pi}_2, \pi_3, \bar{\pi}_4, \ldots \bar{\pi}_k) \ldots F\ (\bar{\pi}_2, \bar{\pi}_3, \bar{\pi}_4, \ldots \pi_k)}{\left[F\ (\bar{\pi}_2, \bar{\pi}_3, \bar{\pi}_4, \ldots \bar{\pi}_k)\right]^{k-2}} \qquad \text{(E-7)}$$

In this, π_2 must be the same in each component set, π_3 must be the same in each set, etc. Similarly, if the general equation for a system involving k pi terms is formed by addition of the component equations, it may be shown that the form is:

$$\pi_1 = F(\pi_2, \bar{\pi}_3, \bar{\pi}_4, \ldots \bar{\pi}_k) + F(\bar{\pi}_2, \pi_3, \bar{\pi}_4, \ldots \bar{\pi}_k) + F(\bar{\pi}_2, \bar{\pi}_3, \pi_4, \ldots \bar{\pi}_k) + \ldots F(\bar{\pi}_2, \bar{\pi}_3, \bar{\pi}_4, \ldots \pi_k) - (k-2)\, F(\bar{\pi}_2, \bar{\pi}_3, \bar{\pi}_4, \ldots \bar{\pi}_k) \quad \text{(E-8)}$$

In general, the possible methods of formation of general equations discussed above are adequate for the majority of engineering problems. Regardless of whether the resultant prediction equation is formed by multiplication or by addition, a constant term of the form:

$$F(\bar{\pi}_2, \bar{\pi}_3, \bar{\pi}_4, \ldots \ldots \bar{\pi}_k)$$

is involved, and this constant can be evaluated from any one of the component equations. As a general policy, the constant should be evaluated from each of the component equations. Each should give the same value as the others. If not, error is present, and the equations should be checked. Tables E-1 and E-2 show detailed calculations for tests of validity.

Table E-1.—Calculations of Validity for the Function To Be a Product

Airplane	$\bar{\pi}_2$	$(\bar{F})^2$	F_1	F_2	$\frac{F_1 \times F_2}{(\bar{F})^2}$	Error percentage
727	0.6	1.16187	1.08461	1.07809	1.006	+0.6
	0.4	2.21877	1.4812	1.4932	0.997	-0.3
	0.2	12.9600	3.5514	3.7861	1.037	+3.7
737	0.6	1.30736	1.14817	1.14271	1.003	+0.3
	0.4	2.3963	1.54775	1.54226	0.996	-0.4
	0.2	6.9485	2.63427	2.63185	0.998	-0.2
747	0.6	1.62691	1.27917	1.2824	1.008	+0.8
	0.4	3.1299	1.76685	1.77516	1.002	+0.2
	0.2	9.5969	3.0864	3.0950	0.996	-0.4
C-141	0.6	2.19635	1.48158	1.48154	0.999	-0.1
	0.4	4.9462	2.21385	2.21192	0.990	-1.0
	0.2	20.79	4.55428	4.55093	0.997	-0.3
F-4	0.6	1.87512	1.38317	1.36896	1.010	+1.0
	0.4	3.84675	1.9518	1.96023	0.995	-0.5
	0.2	18.3486	4.20789	4.29368	0.985	-1.5

$$1/C = (\bar{F})^2 = \left[F\left(\bar{\pi}_2, \bar{\pi}_3, \bar{\pi}_4\right)\right]^2$$

$$(F_1) = F\left(\bar{\pi}_2, \pi_3, \bar{\pi}_4\right)$$

$$(F_2) = F\left(\bar{\pi}_2, \bar{\pi}_3, \pi_4\right)$$

TEST OF VALIDITY:

$$\frac{(F_1)\ (F_2)}{(\bar{F})^2} = 1$$

Table E-2.—Calculations of Validity for Constant Term

Airplane model	$F\left(\bar{\pi}_2, \bar{\pi}_3, \bar{\pi}_4\right) = \pi_1$ (Baseline)				$C = \left[1/_F\left(\bar{\pi}_2, \bar{\pi}_3, \bar{\pi}_4\right)\right]^2$				Average value of predicted C	Deviation from ideal value %	Value of $\bar{\pi}_2$
	Component equation used										
	π_1 vs π_2	π_1 vs π_3	π_1 vs π_4	Ideal	π_1 vs π_2	π_1 vs π_3	π_1 vs π_4	Ideal			
727	1.0714	1.0844	1.0779	1.082	0.8711	0.8504	0.8607	0.8542	0.8607	0.8	0.6
	1.4933	1.482	1.4933	1.482	0.4484	0.4553	0.4484	0.4553	0.4507	-1.0	0.4
	---	3.550	3.789	3.550	---	0.07935	0.06965	0.07935	0.0745	—	0.2
737	1.140	1.148	1.1422	1.149	0.7695	0.7588	0.7665	0.7575	0.7649	+1.0	0.6
	1.554	1.548	1.542	1.549	0.4141	0.4173	0.4206	0.4168	0.4173	-0.1	0.4
	2.640	2.633	2.635	2.640	0.1435	0.1442	0.144	0.144	0.1439	0	0.2
747	1.271	1.279	1.283	1.279	0.619	0.6113	0.6075	0.6113	0.6126	+0.2	0.6
	1.768	1.766	1.775	1.766	0.3199	0.3206	0.3174	0.3206	0.3193	-0.4	0.4
	3.111	3.087	3.096	3.087	0.1033	0.1049	0.1043	0.1049	0.1042	-0.7	0.2
C-141	1.482	1.482	1.482	1.482	0.4533	0.4533	0.4533	0.4533	0.4553	0	0.6
	2.246	2.215	2.212	2.215	0.1982	0.2038	0.2044	0.2038	0.2021	-0.8	0.4
	4.577	4.554	4.548	4.548	0.04773	0.0482	0.04834	0.04834	0.0481	-0.5	0.2
F-4	1.357	1.383	1.369	1.359	0.543	0.5228	0.5336	0.5414	0.5331	-1.5	0.6
	1.972	1.952	1.960	1.952	0.2571	0.2624	0.2603	0.2624	0.2599	-0.9	0.4
	---	4.208	4.293	4.222	---	0.05647	0.05426	0.0561	0.05536	-1.2	0.2

APPENDIX F

MODEL THEORY ANALYSIS FOR GROUND VEHICLES

1. Model Theory

Two common systematic methods can derive modeling laws for a particular physical system. The "equations approach" requires knowledge of the characteristic equations that govern the behavior of the system. The "parameters approach" requires only that the complete set of all variables affecting the system behavior be specified. For our problem, the second approach is more appropriate.

We have already considered the independent variables affecting braking stop distances; by applying conventional techniques of dimensional analysis, we have established the relationship:

$$\left(sg/v^2\right) = F_1\left(\mu, C_L/C_D, \rho v^6/F_e{}^2\right)$$

However, we can rewrite the above equation as:

$$(\mu) = F_2\left(C_L/C_D, sg/v^2, \rho v^6/F_e\, g^2\right) \tag{F-1}$$

The model design conditions follow directly from Eq F-1. By letting the subscript m denote quantities relating to the model and the subscript p denote quantities relating to the prototype, we find that sufficient conditions for the equality of μ_m and μ_p are:

$$\frac{C_{L_m}}{C_{D_m}} = \frac{C_{L_p}}{C_{D_p}} \tag{F-2}$$

$$\frac{S_m v_m}{g_m{}^2} = \frac{s_p v_p}{g_p{}^2} \tag{F-3}$$

$$\frac{\rho_m v_m{}^6}{F_{e_m} g_m{}^2} = \frac{\rho_p v_p{}^6}{F_{e_p} g_p{}^2} \tag{F-4}$$

The conditions given by Eqs F-3 and F-4 can be met under a variety of test constraints. Equation F-2, however, presents a unique problem. No ground vehicle can duplicate the wide variety of C_L and C_D for a single airplane, and certainly not for all the airplanes. Because of this problem, it is not practically feasible to conduct a model test without some measure of model distortion. A systematic technique to account for model distortion has been developed by Murphy Ref. 13 and will be used later.

The model can be tested with the same fluid as the prototype under the same gravitational conditions. That is:

$$g_m = g_p \tag{F-5}$$

and

$$\rho_m = \rho_p \tag{F-6}$$

Simultaneous solution of Eqs F-3 through F-6 results in the following set of simplified design conditions:

$$v_m = \left(\frac{F_{e_m}}{F_{e_p}}\right)^{1/6} v_p \tag{F-7}$$

$$s_m = \left(\frac{v_p}{v_m}\right) s_p \tag{F-8}$$

In generating Eq F-1, if we also considered the weight of the vehicle as an independent variable, the relationship is altered as follows:

$$(\mu) = F_3\left(C_L/C_D, \frac{sg}{v^2}, \frac{\rho v^6}{W g^2}, \frac{F_e}{W}\right)$$

from which:

$$\frac{\rho_m v_m^6}{W_m g_m^2} = \frac{\rho_p v_p^6}{W_p g_p^2} \tag{F-4a}$$

and:

$$\frac{\left(F_{e_m}\right)}{W_m} = \frac{\left(F_{e_p}\right)}{W_p} \tag{F-4b}$$

Substituting Eq F-4b into Eq F-4a gives:

$$\frac{\rho_m v_m^6}{F_{e_m} g_m 2} = \frac{\rho_p v_p^6}{F_{e_p} g_p 2} \tag{F-4c}$$

Equation F-4c is identical to Eq F-4. Hence, Eq F-7 can be modified as:

$$v_m = \left(\frac{W_m}{W_p}\right)^{1/6} v_p$$

or:

$$v_m = (\lambda)^{1/6} v_p \tag{F-9}$$

and:

$$s_m = (\lambda)^6 s_p \tag{F-10}$$

Where $\lambda = W_m / W_p$ is the weight scale ratio for the experiment.

2. Model Distortion

A distorted model is one in which one or more of the design conditions are not satisfied. That is, one of the pi terms is not equal to the corresponding pi term in the prototype. In general, the prediction equation is formulated by dividing the general equation for the prototype by the general equation for the model:

$$\frac{\pi_1}{\pi_{1m}} = \frac{f(\pi_2, \pi_3, \pi_4)}{f(\pi_{2m}, \pi_{3m}, \pi_{4m})} \tag{F-11}$$

If the design conditions for a true model are all satisfied ($\pi_{im} = \pi_i$), the functions are equal and $\pi_1 = \pi_{1m}$. However, if one design condition is violated, the functions may not be equal, whereupon π_1 will not equal π_{1m}.

Under those conditions, two procedures are available for establishing a prediction equation:

- Determine a prediction factor δ so that:

$$\pi_1 = \delta \pi_{1m} \tag{F-12}$$

- Distort additional pi terms in a controlled fashion so that:

$$\pi_1 = \pi_{1m} \tag{F-13}$$

(a) The Prediction Factor, δ.– If one of the design conditions is not satisfied (say $\pi_{3m} \neq \pi_3$), the prediction factor is, by definition from Eq F-11:

$$\delta = \frac{\pi_1}{\pi_{1m}} = \frac{f(\pi_2, \pi_3, \pi_4)}{f(\pi_{2m}, \pi_{3m}, \pi_{4m})} \tag{F-12a}$$

Hence, to evaluate δ, the ratio of the two functions must be evaluated. This determination involves either additional experimental evidence or knowledge of how π_3 influences the function. If, for example, it can be established that:

$$f(\pi_2, \pi_3, \pi_4) = \frac{f(\pi_3)\, f(\pi_2, \pi_4)}{f(\bar{\pi}_2, \bar{\pi}_3, \bar{\pi}_4)} \tag{F-14}$$

it follows that:

$$\delta = \frac{f(\pi_3)}{f(\pi_{3m})} \tag{F-12b}$$

The test for the resolution of a function into the product of two component functions requires that two sets of tests be run in which the degree of distortion is varied. The degree of distortion can be evaluated as a distortion factor a, defined as:

$$\pi_{3m} = a\pi_3 \tag{F-15}$$

Thus $a = 1$ indicates no distortion.

If the log plot of π_1 vs π_3 is a straight line and π_3 satisfies the requirement for combination as a product, it follows from Eq. F-12b that:

$$\delta = \frac{f(\pi_3)}{f(a\pi_3)} \tag{F-12c}$$

and:

$$\delta = \frac{C\pi_3{}^m}{Ca^m\pi_3{}^m} \tag{F-12d}$$

and:

$$\delta = a^{-m} \tag{F-12e}$$

where m is the slope of the line in the log plot. Even if values of π_1 plotted against π_3 do not plot as a straight line, the value of π_1, corresponding to the correct value of π_3 for a true model, can be taken from the curve. If a number of points have been obtained for values of π_3, both less and greater than the desired value, and if the curve is smooth, the value of π_1 may be determined with a high degree of accuracy.

(b) Multiple Distortion.–In some situations, distortion of one factor or dimension will result in the distortion of more than one pi term; two or more factors may be distorted, causing two or more pi terms to be distorted. The prediction factor δ then becomes a function of the distortion factors, and may, in addition, be a function of one or more of the pi terms. It may be determined either algebraically or experimentally.

(c) Compensated Distortion.–One simplification of the prediction equation that is sometimes possible is to adjust the distortion factors in such a manner that the prediction factor becomes unity. Then:

$$\pi_1 = \pi_{1m} \tag{F-13}$$

as it would be in an undistorted model.

If enough is known concerning the effect of each of the pi terms, this can be accomplished algebraically without recourse to experiment (see Figure F-1). In the current problem, $\pi_3 \neq \pi_{3m}$. Using Eq F-12e, we can write:

$$\delta = a^{-\left[C_3 - C_4 \% SP\right]} \tag{F-16}$$

where:

$$\delta = f(\pi_3)/f(\pi_{3m})$$

$$a = \pi_{3m}/\pi_3$$

Here, C_3 and C_4 are the constants determined in the preceding prediction equations. Based on Eq F-16, prediction and distortion factors corresponding to prediction Eqs 4 through 38 are listed in Table F-1. Table F-2 shows the data used for mu-meter evaluation, and Table F-3 shows its detailed analysis.

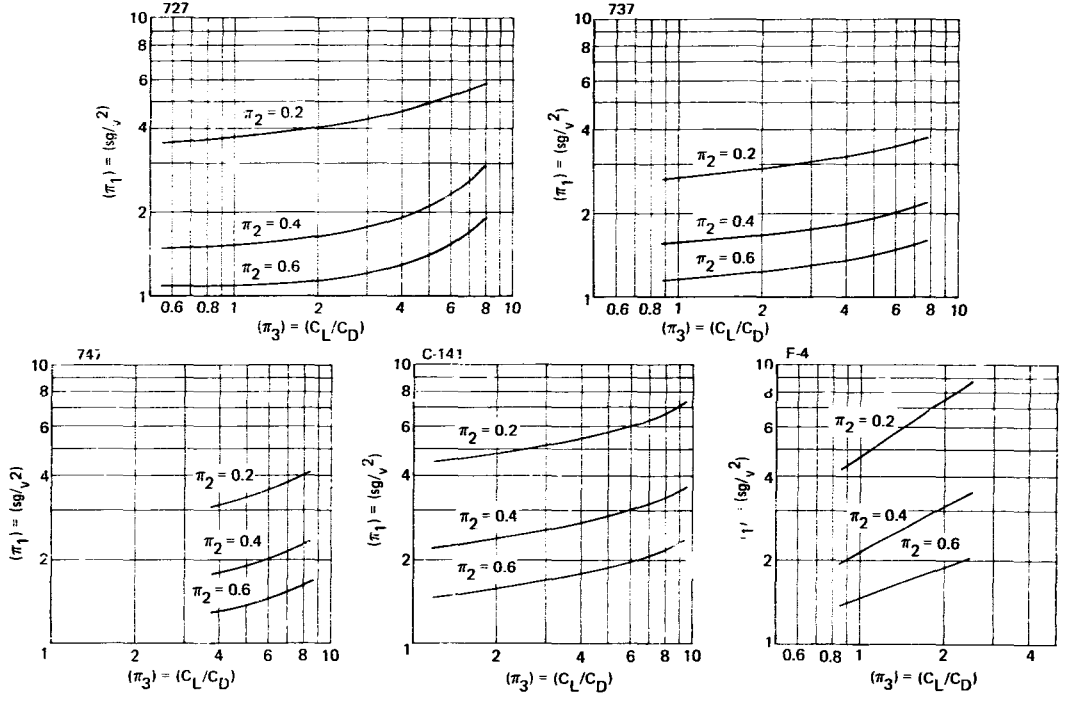

Figure F-1.—Mu-Meter-to-Aircraft Aerodynamic Similiarity

Table F-1.—Prediction Factor δ vs Distortion Factor α for DBV Evaluation

Airplane	Factors	To be used with Eq:
727	$\delta = \alpha^{[0.3375\ \%\ SP\ -\ 0.3125]}$	(4)
	$\delta = \alpha^{[0.3011\ \%\ SP\ -\ 0.309]}$	(6)
	$\delta = \alpha^{[0.1347\ \%\ SP\ -\ 0.2159]}$	(9)
737	$\delta = \alpha^{[0.08113\ \%\ SP\ -\ 0.15668]}$	(12)
	$\delta = \alpha^{[0.08663\ \%\ SP\ -\ 0.16655]}$	(14)
	$\delta = \alpha^{[0.06279\ \%\ SP\ -\ 0.16397]}$	(16)
747	$\delta = \alpha^{[0.11286\ \%\ SP\ -\ 0.14803]}$	(19)
	$\delta = \alpha^{[0.09193\ \%\ SP\ -\ 0.18957]}$	(21)
	$\delta = \alpha^{[0.0818\ \%\ SP\ -\ 0.2365]}$	(23)
C-141	$\delta = \alpha^{[0.13084\ \%\ SP\ -\ 0.21341]}$	(26)
	$\delta = \alpha^{[0.14819\ \%\ SP\ -\ 0.23065]}$	(28)
	$\delta = \alpha^{[0.16567\ \%\ SP\ -\ 0.21614]}$	(30)
F-4	$\delta = \alpha^{-0.3636}$	(33)
	$\delta = \alpha^{[0.52698\ +\ 0.08287\ \%\ SP]}$	(35)
	$\delta = \alpha^{-0.69738}$	(38)

Table F-2.–Mu-Meter Data

Run No.	Surface condition	Water depth (in)	Ambient temperature (°F)	Aircraft gross weight (lb)	Flap angle (deg)	Brake application speed (knots)	Aircraft stopping distance (ft)	Mu-meter average friction reading
10	Dry	– – –	72	113,500	40	98.30	1106	0.810
11	Dry	– – –	72	109,500	30	112.41	1370	0.810
13	Wet	0.010	65	103,500	30	112.64	1744	0.766
14	Dry	– – –	76	136,500	30	119.35	1739	0.760
17	Dry	– – –	75	131,500	40	122.29	1730	0.760
18	Wet	0.010	73	132,500	40	121.70	2392	0.674
21A	Wet	0.010	73	136,500	30	117.11	2202	0.718

Table F-3.—Mu-Meter Data Analysis

Run No.	v (fps)	T_{amb} (^{o}F)	ρ (lb-sec^2/ft^4)	Flaps (deg)	(C_L/C_D) or (π_3)	Calculated F_e (lb)	(sg/v^2) or (π_1)	$(\rho v^6/F_e g^2)$ or (π_4)	$(\mu)_{ap1}$ or (π_2)
10	166.0	72	0.00232	40	0.9627	1946	1.2924	24059	0.518
11	189.8	72	0.00232	30	0.553	1870	1.2252	55850	0.524
13	190.1	65	0.00235	30	0.553	1869	1.5533	57304	0.391
14	201.5	76	0.00230	30	0.553	1833	1.3791	81003	0.439
17	206.2	75	0.00231	40	0.9627	1818	1.3102	94197	0.454
18	205.4	73	0.00232	40	0.9627	1821	1.8256	92272	0.304
21A	198.0	73	0.00232	30	0.553	1844	1.8086	73115	0.318